The Performance Characteristics of a Surface-Modified Cutting Tool

Titus Bitek Watmon

A Thesis submitted in partial fulfilment of the requirements of the University of East London for the degree of Doctor of Philosophy

July 2013

The Performance Characteristics of a Surface-Modified Cutting Tool

Director of Studies: Dr David Xiao
Supervisor: Dr Vijitha M. Weerasinghe
School of Architecture, Computing & Engineering
Docklands Campus,
University of East London.

July 2013

Abstract

In the past, many papers have been presented which show that the coating of cutting tools often yields decreased wear rates and reduced coefficients of friction. Although different theories are proposed, covering areas such as hardness theory, diffusion barrier theory, thermal barrier theory, and reduced friction theory, most have not dealt with the question of how and why the coating of tool substrates with hard materials such as Titanium Nitride (TiN), Titanium Carbide (TiC) and Aluminium Oxide (Al_2O_3) transforms the performance and life of cutting tools. This project discusses the complex interrelationship that encompasses the thermal barrier function and the relatively low sliding friction coefficient of TiN on an undulating tool surface, and presents the result of an investigation into the cutting characteristics and performance of EDMed surface-modified carbide cutting tool inserts. The tool inserts were coated with TiN by the physical vapour deposition (PVD) method. PVD coating is also known as Ion-plating which is the general term of the coating method in which the film is created by attracting ionized metal vapour in this the metal was Titanium and ionized gas onto negatively biased substrate surface. Coating by PVD was chosen because it is done at a temperature of not more than 500^0C whereas chemical Vapour Deposition CVD process is done at very high temperature of about 850^0C and in two stages of heating up the substrates. The high temperatures involved in CVD affects the strength of the (tool) substrates. In this study, comparative cutting tests using TiN-coated control specimens with no EDM surface structures and TiN-coated EDMed tools with a crater-like surface topography were carried out on mild steel grade EN-3. Various cutting speeds were investigated, up to an increase of 40% of the tool manufacturer's recommended speed. Fifteen minutes of cutting were carried out for each insert at the speeds investigated. Conventional tool inserts normally have a tool life of approximately 15 minutes of cutting. After every five cuts (passes) microscopic pictures of the tool wear profiles were taken, in order to monitor the progressive wear on the rake face and on the flank of the insert. The power load was monitored for each cut taken using an on-board meter on the CNC machine to establish the amount of power needed for each stage of operation. The spindle drive for the machine is an 11 KW/hr motor. Results obtained confirmed the advantages of cutting at all speeds investigated using EDMed coated inserts, in terms of reduced tool wear and low power loads. Moreover, the surface finish on the

i

workpiece was consistently better for the EDMed inserts. The thesis discusses the relevance of the finite element method in the analysis of metal cutting processes, so that metal machinists can design, manufacture and deliver goods (tools) to the market quickly and on time without going through the hassle of trial and error approach for new products. Improvements in manufacturing technologies require better knowledge of modelling metal cutting processes. Technically the use of computational models has a great value in reducing or even eliminating the number of experiments traditionally used for tool design, process selection, machinability evaluation, and chip breakage investigations. In this work, much interest in theoretical and experimental investigations of metal machining were given special attention. Finite element analysis (FEA) was given priority in this study to predict tool wear and coating deformations during machining. Particular attention was devoted to the complicated mechanisms usually associated with metal cutting, such as interfacial friction; heat generated due to friction and severe strain in the cutting region, and high strain rates. It is therefore concluded that Roughened contact surface comprising of peaks and valleys coated with hard materials (TiN) provide wear-resisting properties as the coatings get entrapped in the valleys and help reduce friction at chip-tool interface. The contributions to knowledge:

a. Relates to a wear-resisting surface structure for application in contact surfaces and structures in metal cutting and forming tools with ability to give wear-resisting surface profile.

b. Provide technique for designing tool with roughened surface comprising of peaks and valleys covered in conformal coating with a material such as TiN, TiC etc which is wear-resisting structure with surface roughness profile compose of valleys which entrap residual coating material during wear thereby enabling the entrapped coating material to give improved wear resistance.

c. Provide knowledge for increased tool life through wear resistance, hardness and chemical stability at high temperatures because of reduced friction at the tool-chip and work-tool interfaces due to tool coating, which leads to reduced heat generation at the cutting zones.

d. Establishes that Undulating surface topographies on cutting tips tend to hold coating materials longer in the valleys, thus giving enhanced protection to the tool and the tool can cut faster by 40% and last 60% longer than conventional tools on the markets today.

TABLE OF CONTENTS

Chapter 2: Tool Modification Using Spark Erosion Process and Cutting Test Procedures

List of Figures and Illustrative Diagrams

List of Tables

Nomenclature

$ASME: B94.55M$ =   Testing with single-point turning tools 1985

BS EN $ISO3685$ =   Tool-life testing with single-point turning tools 1997

BS EN $ISO4288$ =   Surface Profile including Texture

BS EN $ISO4287$ =   Surface structure Definitions

Al =   Aluminium

Al_2O_3 =   Aluminium Oxide

ω =   Angular Speed

A_R =   Apparent Area

E =   Applied Direct Current in electrical discharge machining

A =   Area

A_S =   area of shear plane

AA =   Arithmetic Average (same as R_a)

A_W =   Average Waviness

BUE =   Built-up Edge

CLA =   Centre Line Average (same as R_a)

CVD =   Chemical Vapour Deposition

θ =   Clearance Angle

$G01$ =   CNC G-Code: Makes a linear feed move to a point

$G00$ =   CNC G-Code: Presets a rapid motion command

CAD =   Computer Aided Design

CNC =   Computer Numerical Control

l_C =   Contact Length

C_U =   Copper

λ_C =   Cut-off length in surface measurements

F_C =   Cutting Force

V_C =   Cutting Velocity / Speed

d_C =   Depth of Crater

ε^p =   Effective Plastic Strain Rate

σ_{eff}	=	Effective Stress
EDMed	=	Electrical Discharge Machined
EDM	=	Electrical Discharge Machining
F_f	=	Feed Force
FEA	=	Finite Element Analysis
FEM	=	Finite Element Method
τ_f	=	Friction Stress
HSM	=	High Speed Machining
HSS	=	High Speed Steel
tm	=	Machining Time
ηm	=	Micrometre / Micron
$EN-3$	=	Mild Steel Grade Free Cutting
l_n	=	Natural Contact Length
F_n	=	normal force
PVD	=	Physical Vapour Deposition
$\pm$	=	Plus or Minus or Equal to
R_C	=	Radius of Curvature
α	=	Rake Angle
R_a	=	Roughness Average
ξ	=	Setting angle
τ_S	=	shear stress
ε	=	Strain Rate
ε_0	=	Strain Rate below which material properties are unaffected by strain rate
F_t	=	Tangential Force
$VT^n = C$	=	Taylor Tool Life Equation
TiC	=	Titanium Carbide
TiN	=	Titanium Nitride
Hv	=	Vickers Hardness (Pascals)
μ	=	coefficient of friction

ALE	=	Arbitrary-Lagrangian Eulerian
A_r	=	real area of contact
C	=	constant in Taylor tool life equation (Eq 2.3)
C	=	The Capacitance
E	=	Young's Modulus of elasticity
f	=	feed in mm/rev
F_C and N_C	=	Force: along and perpendicular to the tool face,
F_c	=	cutting force component parallel to tool face
F_f	=	feed force
F_p	=	cutting force component in power direction (i.e., parallel to V)
F_P and F_Q	=	Force: in the horizontal and vertical direction,
F_R	=	cutting force component perpendicular to F_p and F_Q
F_S and N_S	=	Force: along and perpendicular to the shear plane,
F_S	=	cutting force component parallel to shear plane
Ft	=	Tangential force
Fw	=	total force (in uniformly distributed load)
G-Code	=	Computer Language of Preparatory Command in CNC programming
I	=	Current (EDM Process)
KB	=	Crater width
KF	=	Crater Front distance
KM	=	Crater centre distant
KT	=	Crater Depth
M	=	the machining rate or volume removed per second in EDM,
n	=	revolutions per minute –in machining processes
R	=	Charging Resistance in EDM process
RƐ	=	Tool Nose Corner Radius
S	=	Mean spacing of adjacent local profile peaks
SEM	=	Scanning Electron Microscopy
S_m	=	Mean spacing of profile peaks at the mean line
Ʈ	=	the friction shear stress which is dependent on the contact pressure
t_2/t_1	=	chip thickness ratio
t_c	=	the chip thickness

Ti	=	Titanium
TiAlN	=	Titanium Aluminium Nitride
TiC	=	Titanium Carbide
TiCl	=	Titanium Chloride
TiN	=	Titanium Nitride
TiO_2	=	Titanium Oxide (Minerals Rutile)
Ton	=	Time on (EDM Process)
t_p	=	Bearing Ratio
V	=	cutting speed
v	=	Poisson's ratio
VB	=	average flank wear
VB_{max}	=	maximum depth of flank wear
V_c	=	chip sliding speed
V_d	=	the discharge voltage
W	=	Waviness
W_a	=	Waviness Average
W_c	=	Tungsten Carbide Tool
α	=	Rake angle
δ	=	linear deformation extent of secondary shear zone (Fig)
ε	=	true (ln) strain
$\dot{\varepsilon}^p$	=	the effective plastic strain rate,
η	=	angle between tool face and plane of maximum shear stress (Fig.)
η_p	=	the inelastic heat fraction,
θ	=	temperature
λ	=	chip compression ratio (reciprocal of cutting ratio = l/r)
λc	=	cut off length in surface roughness measurements
ρ	=	radius of curvature of tool tip
σ	=	flow stress
σ_{eff}	=	the effective stress,
σ_n	=	the normal stress
σ_y	=	initial yield stress
τ_s	=	shear yield stress

Υ =   shear strain

Φ =   shear angle

ϕ =   shear plain angle

Acknowledgments

Dedicated to my family

Declaration

I hereby declare that the data/ information recorded in this Thesis was compiled by me for the award of Doctor of Philosophy Degree of the University of East London. I did all Laboratory Experiments, data collection and analysis of results. No part of this Thesis was directly copied from any other work(s) done by somebody else other than citations, which have been referenced. As such, no one has any claims over these materials. No part of this Thesis should be copied for profit making without my expressed consent or published without recognition of my effort.

Titus Bitek Watmon

(**Moto:** For God & My Country)

Chapter 1

Introduction

Performance Characteristics of a Surface-Modified Cutting Tool

This research focuses on the performance characteristics of a surface-modified carbide cutting tool insert. After surface modification by electrical discharge machining (EDM) to generate crater-like surface topography, the insert was coated with Titanium Nitride (TiN) by physical vapour deposition (PVD) method. Comparative cutting tests were carried out using conventional tools coated with TiN as control specimens, and the test specimens were TiN-coated EDMed tools having crater-like surface topography.

1.0   Metal Machining and Man

Metal cutting is central to the modern age, and it was that belief that prompted Juneja to argue that 'wherever metal is used in any manmade object, one can be sure that it must have reached its final stage through processing with machine tools' (Juneja and Sekhon, 1987). Today, most machine tools are computer numerical controlled (CNC). Integrating computers into modern machines has enabled us to produce components that are much better than before, though there is still a need to improve metal cutting efficiency in terms of machinery and cutting tools. The search for efficiency and high productivity has led to the continual research on metal cutting dynamics to enhance cutting tool performance. Consequently, tool coatings with harder substances that can improve tool life have been introduced. At the beginning of coating technology in the 1970s the idea was mainly focussed on high hardness to reduce wear, but as time passed machinists realised the need to have coated tools which give low friction and cutting forces at the chip–tool and tool–work interfaces. Generally, reduced friction leads to less tool wear, lower cutting forces and reduced temperatures, which in turn leads to the improved dimensional accuracy and surface quality of the products being made. Consequently, many different designs of tools are now commercially available in an

attempt to achieve better metal cutting processes.

Dr. M. E. Merchant developed the first scientifically based model in 1945 of orthogonal metal cutting process. Merchant (1945) published paper offered a solution on how to reduce the shear plane angle, and he assumed that the shear flow stress in metal cutting was equal to that obtained from conventional tests. Oxley (1989), on the other hand, came up with a semi-empirical approach.

1.1.0   Motivation for this Work

This research sets out to explain why a TiN-coated metal cutting tool with undulating surface structure has an enhanced performance. Sue and Troue (1990) stated that TiN and TiAlN PVD coatings could reduce friction in tribological contact and increase abrasive wear resistance if the fusion between the substrates and the coatings are firm. Schulz *et al*. (2003) stated that 'cutting edges of cemented carbide tools coated with TiC, TiN or (Ti, Al)N by chemical vapour deposition (CVD) and/or by physical vapour deposition (PVD) processes can show an increase of the service lifetime of tools by a factor of ten compared to uncoated tools' for metal cutting.

The motivation for this work was a result of papers presented by many researchers, (Schulz *et al.*, 2003; Dechjarern, 2002; Fouvry and Kapsa, 2001; Prengel et al., 2001; Jaspers *et al.*, 1998; Bromark, Hedenqvist and Hogmarak, 1995) which explained that coating of cutting tools often yielded decreased wear rates and reduced coefficients of friction. Although different theories are proposed in the literature, covering areas such as hardness theory, diffusion barrier theory, thermal barrier theory, and reduced friction theory, most discussed the coating of plain tool substrates with hard materials such as TiN, Titanium Carbide (TiC) and Aluminium Oxide (Al_2O_3) and the coating's ability to transform the performance of cutting tools. This work looks into the coating of tool inserts with a crater-like (undulating) surface topography with TiN by a PVD process. The crater-like surfaces were created by the EDM method.

The successful application of coating the fine-grained tungsten carbide 6% cobalt substrate with TiN provided excellent toughness and deformation resistance to wear and the PVD coating allows metal cutting speeds to be nearly double the recommended speeds for conventional tool insert of that grade. A variety of engineering coating applications, particularly through the use of hard coating materials such as TiN, TiC, and Titanium

Aluminium Nitride (TiAl)N, to reduce the wear of engineering components in many tribological situations, have stimulated much research work (Arsecularanatne, Zhang and Montross, 2006; Schulz *et al.*,2003; Stoiber *et al.*, 2002; Trent, 1991; Ezugwu, 2001). Stoiber *et al.* (2002) mentioned that today, 'TiN coatings, according to their high hardness, corrosion and wear resistance, are widely used in industrial applications ranging from machining tools to decorative items'. The use of hard coatings has greatly improved the tribological performance of tool and machine elements. In fact, various hard coatings have been widely used to improve the performance and extend the life of cutting tools, dies and moulds (Holleck, 1986; Loffier, 1994). Among these hard coatings, TiN has been successfully used and extensively studied as a protective coating material (Kim. *et al.*, 2003) because of its excellent properties; for instance its high melting point, high hardness and high thermal conductivity.

PVD hard coatings are well-known for providing surfaces with enhanced tribological properties in terms of friction and high wear resistance (Batista *et al.*, 2002) by enhancing machining capability, increasing productivity and generating acceptable surface finishes with moderate power consumption during machining operations. 'When properly applied, PVD coating can extend tool life by up to three times comparative to uncoated tools' (Trent, 1991, cited in Ezugwu, 2001). However Ezugwu (2001) argues that in engineering applications, 'it is necessary to use a sufficiently strong substrate and deposit a coherent, stress-free, defect-free and sufficiently thick TiN coating in order to increase the load bearing capacity, reduce substrate plastic deformation and suppress adhesive failure of the coating/substrate system'.

Tool wear has been a recurrent problem in the metal machining industry and adversely affects the surface finish of the workpiece. A good surface finish has a great influence on the worth of products and satisfaction level of consumers. The causes of tool wear and surface defects that put complex limitations on tool life and the surface finish of products have been the subject of a large number of investigations

Given the above statements, various hard coatings have been widely used to improve the performance and to extend the life of cutting tools, dies and moulds, as mentioned by both Loffier (1994) and Holleck (1986). This research focussed on coating of crater-like surface topography of Electrical Discharge Machined (EDMed) surfaces of modified turning tool inserts. The coating material applied in this case is TiN, though it could have been any other

coating material such as Al_2O_3 or Titanium Chloride ($TiCl_3$) which is readily available on the market today.

1.1.2 Background to the Study

This project aims to further the work of a previous research programme that was based at Imperial College London (Dechjarern, 2002). Before this project started a 'proof of concept' experiments were done at UEL in 2006 which established that there is an operating windows of surface roughness which supports the modified surface structure theory. Figure 1.1 presents a graphical comparison of the rake faces of an EDM-coated tool and a plain-coated tool after 15 minutes of intermittent cutting.
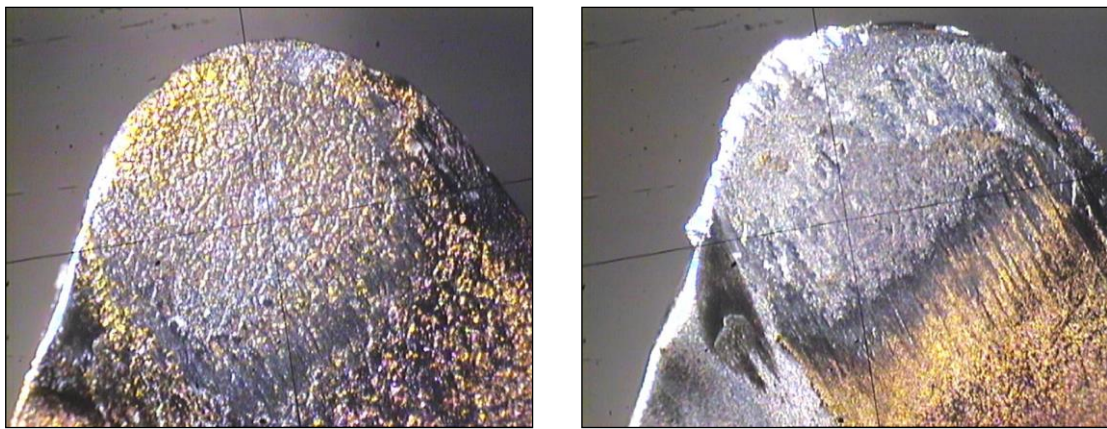
Figure 1.1: Rake Faces After a Cutting Test:
EDM-Modified Tool (left), Plain TiN-Coated Tool (right)

According to Dechjarern, 'if the surface is smooth or too rough it would not work even if coated'. Dechjarern (2002) recommended surface roughness (R_a) values of between 1.4 – 1.8 micrometres as the operating window. This research proposes an extensive study by cutting tests experiments, field tests and computer simulation to substantiate the experimentally observed results on the 'operating window' hypothesis.

A subsequent MBA project at Imperial College identified the need to evaluate the enhanced performance of the EDMed tool in terms of '*increased productivity*' rather than '*tool cost*' (Watson *et al*., 2005). In other words, the information that was needed was to establish how much faster an EDMed tool can cut compared to a plain tool. The MBA project recognised that the increased productivity aspect would be of more interest to industry than that of reduced tool wear. This is because tool wear is associated with tool cost and tool change time, which normally amounts to less than 3% of the total machining cost in a production environment. From the literature, it is not clear whether Watson *et al*. (2005) considered the cost of downtime during tool changeover. The most important mechanisms by which a

4

coating can protect a substrate material are the following, though not exclusively limited to these areas:

a) The wear resistance of the coating itself should be superior to that of the substrate.

b) The coating lowers the friction coefficient and thereby the contact temperature. A decrease in friction also reduces the propensity for severe adhesive wear.

c) The coating acts as a heat barrier owing to the lower thermal conductivity compared with that of the substrate. Thus, the proportion of frictional heat which dissipates into the substrate is reduced which, in turn, lowers the substrate temperature.

d) The coating has lubricating properties because it can generate secondary layers thereby reducing real contact area in the wear surface.

e) Elements of the coating material can diffuse into the substrate and thereby increase its wear resistance long after the original coating–substrate interface has been penetrated.

This work focuses on experimental work and the computer numerical simulation of the cutting process to gain a fundamental understanding of the wear characteristics and the mechanism of enhanced wear resistance of EDM modified surfaces under common cutting process loading conditions.

Tool life is the most important practical consideration in the selection of cutting tools and cutting conditions. Tools which wear out or fail slowly have comparatively long service lives, resulting in reduced production costs and more consistent dimensional and surface finish capabilities. That explains why tool life is the most common criterion used to rate cutting tool performance and the machinability of materials. This project will focus on tool performance higher speed of cutting.

1.1.3   Objectives and Scope of the Study

The project is divided into the EDM machining of tool Inserts, and the coating of the EDMed surface with TiN physical vapour deposition (PVD) technique. Secondly, the research aims to characterise a novel surface topography with the substrates coating combination. Available literatures show that cutting edges of cemented carbide tools coated with TiC, TiN or (Ti, Al)N by chemical vapour deposition (CVD) and or by physical vapour deposition (PVD) processes exhibit an increase in the service lifetime of tools by a factor of ten compared to uncoated tools (Schulz *et al*, 2003, Dobrzanski *et al*, 2004, Batista *et al*, 2002 and Li *et al* 2001).   Further work has indicated a 60% increase in tool life (Dechjarern, 2002 and

Hedenqvist *et al,* 1990). The present work investigated how much faster the tool is able to cut, in addition to carrying out field tests that subjected the tool to real world operating conditions. A further aspect of the work developed a theoretical model that substantiated the experimentally observed results. This research investigated tool wear at the tool and work interface during orthogonal metal cutting. The specific objective of this study is to study the performance characteristics of a surface-modified cutting tool coated with titanium nitride and the inherent properties of the TiN coating substance,

1.1.4 Gap in Knowledge

Since the knowledge of tool coating first became known in the 1980s, tool engineers, materials scientists and other interested parties have been doing research on the benefits of tool coating technology. The gaps in knowledge that remain are:

i. Analysis of available criteria of tool life and tool wear assessment still indicates that the current methods of assessment are subjective and do not correlate with the tribology of metal cutting. They do not account for the cutting regime and thus do not reflect the real amount of the work material removed by the tool during the time over which the measured flank wear is achieved.

ii. The nature of tool wear is not yet clear enough in spite of numerous investigations carried out over the last fifty years. Although various theories have been introduced before to explain the wear mechanism, the complexity of the processes in the cutting zone hampers formulations of a sound theory of cutting tool wear. As a result, there is no universally agreed tool wear formula, which accounts for the work and tool materials.

iii. Knowledge on metal cutting tool life verses tool wear in relation to work material type is a phenomenon not yet well understood.

- this is the area that motivated this study. This research will look into tool wear characteristics of Titanium Nitride (TiN) coated inserts having crater-like surface topography. The cutting speed will be much higher than ever tried before. The work materials will be mild steel grade EN-3 and stainless steel grade 314 and 316.

All past research work on tool coatings used inserts with chip breakers (Wallén and Hogmark, 1989, Hedenqvist, et al 1990, Dobrzanski et al 2004, Hermann, A. J, M., 2000, Batista et al, 2002, MacGinley and Monaghan, 2001, Feinberg, B., 1971, Horlin, N., A., 1971, Suh, and Sanghvi, B.J., 1971) but without crater-like surface topographies. However, in this work, inserts with crater-like surface topographies have been coated for testing. The work focuses

on the complex interrelationship that encompasses the thermal barrier function, and the relatively low sliding friction coefficient of TiN and mild steel. It is therefore, hypothesised that the TiN coatings (materials) will get entrapped in the valleys, and peaks, which may retain the coating longer thereby improving the resistance to wear.

However, it will not be possible to quantify the wear because there are still no universal wear equations due to the complexity of the wear process, which depends on the materials, contact conditions and environmental parameters in a number of different combinations.

1.1.5   Structure of the Thesis

Chapter 1, introduces the motivation and background that generated the enthusiasm to do this research, and introduces the concept of cutting tool modification and modern coating techniques with hard substances, which enhances the tribological properties in terms of the low friction, and high wear resistance of Titanium. Available literatures indicate that Titanium is the ninth most abundant element and the fourth most abundant metal in the earth's crust (Kraft, 2003).

This chapter continues to provide a literature review of various scholars and researchers, which provided the background to this research. The analysis of information and data of published works provide the rationale for the experimental work in this project. It covers literature reviews on EDM processes and the tribology of rough surfaces in sliding friction. A detailed description of surface engineering such as surface treatment, coating by PVD, and surface modification are also discussed.

This chapter also looks at the comprehensive analysis of the effect of coated EDMed surface roughness on the contact point between the tool and the workpiece interface, including the properties and effects of TiN coating technology.

Chapter 2 discusses the tool preparation before coating the surface with TiN and the experimental approach that followed. A detailed study of EDM surface characteristics is described and the general procedures for the cutting tests and investigation into progressive tool wear.

Chapter 3 concentrates on the study of the tool surface modification process using the EDM method, the tool surface treatment and continues to investigate the influence of modified surface and the coating material (TiN). The chapter goes on to examine tool life

requirements and attempts to understand the ways in which metal cutting tools fail. Broadly, tool failure may result from wear, plastic deformation, or fracture (chipping). Tool wear can be categorically classified by the area of the tool affected or by the physical mechanisms which produce it. The EDM process left a matt surface finish on the inserts, which was covered in small craters of a diameter-to-depth ratio of about 5 to 50 μm. The formation of these craters (valleys) is mainly a consequence of the discharge action. The degree of surface roughness depends on the size of the craters, as a result of energy per discharge during cutting.
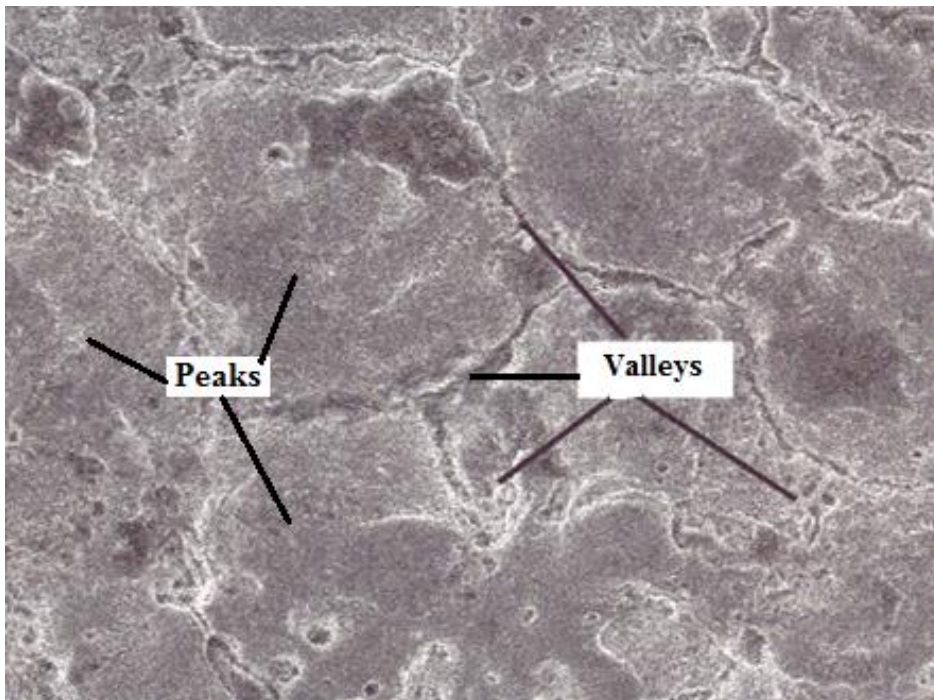
Figure 1.2: SEM image of an EDMed surface showing matt surface with valleys and peaks

Chapter 4 discusses the cutting test experiments and the enhanced tool wear characteristics of the modified surface structures. Since the primary goal of this research has been to develop a method for enhancing the performance of a coating tool with novel surface structures for improved production and tool life, from a consideration of tool failure mechanisms. It therefore, gives a detailed account of the experimental procedures, including the cutting processes and parameters. It goes on to discuss about sliding contact conditions between materials, which generate frictional heat in the contact zone. The heat can induce significant changes in wear rates and mechanisms in either one or both components (materials). It ends by pointing out that a key factor in the wear rate of virtually all tool materials is the temperature reached during machining operation.

Chapter 5 begins with a literature review of current finite element modelling of metal cutting, and the general approaches that need to be understood in computer modelling and simulations. The effects of surface roughness on the cutting performance of TiN-coated tools is discussed, as well as how the numerical modelling of the cutting process will be carried out to investigate the effect of the crater-like surface topography on the performance of the tool. In-depth consideration of sliding friction conditions at the chip–tool and work–tool interfaces could possibly lead to a contribution to knowledge.

Chapter 6 discusses the final experimental and simulation results, which show that the EDMed TiN-coated tool inserts have properties that are resistive to wear during machining, and this phenomenon leads to a contribution to knowledge.

Chapter 7 summarises the research findings and gives detailed conclusions, with recommendations for the implementation and possible future work in the study of the performance of a surface-modified cutting tool.

1.1.6   Contribution to Knowledge

Tools used under the same conditions for different operations may have quite different usable lives, depending on a number of things, such as workpiece material, coolant used, feed rates selected, cutting speeds and critical tolerances or requirements. For that reason, the methods for predicting tool life are primarily only useful for comparative purposes. For example, when ranking expected levels of tool life for different work materials, tool materials, or cutting conditions, they cannot logically be expected to yield an accurate estimate of tool life for a given application unless prior application of data for similar parts are available. Based on these statements, this study contribution to knowledge orientates on the establishment of the fact that in the coating process the TiN particles fills up the valleys following the crater-like profile of the EDMed modified tools; thereby increasing the surface area of the coatings and as a result the TiN pockets in the valleys continue to provide wear resistance to friction. Thus, the summarised contributions to knowledge in this study;

a. relates to a wear-resisting surface structure for application in contact surfaces and structures in metal cutting and forming tools with ability to give wear-resisting surface profile.

b. provide knowledge for increased tool life through wear resistance, hardness and chemical stability at high temperatures because of reduced friction at the tool-chip and work-tool interfaces, which leads to reduced heat generation at the cutting zones.

9

c. provides technique for designing tool with roughened surface comprising of peaks and valleys covered in conformal coating with a material such as TiN, TiC etc which is a wear-resisting structure with surface roughness profile compose of valleys which entrap residual coating material during wear thereby enabling the entrapped coating material to give improved wear resistance.

Undulating surface topographies on cutting tips tend to hold coating materials longer in the valleys, thus giving enhanced protection to the tool and the tool can cut faster by 40% and last 60% longer than conventional tools on the markets today.

1.2.0 Literature Review

The overall background of this project including discussion on tool wear and the friction mechanisms of coated cutting tool are presented in the section below.

1.2.1 Tool Wear

Tool wear in machining is the gradual failure of cutting tools because of their usage, which involves loss of particles or material at the contact point between the tool and the workpiece. The contact between tool and workpiece generates heat, which culminates in the gradual failure of cutting tools after regular operation. Tool wear or failure is a term associated with tipped tools, tool bits, or drill bits that are used with machine tools, and is described by wear rate (volume loss per unit area per unit time). Tool wear is dependent on the temperature, cutting velocity and stresses due to friction generated at the tool–chip and tool–work contact interfaces. The rate at which cutting tools wear out depends on:

i.   maximum temperature reached,

ii. tool and workpiece materials,

iii. tool shape,

iv. cutting fluids,

v.   machine tool characteristics,

vi. process parameters (such as cutting speed, feed rate, depth of cut, coolant use and coefficient of friction).

1.2.2 Crater and Flank Wear

There are two main types of tool wear during turning operations on a lathe; these are *flank wear* and *crater wear.*

    a) *flank wear* is when a portion of the relief face erodes the already machined workpiece surface. Flank wear occurs on the relief face of the tool and the side relief angle and is generally attributed to the rubbing of the tool along the machined surface, thus causing adhesive and or abrasive wear, which in turn generates high temperatures. This affects tool-material properties as well as the work surface and tool life.

    b) *crater wear* is where the contact between the tool and chips erodes the *rake face.* Crater wear can occur when the spindle speed is too low or if the feed rate is too high. In orthogonal cutting this type of wear typically occurs at locations where the tool temperature is the highest, and it occurs approximately at a height or distance equalling the depth of cut.

1.2.3 Wear Equation

The mechanics of wear is a very complex process to analyse because it depends on the material contact conditions and environmental parameters in a number of different combinations, thus it has not been possible to formulate a universally accepted equation for wear (Holmberg and Mathews, 2009). Holmberg and Mathews point out that many authors developed wear equations for different wear modes, but all of them are quite limited in their range of validity.

Archard (1953) both observed that 'the worn out volume is directly proportional to the normal load and the distance of movement and is inversely proportional to the hardness of the material'. They the formulated and presented the wear relationship as

$$V = K^{'} \cdot \frac{w \cdot s}{H} \qquad\qquad \text{Equation 1.1}$$

Where V is the worn volume, w is the normal load, s is the distance moved, H is the hardness and $K^{'}$ is a constant, frequently called the coefficient of wear. This relationship is not a universal wear equation because there are several examples of tribological contact where it is invalid. Meanwhile, Holm and Archard's wear relationship is often used for formulating the wear rate (also called specific wear rate) which is a practical and more general value for wear. Thus, their wear equation is (Holm, 1946; Archard, 1953)

$$K = \frac{V}{w \cdot s}$$ Equation 1.2

Which is normally given with dimensions (10^{-6} mm^3/Nm). It is not an ideal way of expressing wear but it has general support from researchers. There is clear physical argument for using the wear rate as defined above because it is the worn volume divided by the mechanical energy input into the contact energy (Holmberg and Mathews, 2009). The contact energy input can be described as the product of the normal load, the velocity and the applied time, which again is the same as the product of load and distance. Holmberg and Mathews (2009) continued by stating that this way of expressing wear should be taken into practice as widely as possible, to make it possible to compare and utilise wear data produced under different contact conditions.

1.2.4 Tool Life Equation

Tool life T is the cutting time at the end of which a given tool may be said to be unusable based on a selected tool failure criterion. A tool life equation is an empirical relationship between the tool life and one or more variables of the cutting process, such as cutting speed, feed rate and depth of cut. In 1907, Taylor published the following empirical formula for calculating cutting speed:

$$VT^n = C$$ Equation 1.3

Where V is the cutting speed, T is the time (in minutes) that it takes to develop a certain flank wear-land and n is an exponent that depends on the tool and workpiece materials and cutting conditions, and is a constant. Note that C is the cutting speed at $T = 1$ *(a one minute tool life)*. Thus, each combination of workpiece and tool material and each cutting condition has its own n and C values, both of which are determined experimentally. Cutting speed is the most significant process variables in tool life; however, depth of cut (d) and feed rate (f) are also important. The equation (1.3) can be written as shown in equation 1.4, and represented graphically in a log-log graph.

Log V + n log T = log C Equation 1.4

or Log T = (1/n) log C − (1/n) log V Equation 1.5
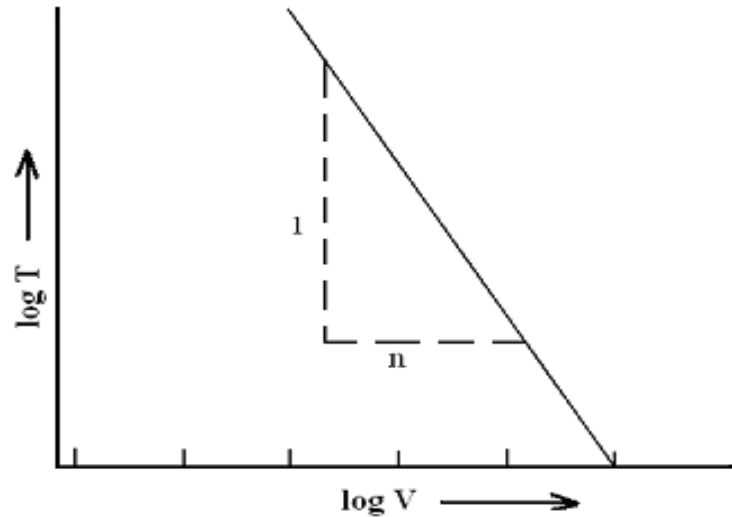
Figure 1.3: Taylor's Tool Life Plot on Log-Log Scale

On a log-log graph, therefore, the Taylor's tool life equation represents a straight line, as shown in Figure 1.3, above which the exponents n, n_1, n_2… and constants C_1 depend upon tool and work materials, tool geometry and type of coolant used. The type of coolant is important as its correct usage is important in enhancing the performance of cutting tools. Thus, Taylor equation (1.3) can be modified as follows:

$$VT^n d^x f^y \quad = \quad C \qquad\qquad \text{Equation 1.6}$$

Where d is the depth of cut and f is the feed rate (mm/rev) in a turning operation. The exponents x and y must be determined experimentally for each cutting condition. Taking $n = 0.15$, $x = 0.15$ and $y = 0.6$ as typical values encountered in practice, we see that cutting speed, feed rate, and depth of cut are of decreasing order of importance. Equation 1.4 above can be rewritten as

$$T \quad = \quad C^{1/n} V^{1/n} d^{-x/n} f^{y/n} \qquad\qquad \text{Equation 1.7}$$
$$\text{Or} \quad T \quad = \quad C^7 V^7 d^1 f^4 \qquad\qquad \text{Equation 1.8}$$

For a constant tool life, the following observation can be made:

- If the feed rate or depth of cut is increased, the cutting speed must be decreased, and vice versa,

- Depending on the exponents, a reduction in speed can result in an increase in the volume of the material removed because of the increased feed rate and/or depth of cut.

13

1.2.5 Feedrates and other Factors that Influence Tool Wear

Many researchers on metal cutting look at metal cutting speed as the main factor that influences tool wear as well as tool life. Yet there are other parameters and characteristics of cutting processes, which are ignored because of contradicting results presented by different authors on the influence of cutting feed, depth of cut, and workpiece properties. However, the geometry of the cutting tool affects tool life as this geometry defines the magnitude and direction of the cutting force and its components.

When the machining process is carried out at high speed there is bound to be high contact temperatures at the tool–chip and tool–workpiece interfaces, which leads to softening of the tool material. The softening effects therefore promotes diffusion and chemical (oxidation) wear, and high contact pressures at these interfaces and the tool flank sliding over the freshly machined surfaces of the workpiece promotes abrasive and adhesion wear (Olson, Stridh and Söderberg, 1988; also cited by Astakhov, 2006).

Cutting tool wear is a product of differing physical, chemical, and thermo-mechanical occurrences. Various theories have already been introduced to explain the wear mechanism, but the complexity of the processes in the cutting zone hinders the formulation of a sound theory of cutting tool wear due to the mechanisms of wear, especially by adhesion, abrasion, diffusion and oxidation, which occur instantly. Thus, the identification of the dominant mechanism is far from simple, and most interpretations are subject to controversy (Schey, 1983).

These interpretations are highly general and are based on the evaluation of the cutting conditions, possible temperature and contact stress levels, relative velocities, and many other process parameters and factors (Astakhov, 2006; Childs *et al*., 2000; Gordon, 1967; Jawahir and Van Luttervelt, 1993; Loladze, 1958; Van Luttervelt *et al*., 1998; Olson, Stridh and Söderberg, 1988; Schey, 1983; Stephenson and Agapiou 1996; Trent and Wright, 2000; Usui and Shirakashi, 1982; Shuster, 1988). Makarow (1976) used the tool–work thermocouple to prove that cutting temperature is the main factor at the tool–chip and tool–workpiece interfaces. So far temperature is the most suitable parameter to relate the tribological conditions with tool wear. Makarow (1976) analysed a numerous experimental data, and formulated the law which was presented as the first metal cutting law (Astakhov, 2004; Makarow, 1976). Astakhov (2004) argued that 'the pure geometrical characteristics of tool wear as the depth of the crater KT and relief face or flank wear-land VB are unsuitable for

14

proper wear characterization', because they do not account for the tool geometry (the flank angle, rake angle, cutting edge angle, etc.) so they are not suitable for comparing the wear parameters of cutting tools with different geometries. Astakhov (2004) goes on to say

> .….they do not account for the cutting regime (the cutting speed and feed(s)) and, thus, they do not reflect the real amount of the work material removed by the tool during the tool operating time, which is defined as the time needed to achieve the chosen tool life criterion (KT or VB).

Marinov (1996) introduced an approach formula to objectively evaluate tool wear and surface wear rate as radial wear per 1,000 sm^2 of the machined area (S) as follows:

$$h_s = \frac{dh_r}{ds} = \frac{(h_r - h_r - i)100}{(l - l_i)f} (\mu m / 10^3 sm^2)$$ Equation 1.9

(Marinov, 1996)

Where h_{r-i} and l_i are the initial radial wear and the initial length of the tool path, respectively, and l is the total length of the tool path. This equation proves that the surface wear rate is inversely proportional to the overall machined area, and it does not depend on the selected wear criterion (as cited in Astakhov, 1998).

The metal cutting process involves many different parameters, particularly cutting speed, cutting feed (feed rate), and depth of cut, and these parameters affect the tool life (Zorev, 1966). The uncut chip thickness or the cutting feed has a direct influence on the quality, productivity, and efficiency of machining. It is believed that the tool life decreases (and thus tool wear increases) with increasing cutting feed (Childs *et al*., 2000; Gorczyca, 1987; Zorev, 1966). This hypothesis comes from the generally adopted equation for tool life. For example, generalising the experimental data, Gorczyca (1987) proposed this equation:

$$T = \frac{48.36 x 10^6}{v^4 f^{1.6} d_w^{0.42}}$$ Equation 1.10

If the cutting speed (*v)* and the depth of cut (*d_{w)}* are both constant, then it follows from the above equation that tool life decreases when cutting feed (*f)* is increased.

Incidentally, Taylor (1907) in his discussion *on the art of metal cutting* did not include cutting feed in his tool life equations because he did not consider this parameter as having a significant influence on tool life. Other researchers found that the experimentally obtained relation 'tool wear−cutting feed' has a distinctive minimum. Such a great variation in the

experimental results can be explained by the fact that the cutting tests were carried out under variable cutting speeds, which resulted in different cutting temperatures (Astakhov,2006).

In fact, the effect of cutting feed (the uncut chip thickness) on the surface wear rate (Astakhov, 2004) is of prime interest when maintaining the area of the machined surface constant (or the volume of the removed work material) in contrast to the length of the cutting path, because the area of the machined surface (or the volume of the removed work material) does not change with the cutting feed, while the length of the tool path does. This follows that if the cutting feed (f) is increased but the cutting speed (v) is kept constant, the given length of the tool path decreases, thereby the cutting time decreases as well as the corresponding tool wear.

1.2.6 Laws of Friction

In 1699, Amontons published his rediscovery of the laws of friction first put forward by Leonardo da Vinci. Though they were received with some misgivings, the laws were verified by Charles-Augustin de Coulomb in 1781.

The three laws of friction published by Amontons (taken from Shaw, 2005) state that:

  i. The force of friction is directly proportional to the applied load (Amontons 1st Law)

  ii. The force of friction is independent of the apparent area of contact (Amontons 2nd Law)

  iii. Kinetic friction is independent of the sliding velocity (Coulomb's Law).

These three laws only apply to dry friction, in which the addition of a lubricant significantly modifies the tribological properties. A tribological property of the cutting tool is also affected by cutting speed, as the speed increases during machining the tool life is rapidly reduced (Jacobson, Wallén and Hogmark, 1987). On the other hand, if cutting speeds are low, tool life is long, but the rate at which material is removed is also low.

1.2.7 Machinability and Composition of Steel Materials

Carbon presence in steel workpiece materials greatly affects its machinability. High-carbon steels are difficult to machine because they are tough and because they may contain carbides that abrade the cutting tool, while low-carbon steels are troublesome because they are too soft or '*gummy*' and stick to the cutting tool, resulting in a built-up edge that shortens the tool life (Madhaven *et al.*, 1988). Therefore, the steel that has the best machinability is one with medium amounts of carbon, about 0.30 – 0.59%. Steel manufacturers usually add chromium, molybdenum and other alloying metals as a means to improve steel strength. However, most

of these metals also decrease machinability. Inclusions of oxides in steel may abrade the cutting tool, thus machineable steel should be free of oxides.

There are varieties of additives that can be added to steel to make the alloy easier to machine, these can be both metal and non-metal. Such additives may work by:

- lubricating the tool–chip interface,
- decreasing the shear strength of the material, or
- increasing the brittleness of the chip.

Sulphur (S) and lead (Pb) have been the most common additives, but bismuth (Bi) and tin (Sn) are increasingly popular for environmental reasons. Lead (Pb) acts as an internal lubricant in the cutting zone but has poor shear strength, thus it allows the chip to slide more freely past the cutting edge. When it is added in small quantities to steel, it can greatly improve machinability while not significantly affecting the steels strength. Sulphur (S) improves the machinability of steel by forming low shear strength inclusions in the cutting zone. These inclusions are stress risers that weaken the steel, allowing it to deform more easily. Mild steel EN-3 is easier to machine because of the addition of sulphur (0.6%) and phosphorus (0.06%). Kalpakjian and Schmidt (2002) stated that stainless steels have poor machinability compared to regular carbon steels because they are tougher, gummier and tend to work harden very rapidly. Kalpakjian continues to say that slightly hardening the steel may decrease its gumminess and make it easier to cut. On the other hand, aluminium (Al) is much softer than steel, and techniques to improve its machinability usually rely on making it more brittle. Aluminium alloy grades 2007, 2011 and 6020 have good machinability.

There are many factors affecting machinability, but there is no widely accepted way to quantify it. Instead, machinability is often assessed on a case-by-case basis, and tests are tailored to the needs of a specific manufacturing facility. Materials with good machinability require little power to cut, and can be cut quickly to obtain a good surface finish. Common metrics to measure machinability for comparison include:

    i.   tool life,

   ii.   surface finish,

  iii.   cutting temperature, and

  iv.   power consumption.

1.2.8   Shear Zones

The primary shear zone is a rather distinct narrow region in which the workpiece material is bent into the direction of the tool rake face, thus forming a chip (Burns and Davies, 1997). The friction at the tool-chip interface causes plastic deformation in the secondary shear zone, resulting in high temperatures. In the secondary shear zone high friction causes the chip to adhere to the rake face and hence it is called the sticking zone. It is in this zone that most of the deformation takes place. In the subsequent zone the chip will start to slide along the rake face until it leaves the tool, this part is the sliding zone. However, there are features of metal cutting which make the process complex. The complexity lies in the fact that:

> *i.* The chip has an unconstrained free surface, thus the process geometry in cutting is not defined by the tool but merely depends on the workpiece material and the cutting conditions.
>
> *ii.* The frictional conditions at the rake face form a complex system of interactions with the chip. The unconstrained chip geometry is highly influenced by the frictional conditions at the chip–tool interface. In turn the frictional conditions are dependent on the contact length between chip and tool and as a result of the chip geometry.
>
> *iii.* The tool is in contact with new and fresh metal surfaces that are chemically highly active and lead to adhesion and diffusion reactions between chip and tool.

Following on from the above statement, there is evidence that there is a wide range of mechanical and chemical interactions taking place at the cutting zone. Understanding the basics of chip formation involves knowledge of several fields of engineering, including solid state physics, engineering mechanics and plasticity, material behaviour, tribology, basic concepts of chemistry and physics and thermodynamics and heat transfer (Shaw, 1984).

Others, such as Lee and Shaffer (1951) as well as Palmer and Oxley (1989), based their analyses on a thick shear deformation zone, proposing '*shear angle prediction'* models in accordance with the laws of plasticity.

The shear angle is defined as the angle between the direction of the cutting speed (*V*) and the shear plane. It is further assumed that the shear stress (τ_s) and the normal stress (σ_s) on the shear plane are constant; the resultant force (*F*) on the chip, applied at the shear plane, is in equilibrium to the force applied to the tool over the chip–tool contact zone on the rake face, and an average constant friction is assumed over the chip-rake face contact zone (Altinas,

2000). From the force equilibrium, the resultant force (F) is formed from the feed (F_f) and tangential (F_t) cutting forces, which means:

$$F = \sqrt{F_t^2 + F_f^2}$$
Equation 1.11

The feed force (or thrust force) is in the direction of the uncut chip thickness and the tangential cutting force (or power force) is in the direction of cutting velocity. The cutting forces acting on the tool will have equal amplitude but opposite directions with respect to the forces acting on the chip.

1.2.9   General Mechanics of Metal Removal

In orthogonal machining, cutting is assumed to be uniform along the cutting edge, therefore it is a two-dimensional plane strain deformation process. Hence, the cutting forces are only exerted in the directions of velocity and uncut chip thickness, which are called the tangential force (F_t) and feed force (F_f). However, in oblique cutting the cutting edge is orientated with an inclination angle (i), and the additional third force acts in the radial direction (F_r)

Referring to figure 1.4 it can be seen that as the edge of the tool penetrates the workpiece, the material ahead of the tool is sheared over the primary shear zone to form a chip. The sheared material/chip partially deforms and moves along the rake face of the tool, which is called the secondary deformation zone (Altinas, 2000).

The friction area, where the flank of the tool rubs the newly machined surface, is called the tertiary zone. The chip initially sticks to the rake face of the tool, which is called the *sticking region*. The friction stress is approximately equal to the yield shear stress of the material at the sticking zone, where the chip moves over a material stuck to the rake face of the tool. The chip stops sticking and starts sliding over the rake face with a constant sliding friction coefficient (Trent and Wright, 2000). The chip leaves the tool as it begins to lose contact with the rake face of the tool. The length of the contact zone depends on the cutting speed, tool geometry, and material properties.
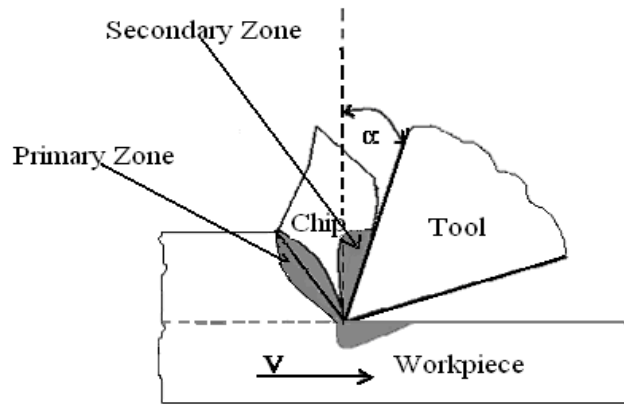
Figure 1.4 Illustration of how Material ahead of the Tool is sheared

There are basically two types of assumption in the analysis of the primary shear zone. This led Merchant to develop an orthogonal cutting model by assuming the shear zone to be a thin plane.

1.2.10   Geometry of Tool Bits and Holders

The geometry of the tool tip plays an important role in tool wear. Single-point cutting tools are non-rotating cutting tools used in lathe machines, shapers and planers. The cutting edge is designed to suit a particular machining operation and may be shaped as needed. Tool holders when in operation hold single point cutting tools in the form of inserts rigidly. Klopstock (1926) was the first to show that the tool life and cutting forces could be favourably altered by restricting the contact length between the chip and tool.

a) **Back and Side Rakes**

The back rake helps control the direction of the chip, which naturally curves into the work due to the difference in length between the outer and inner parts of the cut. It also helps counteract the pressure against the tool from the work by pulling the tool into the work. Side rakes along with back rakes control the chip flow and partly counteract the resistance of the work to the movement of the cutter, and can be optimised to suit the particular material being cut. Brass for example requires a back and side rake of zero degrees, while aluminium uses a back rake of 35 degrees and a side rake of 15 degrees (Astakhov, 1998).

b) **Nose Radius**

The nose radius makes the finish cut smoother as it can overlap the previous cut and eliminate the peaks and valleys that a pointed tool produces. Having a radius also strengthens the tip because a sharp point is quite fragile. All the other angles are for clearance in order that no part of the tool besides the actual cutting edge touches the

20

work. The front clearance angle is usually 8 degrees, while the side clearance angle is 10 –15 degrees and partly depends on the expected rate of feed.

c) Tool Insert Materials

Cemented carbide, also called tungsten-carbide cobalt, is a hard material used in machining tough work materials such as carbon steel or stainless steel. Carbide tools can also withstand higher temperatures than standard HSS tools. Originally all tool bits were made of high carbon tool steels with appropriate hardening and tempering.

1.2.11   Uses of Coolant in Heat Removal

According to Timings (1998) the correct usage of cutting fluids is important in enhancing the performance of cutting tools. To obtain optimum rates of metal removal and maintain optimum tool service life, it is necessary to lubricate and cool the chip–tool interface zone. The following are factors likely to cause excessive heat during a metal cutting operation:

  i. The cutting speed is too high,

  ii. there is friction between the tool and workpiece,

  iii. the tool is worn or is an incorrectly ground cutting tool,

  iv. there is formation of a build-up edge on the cutting face of the tool.

In addition to cooling, cutting fluids aid the cutting process by lubricating the interface between the tool's cutting edge and the chip. Cutting fluids may be made from petroleum distillates, animal fats, plant oils, or other raw ingredients. Depending on which type of cutting fluid is being used, it may be referred to as coolant, cutting fluid, cutting oil, cutting compound, lubricant or compressed air (Timings, 1998). Every kind of machining (e.g. turning, boring, drilling, milling, broaching, grinding, sawing, shaping, reaming, tapping) can benefit from one kind of cutting fluid or another, depending on the workpiece material. Cast iron and brass are often machined dry. Interrupted cuts such as milling with carbide cutters are carried out dry due to damage to the cutters caused by thermal shock. Holmes (1971), in his paper "*Factors affecting the selection of cutting fluids"*, pointed out that the properties of a good cutting fluid are based on its ability to:

  i. keep the workpiece at a stable temperature (critical when working to close tolerances). Very warm is okay, but extremely hot or alternating hot-and-cold should be avoided,

  ii. maximise the life of the cutting tip by lubricating the working edge and reducing tip welding,

iii. ensure safety for the people handling it (toxicity, bacteria, fungi) and for the environment upon disposal,

iv. prevent rust on machine parts and cutters.

1.3.0 Electrical Discharge Machining

Electrical discharge machining (EDM) is one of the most important abrasion-less machining methods for ceramics and carbides. Since EDM does not involve any physical contact between the electrodes and workpiece it can be performed regardless of the hardness and strength of the workpiece materials. However, the thermal action of the EDM process is known to yield a relatively poor surface integrity, including craters, microcracks and unfavourable residual stresses, on the machined components. All EDM surfaces can be regarded as 'possessing a Gaussian height distribution, with a surface skewness between ±1, and a kurtosis of about 2.5 – 3' (Dechjarern, 2002). TiN-coated tungsten carbide and HSS tools are frequently used in metal cutting operations and increasingly replace uncoated inserts, drills and taps. It has been proven by other authors that coatings applied to tool inserts 'considerably improve the tool life performance by suppressing the mechanisms of tool edge wear' (Tecvac Ltd., 2012); Söderberg, Jacobson and Olsson, 1987 also cited in Wallén and Hogmark, 1989). Investigations into the TiN-coating of carbide and HSS tools are numerous. Most of the researchers have quantified the benefits of using 'coated tools in terms of prolonged tool life' (Thornley and Upton, 1987; Soliman, Abu-zeid and Merdan, 1987; Redford, El-Bialy and Mills, 1986; Walker, 1981; Ohishi *et al.*, 1987).

1.3.1 Tribological Characteristics of EDM Process

Puertas and Perez (2003) state that Electrical discharge machining (EDM) is a non-traditional manufacturing process based on removing material from a part by means of a series of repeated electrical discharges (created by electric pulse generators at short intervals) between a tool, called the electrode, and the part being machined in the presence of a dielectric fluid.

The level of generator intensity represents the maximum value of the discharge current intensity. The pulse time is the duration of time that the current is allowed to flow per cycle, and the duty cycle is the percentage of the pulse time relative to the total cycle time. In addition, none of these processes within EDM require force, because the Anode never touches the Cathode. Another factor to consider in the EDM process is the speed of the material removal process, as in most cases it is measured by cubic centimetres per hour. Several factors control the material removal rate. The most important of these is the melting

temperature of the workpiece material. According to Fellers and Hunt (2001), 'erosion rates are not affected by the material hardness but by the melting temperature of the material being machined'; thus the lower the melting temperature of the work material the faster the removal rate.

Figure 1.5 shows an SEM picture of a typical eroded surface obtained with current (I) = 1.5 ampere and T_{on} = 0.2 milliseconds. During each electrical discharge, intense heat is generated, causing local melting or even evaporation of the workpiece material. With each discharge, a crater is formed on the workpiece. It can be seen that valley areas consist of a pool of molten metal, overlapping craters created by EDM and other features include peaks and deep cracking valleys. Aleksandrov and Barash (1970) have also reported this phenomenon. The three dimensional nature of the EDM surface is discussed in detail is in section 2.1.3 in next chapter.
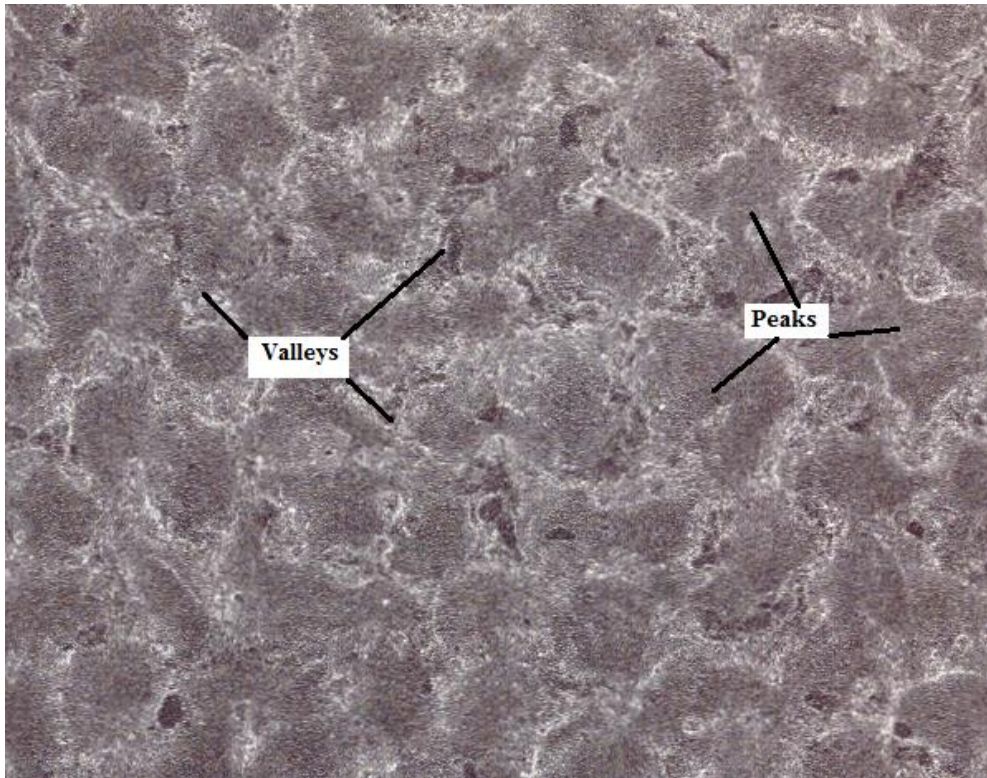
Figure 1.5: SEM image of an EDMed Tool Surface
produced with I =1.5 amp and T_{on} = 0.2 ms, the surface finish (Ra) = 1.46 μm

1.3.2   State of the Art Modified Tool and its Applications

The modified inserts possess crater-like surface topography with deep cracks/ valleys. During the physical, vapour deposition coating process, thin film of the coating materials (TiN) flows over the contour of the surface topography into and out of the valleys covering the peaks and troughs. In this study it was established that the undulating surface topography is only

effective at a narrow window of between 1.4 and 1.8 µm. If the tool surface is smooth or too rough beyond 1.8 µm the novel idea won't work. The coating element, which flows down deep into the valleys, is entrapped behind the peaks. It is the entrapped films, which protects the substrates from excessive heat the tool life.
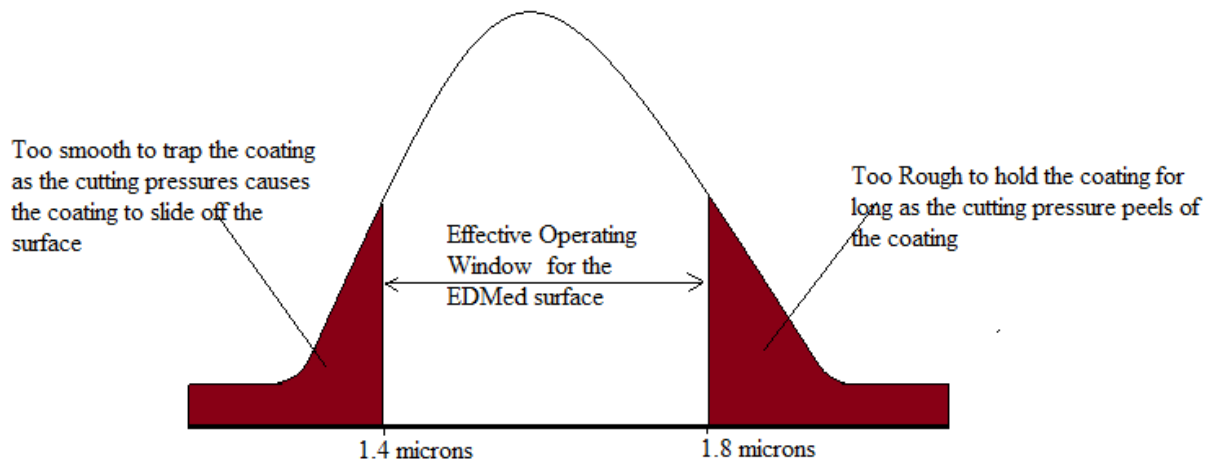
Figure 1.6: Illustration of the Normal Distribution Chart for the operating "Window".

During machining processes, the TiN films entrapped in the valleys behind the peaks continue to offer resistance to wear because of its low coulomb friction coefficient. The coating material could be any other coating materials, for instance; TiCN, which is suitable for interrupted metal cutting and TiAlN is recommended for dry high speed machining. Mostly TiN is good for general-purpose use in metal machining. The performance of the modified tools is discussed exhaustively in chapter three of this report.

1.3.3 Uses of EDM

The EDM process is used in various fields and industries such as medicine, construction, automotive, and aeronautics and space. Puertas and Perez (2003) explain that there are two basic types of EDM

> … die sinking and wire EDM. Die sinking EDM reproduces the shape of the tool used (electrode) in the part being machined, whereas in wire EDM a metal wire (electrode) is used to cut a programmed outline into the piece being machined.

There are different variables when using EDM for ceramic materials, such as 'surface roughness, material removal rate, and electrode wear' (Puertas and Perez, 2003). An advancement of EDM is that it produces high accuracy components from high nickel-based alloys for aircraft engines and land-based wind turbine markets. EDM can be used to make:

a) fixtures,

b) collets and jet engine blade slots,

24

c)   mould cooling ribs, and

d)   reinforcing ribs.

1.3.4   Advantages of EDM

EDM is a method of machining parts that cannot be achieved by conventional machines, and as the tool does not touch the workpiece there are no cutting forces generated, therefore:

a)   very fragile parts can be machined,

b)   the shape and the hardness of the materials being machined do not present a great challenge,

c)   the EDM process leaves no burrs but generates debris (material) which gets flushed away by the dielectric fluid,

d)   EDM can replace many types of contour grinding operation and eliminate secondary operations such as deburring and polishing,

e)   EDM is at an advantage when secondary operations are too labour-intensive for traditional machines,

f)   EDM allows the cutting of complex shapes without distortion.

1.4.0   Titanium

Titanium is the ninth most abundant element in the earth's crust and is primarily found in the minerals rutile (TiO_2), Ilmenite ($FeTiO_3$) and Sphene ($CaTiSiO_5$). Titanium makes up about 0.57% of the earth's crust. The pure elemental metal was not made until 1910 by Mathew A. Hunter, who heated $TiCl_4$ together with sodium in a steel bomb at 700–800 °C. Titanium has a characteristic of hardness, which is difficult to measure, as the coatings are exceptionally hard though the thinness of the coating causes conventional hardness tests to penetrate into the substrate. The hardness of titanium is estimated as ~85 on the Rockwell hardness C scale, which is approximately 2500 Vickers Hardness or 24.5 Gigapascals (Hermann, 2000; also cited by Clapa and Batory, 2007).

1.4.1   Titanium Coatings on Cemented Carbides and Cermets

The wide choice of the coating techniques and types available provides some solutions to the growing need for modern surface modification methods. There is increased interest amongst researchers in coating with TiN, Al_3O, etc. to improve resistance to wear and corrosion. High performances in tool applications – drilling and turning – have been reported for these coatings. In addition to enhanced wear resistance, TiN coatings can also 'provide wear and oxidation resistance, especially at high temperatures' (Dobrzanski *et al.*, 2004; also mentioned in Batista *et al.*, 2002; Cekada *et al.*, 2002; Navinsek *et al.*, 2001). According to Dobrzanski

(2004), depositing the TiN + multiTiNlSiN + TiN coating on cemented carbides and cermet substrates results in a significant increase in the surface layer hardness, in the range of 3200–3520 HV0.07. This gives a hardness increase on the surface layer, compared to the uncoated substrate hardness, of about 40%. Dobrzanski (2004) also states that there is indication of an increase in wear resistance, which exhibits an increase in tool flank life. This means that depositing a coating on the substrate reduces the wear rate of tool flanks.

1.4.2   TiN Physical Properties

In most literature, 'TiN is often considered to play the role of a thermal barrier, protecting the heat-sensitive tool substrate from thermal softening' (Deller, 1982); the aim of this study is to investigate the performance characteristics of the coated EDMed tool to establish how much faster and for how long it can cut before wearing out compared to a plain-coated tool (control specimens). Hedenqvist, Olsson and Söderberg,(1988); Yin-Yu, Da-Yung and Chi-Yung, (2005) all agree with Deller (1982). However, from Table 2.1 it can be seen that the thermal conductivity of TiN differs from that of HSS. A simple temperature distribution analysis was performed by Hedenqvist, Olsson and Söderberg (1988) using FEA for a tool surface temperature of 600 ^{0}C using the data as given in Table 1.1 on the next page.

Table 1.1 Physical Properties of TiN and HSS

Parameters	TiN	High Speed Steel (HSS)
Density (g cm^{-3})	5.2–5.44	8.16–8.26
Melting temperature (^{0}C)	2948 ± 50	1450–1500
Thermal Conductivity (W m^{-1} K^{-1})	24 (400 K) 67.8 (1773 K)	16.8–23.9 (300 K) 25.1–28.5 (773 K)

Source: Hedenqvist *et al,* (1990)
(Paper: How TiN coatings improve the performance of HSS cutting tools, International Journal of Surface and Coating Technology. 41 (1990) pp.243-256)

The results show that the maximum equilibrium temperature of the substrate is reduced by less than 5 ^{0}C by the addition of a TiN coating of 5µm thickness. This clearly demonstrates that TiN acts as a thermal barrier.

1.4.3   TiN and HSS Mechanical Properties

The mechanical properties of TiN and HSS are given in Table 1.2. As can be seen the available data indicates that the Young's modulus of TiN is higher than that of HSS, indicating a stiffer behaviour. As for most ceramics, the Young's modulus of TiN is expected to decrease with increasing temperature. The mismatch in thermal expansion between TiN and HSS is of importance since it will cause thermal stresses, which may influence the performance of the coating.

Table 1.2 Mechanical properties of TiN and HSS at room temperature

Parameters	TiN	HSS
Young's Modulus (GPa)	251 – 616	229 – 237
Thermal expansion (K^{-1})	8×10^{-6}	$8.4 – 10.7 \times 10^{-6}$
Hardness (HV)	2,000 – 2,500	700 – 1,000

Source: Hedenqvist *et al.* (1990)
(Paper: How TiN coatings improve the performance of HSS cutting tools, International Journal of Surface and Coating Technology. 41 (1990) pp.243-256)

For HSS, the room temperature hardness is strongly dependent on the heat treatment. However for cutting tool applications, the hardness at elevated temperatures, i.e. hot hardness, is of greater significance (Holmberg and Mathews, 2009). According to Hedenqvist *et al.* (1990), for HSS there is a continuous moderate decrease in hardness with increasing temperature up to the tempering temperature (approximately 600 ^{0}C). Above this point the decrease is relatively steep.

1.4.4 TiN Chemical Stability

Many tool tests revealed that even when the coating has been partially removed, e.g. by edge wear or by regrinding, a prolonged tool life is still obtained (Hogmark, (1989); Smith *et al.*, (1988); Sundqvist, Sirvio and Kurkien, (1983). To explain this fact Kassman *et al.* (1989) tried to prove the presence of a 'smearing mechanism'. Through an atomistic wear process, TiN material was assumed to be continuously transferred from the coated region of the edge on to the uncoated, thereby modifying the contact conditions and reducing the wear rate.

1.4.5 Benefits of TiN Tool Coating

Pure titanium melts at 1670 ^{o}C and has a density of 4.51 gcm^{-3}. This therefore makes it ideal for use in components, which operate at elevated temperatures, especially in turning operations where large strength-to-weight ratios are, required (Carbide Insert). This can be obtained by fulfilling any or all of the following performance requirements.

1.4.6 Increased Wear Resistance of The Composite Tool

It is important to note that the temperature at the tool and workpiece interface can reach up to 700 ^{0}C. TiN has a very high melting point (2948 ^{0}C) (Birkholz, et al, 2010) and this gives protection to the substrates (tool) during cutting. Thus, the coating acts as a heat barrier to the substrates. The requirement of high wear resistance is usually essential. It is naturally the wear resistance of the substrate tool, rather than the inherent wear resistance of the coating, that is of interest. The tool life limiting wear rate varies between different cutting applications.

1.4.7   Increased Production Rate

According to Söderberg, Jacobson and Olsson (1989) coating metal cutting tools with TiN has great benefits. One such benefit is the increase in the rate of production rather than the total production per cutting edge. That is, the improved properties of the cutting edge are used to increase the cutting speed, the feed, the depth of cut or any combination of these parameters, in order to obtain production at a higher rate rather than to obtain an increased tool life. The capability to cut at much higher speeds has generated more interest in the metal machining industry than reduced tool wear, which is associated with the tool cost and tool change time and which normally amounts to less than 3% of the total machining cost (Rao, Kumar and Shaw, 1978). The ability to increase productivity makes more sense than reduced tool wear, and for unmanned production tools like these are more important.

1.4.8   Improved Cutting Performance

The cutting performance of tools also includes reduced cutting and thrust forces, chip appearance and the resulting surface finish (Shaw, 2005). A reduced cutting force is beneficial, primarily because it demands less motor power of the cutting machine while a reduced thrust force gives lower machine stability.

1.5.0   Finite Element Analysis

The finite elements method employs a number of finite points (nodal points) covering the area of the function to be assessed. The sub-domains within these nodal points are called finite elements. The primary objective of any model is to realistically replicate the important parameters and features of the real model (Hieronimus, 1977). The simplest mechanism to achieve modelling similarity in structural analysis is to utilise pre-existing digital blueprints, design files, CAD models and/or data by importing that into a FEA environment. Once the finite element geometric model has been created, a meshing procedure is used to define and break the model up into small elements. In general, a finite element model is defined by:

    i.   a mesh network which is made up of the geometric arrangement of elements and nodes,

   ii.   nodes representing points at which features such as displacements are calculated,

  iii.   FEA packages use node numbers to serve as an identification tool in viewing solutions in structures such as deflections,

  iv.   elements are bound by sets of nodes, and define the localised mass and stiffness properties of the model,

v. elements are also defined by mesh numbers, which allow reference to be made to corresponding deflections or stresses at specific model locations (Hieronimus, 1977).

Following from above it is clear that the FEM application has many advantages in solving complex engineering challenges/processes, which are not easily understood. The advantages are as follows:

i. nonlinear geometric boundaries can be formulated, especially in chip formations,

ii. the generation of friction in metal cutting can easily model chip flow to identify the sliding and sticking friction points and impacts on the tool and work surface finish,

iii. it is possible to model the interactions between the tool and workpiece,

iv. material properties of both the tool and workpiece can be used as a function of strain, strain rate and temperature distributions,

v. machining variables such as cutting force, feed force, and localised stress can be obtained.

A more recent FEM for use in studies of the metal cutting problem is one called the Arbitrary Lagrangian Eulerian (ALE) method. This is well suited to problems involving very large strains that have characteristics of both solid and fluid flow. In this approach, the nodal points of the finite element mesh are neither attached to the work material nor fixed in space. The mesh points may have an arbitrary motion best suited to the problem. A detailed description of the ALE approach is presented in Movahhedy, Gadala and Altintas (2000). In all FEM applications, the Von Mises yield criterion is employed, and this represents an analytical weakness when the strains involved are very large, as in metal cutting chip formation.

1.5.1   Von Mises Yield Criterion

Von Mises (1913) suggests that the yielding of materials begins when the second deviatoric stress invariant J_2 reaches a critical value k. For this reason, it is sometimes called the J_2-*plasticity* or J_2 *flow theory*. It is part of a plasticity theory that is best applied to ductile materials, such as metals.

1.5.2   Yield Strength

The yield strength or yield point of a material in engineering and materials science is the stress at which a material begins to deform plastically. Prior to the yield point the material will deform elastically and will return to its original shape when the stress applied is removed. As the load is increased, the specimen begins to undergo permanent (plastic) deformation at some level of stress. Beyond this stress, the stress and strain are no longer proportional, as they were in the elastic region. The stress at which this phenomenon

occurs is known as the yield stress (Y) of the material. There are many types of elastic moduli, but the three primary ones are:

- Young's modulus (E)which describes tensile elasticity, or the tendency of an object to deform along an axis when opposing forces are applied along that axis; it is defined as the ratio of tensile stress to tensile strain. It is often referred to simply as the elastic modulus.

- The shear modulus or modulus of rigidity (G or μ) which describes an object's tendency to shear (the deformation of shape at constant volume) when acted upon by opposing forces; it is defined as shear stress over shear strain. The shear modulus is part of the derivation of viscosity.

- The bulk modulus (K) describes volumetric elasticity, or the tendency of an object's volume to deform when under pressure, which is defined as volumetric stress over volumetric strain, and is the inverse of compressibility. The bulk modulus is an extension of Young's modulus to three dimensions.

    (a) A thicker hard coating has a better load-carrying capacity than a thinner one but generates higher stresses at the coating/substrate interface (Holmberg *et al.*, 2006).

    (b) A stiffer coating (high *E* modulus) has a better load-carrying capacity than a more compliant one (low *E* modulus) but generates higher tensile stresses in the coating and lower tensile stresses in the substrate with the same indentation depth (Holmberg *et al.*, 2006; Karl and Komvopoulos, 1996, 1997).

    (c) High-friction sliding promotes plasticity and intensifies the Von Mises and first principal stresses in both the coating and the substrate, thus increasing the tendency towards yielding and cracking in each of them (Ye and Komvopoulos, 2003).

    (d) Coating thickness exhibits a more pronounced effect on the temperature rise from frictional heating at the coating surface and the coating–substrate interface than the layer's thermal conductivity. Frictional heating and shear surface traction may significantly intensify the stress field; the likelihood of yielding and cracking in the coated surface increases with decreasing coating thickness (Ye and Komvopoulos, 2003).

Chapter 2

Tool Modification Using Spark Erosion Process
and Cutting Test Procedures

In this chapter, the procedures for electrical discharge machining (EDM) of the carbide tool inserts and subsequent coatings of the inserts with TiN and the detailed experimental procedures of the cutting tests are presented. The work is divided into sections, beginning with a brief literature review as an introduction to EDM processes, then continues with the research concept, TiN coating, and ends with the design procedure for computer simulation / modelling.

2.0   Introduction

EDM is a non-traditional manufacturing process based on removing material from a part by means of a series of repeated electrical discharges (created by electric pulse generators at short intervals) between a tool, called the electrode, and the part being machined, in the presence of a dielectric fluid (Kuldeep, et al, 2010; also mentioned by Tomadi *et al.,* 2010; Pandey and Shah, 1980).

2.1.0   Tool Modification Processes by EDM

The EDMed surfaces consisted of a large number of craters (valleys) that are formed from the discharge energy. Generally, the surface finish of an EDMed component depends on the energy released per spark. In this experiment, a copper electrode was used because copper does not vaporise and is a good conductor of electricity, with the added benefit of being machined very easily for re-shaping to the required details whenever necessary. Other types of electrode that could be used are tungsten and graphite. During the process, the discharges that revealed the 'sparks' actually created the crater-like surface on the workpiece. Figure 2.1 is an illustration of the basic setup and principle of the working of an EDM machine.

The main components of the machine are the worktable, tool holder, precision slides for the tool holder in the two horizontal directions (x and y), dielectric tank, and pulse generating

system, a DC power supply and a filter for refining the used dielectric fluid. Both electrode and workpiece were immersed in dielectric fluid. The fluid created a course for the electric discharge. The EDM fluid (electrolyte) used had a high dielectric strength. Dielectric strength is important; though too high a strength would force a smaller gap and could lead to greater wear on the electrode. Most quality dielectric fluids are odourless, but there are some that do produce an odour, which generally means the quality is not as high.
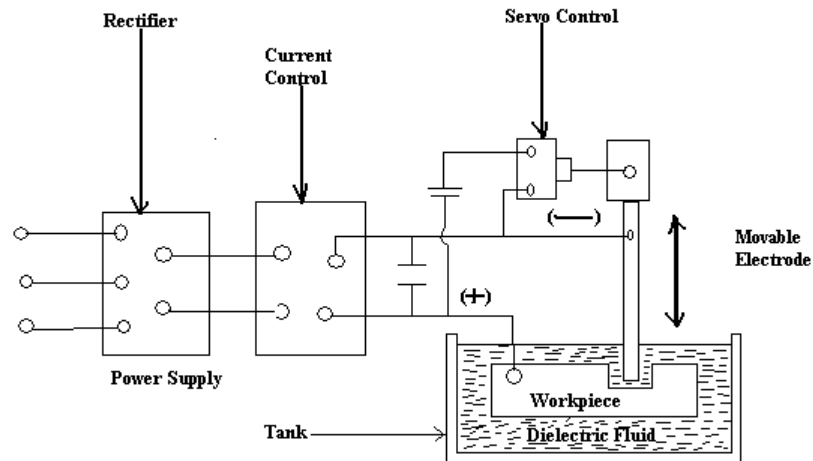
Figure 2.1 Schematic drawing of the Electrical-Discharge System Setup.

The dielectric fluid allowed the tool to cool and removed any waste products remaining. The fluid also controls the discharge, and impacts on the surface finish.

2.1.1 EDM Metal Removal Rate

The material removal rate (MRR) in EDM was affected by three parameters.

(a) **The On-time** (pulse time of 50 milliseconds), typically this is the erosion time. In other words, the duration of time (μs) the current is allowed to flow per cycle. The amount of material removed is directly proportional to the amount of energy applied during this On-time cycle, which is influenced by the peak current and On-time length.
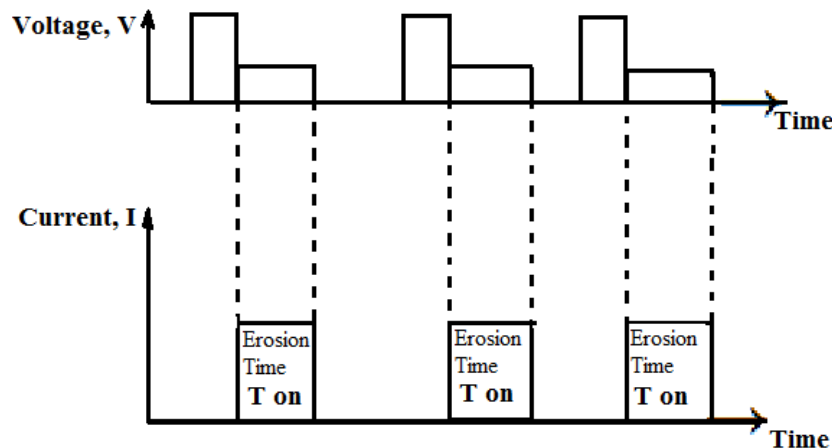
Figure 2.2: Voltage and Current (*I*) characteristics for EDM machine (McGough, 1988)

32

(b) **The Off-time** (pause time), is the interval in-between sparks at the On-time. The Off-time affects the speed and the stability of the machining. In a situation where the off time is too short, sparking will be unstable.

(c) **The Arc gap** (gap / break) is the distance between the electrode and the part during the EDM process.

Mathematically, let us assume that the volume of metal removed per second is proportional to *N,* the number of sparks per second, and the energy content of the sparks. The number of sparks per second *N* is given by:

$$N = \frac{1}{RC} \ln\left(\frac{E}{E - Vd} \right)$$ Equation 2.0

Where *R* is the charging resistance, *E* the applied DC source voltage and V_d the discharge or breakdown voltage. Therefore *M*, the machining rate or volume removed per second, may be expressed as follows:

$$M \alpha N x \frac{1}{2} CV_d^2$$ Equation 2.1

Where *C* is the capacitance and V_d the discharge voltage.

$$M = \frac{V_d^2}{R} \ln\left(\frac{1}{1 - (V_d / E)} \right)$$ Equation 2.2

Where *d* is a constant of proportionality. *M* could be written as follows:

$$M = \lambda \frac{E^2}{R} \left(\frac{V_d}{E} \right)^2 \ln\left(\frac{1}{1 - (V_d / E)} \right)$$ Equation 2.3

Consequently, *M* is a function of V_d / E for constant values of *E* and *R*. For maximising *M,* we differentiate *M* (equation 4.4) with respect to V_d / E and equate the resulting expression to zero. The value of V_d / E corresponding to the maximum *M*. Hence for a given value of *E*, the optimum value of V_d can be obtained from equation 2.3. Thus knowing the dielectric properties of the medium, the gap between the tool and the workpiece was determined. The control circuit of the servo-motor was made compatible with V_d

2.1.2 Electrical Discharge Machined Surface Finish

After EDM machining the workpiece surfaces were seen covered in small craters. The formation of these craters was mainly a consequence of the electrical discharge action, although it could have been affected the dielectric fluid as explained above, and the electrode used had to be machined in order to reshape it to the desired detail for subsequent machining. As the removal rates are directly related to the percentage of discharges doing useful work, it

was important that any variation in the correct gap due to metal erosion, or any short circuit caused by debris affecting the useful spark discharges, were controlled and regulated. The degree of surface roughness depended on the size of craters, which in turn depended on the energy per discharge used during the machining operation. It is widely known that the surface roughness of the work was usually found to decrease with a rise in pulse frequency and with a reduction in current. Thus, rougher surfaces were produced using longer pulse lengths.
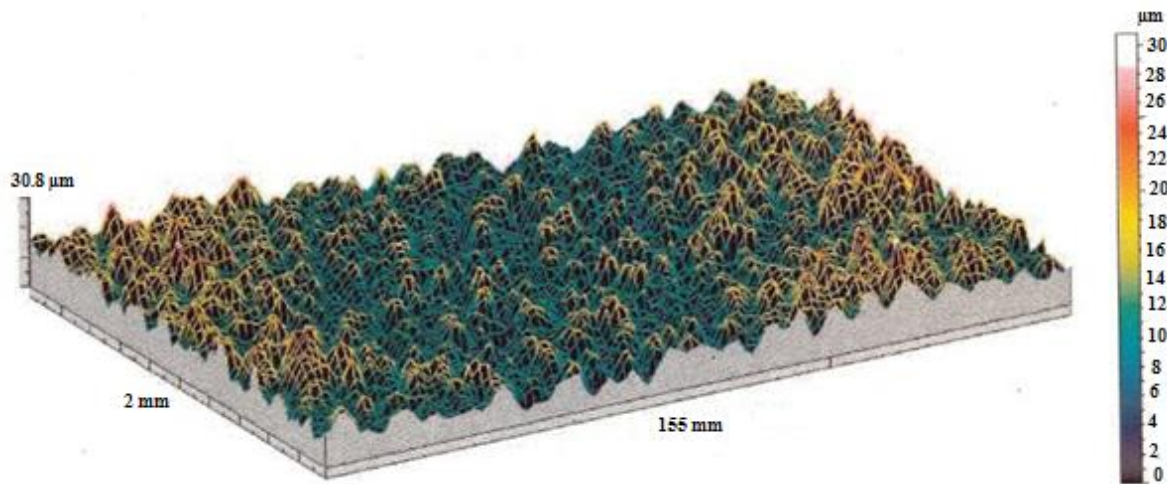
Figure 2.3: Showing 3D SEM profile of EDMed tool surface discussed in section 1.3.1 as figure 1.4 about discussion on characteristics of EDM Process

According to Sayles and Thomas (1978), spark eroded surfaces have been found to possess asperity heights which can be reasonably approximated by a Gaussian distribution. Dechjaren (2002) also stated that all 'EDM surfaces can be regarded as possessing a Gaussian height distribution, with a surface skewness between ±1, and a kurtosis of about 2.5− 3'. Deng and Lee (2000) stated that a higher surface roughness of the EDMed surface can be attributed to the existence of surface cracks, craters and droplets. Ramasawmy and Blunt (2002) shared the same view in their work on the 3D surface characterisation of an electro-polished EDMed surface and the quantitative assessment of process variables.

2.2.0 Preparation for Inserts Modification Process
2.2.1 Identification of Inserts
Rank Taylor Hobson surface roughness measurement machine was used to inspect all the tool specimens to ensure that they did not have any surface defects since the research involves surface modification and all were found to be uniform, each registering a surface finish reading of 0.15 μm. All inserts were numbered using an electric engraver on the bottom face of the insert, as seen below in Figure 2.4(a), this was done before taking them for EDM and subsequent coating.
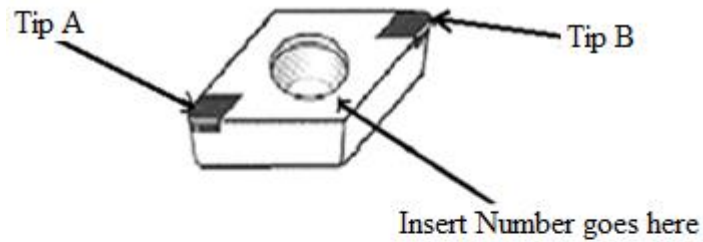
Figure 2.4(a): Showing Front Face of an Insert
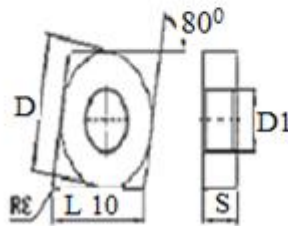
Figure 2.4(b): Showing the Tool Design

Figure 2.4:   Kennametal Inserts CNMA 432 K313X03
(Courtesy of Kennametal Inc. Catalogue 4010-GB, 2010 p. A43)

Figure 2.4 (b) presents the following parameters:

- Thickness (S) = 4.76 mm
- Theoretical diameter of the inscribed circle (D) = 12.70 mm
- Inside Diameter (D1) = 5.16 mm
- Corner Radius (Rε) =0.8 mm
- Length (L) = 10.00 mm
- Rake Angle = 5^0
- Relief/ Flank Angle = 5^0

These parameters are standard pre-requisite for turning mild steel at 250 m/min cutting velocity.

2.3.0   The Novel Surface Modification Process

Each corner of the insert was EDMed at the same current and On-time set-up as given below. The surface was first machined to a shallow depth using an Electric Discharge Machining (EDM) process to produce a characteristic crater-like surface topography.   Earlier experiments had identified that for the tool to work effectively it should have surface roughness within a narrow 'window' of between R_a values of 1.4 µm and 1.8 µm. The novel surface modification process was as follows:

a) The surface was first machined to a shallow depth using an EDM to produce a characteristic crater-like surface topography.

35

b) The crater-like surface was then coated with TiN to a thickness in the order of 4 microns (see Figure 2.4). The figure shows a cross-section of the TiN-coated surface as a hard wear-resistant coating material.
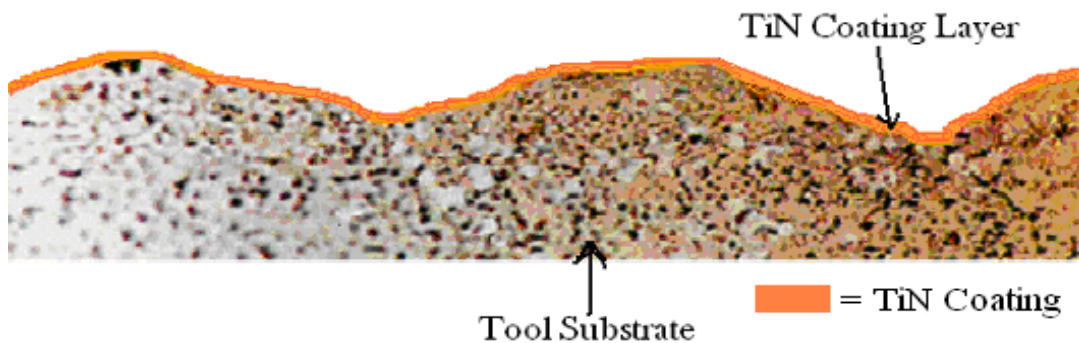
Figure 2.5: Micrograph showing a section through a surface-modified tool
(With permission from Vijitha Weerasinghe, 2002)

2.3.1 Apparatus

- Surface roughness measurement machine –Rank Taylor Hobson
- Cu-W 12 mm diameter EDM electrodes
- Digital Blue QX5 Microscope
- Eurospark Electrical Discharge Machining appliance –hybrid version pulse or relaxation (pulse mode used)

Thus, the parameters capable of producing these surface roughness (Ra) values for the particular electrodes are as follows:

i. On Time (T_{on}) = 50 µs

ii. Current (I) = 1 Ampere
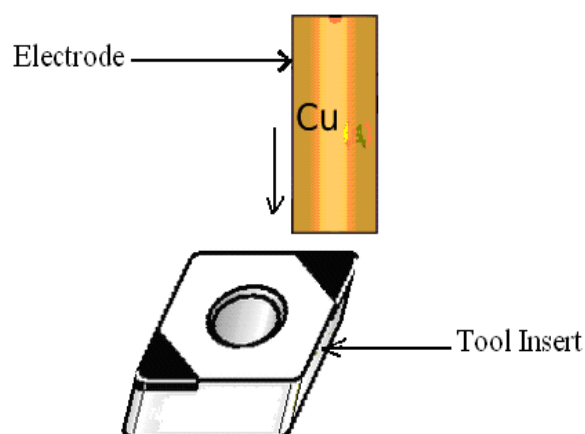
Figure 2.6: Approach of the Electrode to the Workpiece

2.4.0 Requirements for Surface Preparation for Coating

Proper surface preparation was essential for the success of the coating scheme, as the performance of the coating was directly dependent upon the correct and thorough preparation of the surface prior to coating. By convention, some of the various methods of surface preparation of steel should be done to the ISO 8504-2:2000 standards dealing with surface preparation methods –Part 2: Abrasive blast-cleaning and this are explained in appendix VIII. Tecvac the coating company was instructed to observe this standard when applying the TiN coating.

2.4.1 Benefits of TiN Coatings

Many authors have discussed the performance of turning, drilling, and tapping HSS tools coated with thin layers of TiN by the PVD method (Bromark, Hedenqvist and Hogmark, 1995; Ghani, Choudhury and Masjuki, 2004; Harju *et al.*, 1990; Kwostubhan *et al.*, 2003; Prengel *et al.*, 2001; Spur and Byrne, 1990; and Bienia *et al.*, 1990). TiN coatings were found to be most beneficial when turning at high speed, but were of little value on taps which cannot be operated at speeds high enough to take advantage of this coating (Shaw, 2005). This requires sufficient adhesion to the substrate in order for the tool to have enhanced wear resistance. A brief comparison of coating material properties is given in appendix V, and a comparison of Vickers Hardness levels. It was relevant to use TiN coating because TiN reduces friction and resists adhesive wear and BUE formation, as well as increasing oxidation resistance. It also acts as a chemical barrier to diffusion wear when cutting ferrous materials with carbide tooling (Dobrzanski *et al.*, 2004).

TiC is known to provide superior abrasive resistance. Meanwhile TiAlN has superior ductility and is stable at higher temperatures than TiN and TiC (Stephenson and Agapiou, 2006, also mentioned by Bhat and Woerner, 1986; McCabe, 2001).

2.5.0 Modified Tool Surface Finish
2.5.1 Definitions

Many parameters can be used to describe surface workpiece finishes, and these are explained in BS EN ISO 8503-4:2012 (see appendix IV) for surface structure definitions and profile, including texture, and ISO 4288 (1996) which specifies rules and procedures for surface assessment. Those in most common use in the metal cutting industry include:

- R_a, which is defined as the arithmetical mean deviation of the assessed profile (see Figure 2.9 in section 2.7.0).

The surface topography of the machined tools were measured before and after the coating of the tool surface, using a Taylor Hobson Talysurf Series 2. For each insert, five individual measurements were taken at random locations on the surface of the tool and the cut-off length (λc) was set at 0.25 mm according to BS EN ISO 5436-1 detailed in appendix VIII

In the previous work, experimental evidence had indicated that for the EDMed tool insert surface to be effective it must have surface roughness (Ra) values between 1.4–1.8 µm. Thus, a number of EDMed inserts were produced within the surface roughness range that was previously identified by Dechjarern (2002).

2.5.2   Application of the TiN Coating by PVD

After modifying the inserts the specimens were sent for coating to Tecvac Limited, a specialist coating company in Cambridgeshire for surface preparation (blasting) and coating in accordance with BS EN ISO 8503-2:2012(E) (*surface roughness characteristics of blast-cleaned substrates*).   The tools were coated with TiN by the physical vapour deposition (PVD) process under vacuum at a workpiece temperature of about 480 ^{0}C. According to Tecvac Ltd. (2012), this method results in coatings which are very smooth and require no post-coating processing. The PVD technique creates lower residual stresses than the Chemical Vapour Deposition (CVD) method. CVD is a thermochemical process conducted at temperatures between 950 ^{0}C to 1050 ^{0}C. A typical cycle for CVD is normally long, consisting of three hours of heating, four hours of coating and six to eight hours of cooling to room temperature. The long hours of heating creates mechanical stresses in the substrates. PVD can be performed at a lower temperature (Holubar, Jilek and Sima, 2000; Wu, 1998; Zhang, 1993) without creating mechanical stresses in the substrates. PVD coatings can be deposited at temperatures between 400 – 600 ^{0}C (Grzesik, 2000; Takadoum *et al*., 1997; Tecvac, 2012).

2.5.3   Test Concepts

This research was exploratory; it involved metal cutting experiments and data collection. Initially fifty (*CNMA 432, grade K313)* inserts were acquired from Kennametal Inc., a tool manufacturer for the tests. Each insert/ specimen had four cutting tips this means a total of two hundred cutting tips were available for the cutting test experiment and data collection. First, these inserts were numbered /marked with an electric engraver on the bottom face. The research focussed on the analysis of the tool wear and work-based wear criterion by the

detailed examination of the tool performance. The experiments were divided into two sets of tests:

a) <u>Tool-based wear criterion</u> design to establish the emergence of flank wear on the tool.

b) <u>Work-based wear criterion</u> to analyse the impact of cutting speed on the surface roughness (finish) as the cutting operation progresses and the tool begins to wear (tool life).

2.6.0   The Research Concepts and Plans

In order to maintain a clear goal for the cutting experiments, research plan and concepts were drawn up as indicated in Figure 2.7 below. All the different stages in the experimental plan were strictly followed for consistency in the project.

Research Concepts

Study: Performance characteristics of a surface-modified cutting tool insert

Available: Plain carbide tools without surface structure

Carry out literature search or reviews on EDM and TiN properties and coating characteristics

Generate crater-like surface topography on tool rake-face by spark erosion

Ensure that the tool surface roughness is between (R_a 1.4 – 1.8 µm)

Send the inserts to Tecvac Ltd. for surface preparation and coating

Apply TiN coatings by PVD to a thickness of 4 µm

Use the insert to...

Conduct cutting tests at various cutting speeds of 250, 300,325 and 350 m/min

- Establish the highest cutting speed and conditions, collect data.
- Create simulation models to substantiate experimental results

Write-up

Figure 2.7: Design of the Research Concepts

39

2.6.1 Preparation of Workpiece Billet

The billets were free cutting mild steel. Both ends of the billet were machined and each billet was centre drilled on one end for location at the tailstock. The centre-drilled point is needed for firmly holding the work in the chuck. Free cutting steels produce small chips when machined, and because it produces smaller chips the cutting force is also reduced as the length of contact between the workpiece and the cutting tool (in the stiction area) is reduced. These steels offer good machinability due to their contents of sulphur and lead. Thus reducing friction, heat, power required for machining, and wears on the tool due to friction between the chip and tool rake face. These features of good machinability reduce the chance of chip entanglement during machining.

2.6.2 Equipment Used for Cutting Tests

a) <u>Tool inserts:</u>   Kennametal tungsten (WC) cemented carbide inserts; CNMA 432, grade K-313

b) <u>Tool Holder:</u>   Kennametal MVJNR2525M16

c) <u>Work billets:</u>   75.00 mm diameter with length of 300 mm, mild steel EN3 (non-free cutting). Free machining steel forms small chips when machined. This increases the machinability of the material because small chips reduce the length of contact between the workpiece and the cutting tool, thus reducing friction, heat, power required to machine and wear on the tool. It also reduces the chances of chip entanglement.

d) <u>Lathe:</u> 30 HP (horsepower) Hitachi Seiki CNC Turning centre

2.6.3 Objectives of the Experiments

To investigate the effect of various cutting speeds (250 m/min to 350 m/min) on tool life with its eventual impact on work surface finish.

2.6.4 Experimental Plan and Cutting parameters used in the Cutting Test

Cutting speed of 250 m/min was the tool manufacturer's (Kennametal Inc.) recommended maximum speed. However, in order to satisfy the quest of this research the speed was increased by a multiple of 10% until a maximum speed that the machine tool could accommodate of 350 m/min was achieved before self-induced machine vibrations were observed. Self-induced machine vibrations are a function of both speed and how near the speed to a machine resonance and the cutting forces are.

Table 2.1: Experimental Plan and Cutting parameters used in the Cutting Test

Cutting Speed (V)	% Increment	Spindle Speed (N) rpm	Feed Rate (f) (mm/rev)	Depth of Cut (d)	Number of Cuts to approximate 15 Minutes cutting Time
250 m/min	Nil	1061	0.28	1 mm	23
300 m/min	20%	1273	0.28	1 mm	27
325 m/min	30%	1379	0.28	1 mm	29
350 m/min	40%	1485	0.28	1 mm	32

2.6.5 Rationale and Choice of Parameters for the machining tests were;

- Billet length = 300 mm

- Billet initial (Work) diameter (Ø) = 75 mm. The spindle speed (rpm) increased as the work diameter reduces.

- Surface finish settings cut-off (λc) = 0.8 mm.

- Length of cut = 200 mm,

The choice for the cutting speeds (parameters) was dependent on the tool manufacturer's recommendation for this particular type of inserts and work material (Mild steel EN-3) which was 250 m/min. as explained in the previous page the speed was incrementally increased to satisfy the objectives of the experiment.

2.6.6 Calculations of the Spindle Speeds

The spindle speeds for each cutting speed were determined by calculations

i. Cutting Velocity (V_c) of 250 m/min

Spindle Speed $n = \dfrac{V \times 1000}{\pi d}$ 　　　　　　　　　Equation 2.4

Therefore substituting n to get the spindle speed for the recommended cutting speed

(velocity) we have $n = \dfrac{250 \times 1000}{\pi \times 75} = 1061 rpm$

ii. Cutting velocity (V_c) of 300 m/min

$$n = \frac{V \times 1000}{\pi d} = \frac{300 \times 1000}{\pi \times 75} = 1273 rpm$$

iii. Cutting velocity (V_c) of 325 m/min

$$n = \frac{V \times 1000}{\pi d} = \frac{325 \times 1000}{\pi \times 75} = 1379 rpm$$

iv. Cutting velocity (V_c) of 350 m/min

$$n = \frac{V \times 1000}{\pi d} = \frac{350 \times 1000}{\pi \times 75} = 1485 rpm$$

2.6.7 Machining Time

The machining time for each speed shall be calculated as follows:

Machining Time (*tm*)

$$tm = \frac{Turning\ Length}{Feed/Minute} = \frac{L}{fxn}$$

Equation 2.5

Where:

L = turning length

f = feed in mm/rev

n = revolutions per minute (feed per minute (s) = $s \times n$)

2.6.8 Experimental Procedure Machining

The cutting procedures in this experiment began with the control specimen. Coolant was used at all times, and the coolant nozzle remained in the same location at all times during the course of the experiments. After each cut of 200 mm length the machine was stopped and the swarf generated cleared. After every 5 cuts, the workpiece surface finish was measured and a picture of the rake face and flank of the tool were taken at 10x and 60x magnifications. Good illumination of the specimen during the inspection, measurement and photography of the component was consistently maintained. The specimens were constantly positioned in the same location. The plan was to take up to 22 cuts (approximately 15 minutes cutting time). In the case of no appreciable wear, a further 5 cuts were taken. The machining time (*tm*) for the manufacturer's recommended cutting speed of 250 m/min was calculated to determine the length of time it takes to make one pass using equation 2.5

Thus by substituting the cutting parameters into equation 2.5 the time for each cut / pass would be

a) Cutting speed of 250 m/min

$$tm = \frac{L}{s\ x\ n} = \frac{200\ mm}{0.28\ mm/rev\ x\ 1061\ rev/min} = 0.6732\ min$$

This means that 1 pass is completed in 0.673 minutes.

With the length of time now known for every pass or cut the machine took to complete a pass, the number of passes possible in 15 minutes was computed. This gives a total number of cuts for this particular speed to be 22 passes. The cutting tests started with the control specimen (insert), and the same procedure was repeated with the test (EDMed) specimen as explained above.

b) Cutting speed of 300 m/min

$$tm = \frac{L}{s \times n} = \frac{200\,mm}{0.28\,mm/rev \times 1273\,rev/min} = 0.5611\,min$$

15 minutes of cutting time will equate to 27 cuts, and the process was started by machining the control specimen (insert) then the same procedure was repeated with the test (EDMed) specimen as given above.

c) Cutting speed of 325 m/min

$$tm = \frac{L}{s \times n} = \frac{200\,mm}{0.28\,mm/rev \times 1379\,rev/min} = 0.5180\,min$$

15 minutes of cutting time will equate to 29 cuts, and the process was started by machining the control specimen as above.

d) Cutting speed of 350 m/min

$$tm = \frac{L}{s \times n} = \frac{200\,mm}{0.28\,mm/rev \times 1485\,rev/min} = 0.4810\,min$$

15 minutes of cutting time will equate to 31 cuts and the process was started with control specimen, the same as in (a) above.

2.7.0 Work Surface Measurements

During the experimental work surface measurements were taken after every five cuts/ passes using a Taylor Hobson Talysurf Series 2. For each mild steel test specimen, five individual measurements were taken at random locations on the surface of the cylindrical workpiece according to BS EN ISO 5436-1 (*Surface texture: Profile method; Measurement standards-Part 1: Materials Measures*) standard on surface measurement see appendix IV.
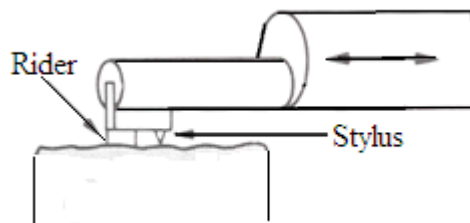
Figure 2.8: Measurement Techniques

The surface profile measurement was 5 mm long, and the filter cut-off length (λc) is set at 0.8 mm. The parameters were calculated relative to a reference (centre) line, fitted through the surface profile such that the area between the profile and mean line above the line is equal to that below the line, as shown in appendix III.

2.7.1 Cutting Tests Results

The results show the following:

<u>Wear on rake face:</u> Wear on rake face takes place in the form of a crater away from the cutting edge in a zone where the temperature is highest. Primary mechanism is by way of abrasion caused by the chip rubbing against the tool surface. Results show that at all speeds, the EDMed surfaces have a much higher resistance to wear. Whereas the TiN coating on the rake faces of the control specimens appear visibly to be worn off after a short duration of cutting, the coating on the EDMed surfaces is visibly held for a much longer duration of cutting as shown in appendices 1A - 1C. However, although the coating is worn off by way of a crater, the remaining coating (along the rim of the wear scar) continues to offer resistance to wear (Sundqvist *et al*, 1983, Wallén and Hogmark, 1989, also cited by both Smith et al, 1988 and Stjernberg K, 1985). Furthermore, it is capable of carrying the full load of the chip without collapsing. Wallén and Hogmark (1989), have compared the profile of wear scars produced on uncoated and TiN coated cylinders in a crossed-cylinders wear test. They found that the presence of the TiN rim produced a concave wear scar while the scar on the corresponding uncoated specimen was flat. In regard to the EDMed surface, it can be postulated that the sliding friction is likely to be less and islands residual TiN coating is likely to remain in the 'valleys' of the surface topography.

Table 2.2: Results for Control Specimen at 250 m/min cutting speed

250 m/min (Kennametal Inc. Recommended Cutting Speed)							
Control Specimen	**1st (µm)**	**2nd (µm)**	**3rd (µm)**	**4th (µm)**	**Average (µm)**	**Power Load**	**Machine Time (mins)**
After 5 Cuts/ Passes	2.46	2.60	2.65	2.47	**2.54**	60%	3
After 10 Cuts/ Passes	3.41	3.61	3.97	3.80	**3.69**	60%	6.7
After 15 Cuts/ Passes	3.46	3.32	3.56	3.77	**3.52**	63%	10
After 20 Cuts/ Passes	3.05	2.89	2.86	2.99	**2.94**	65%	13
After 25 Cuts/ Passes	2.94	3.02	3.09	2.88	**2.98**	60%	16
After 30 Cuts/ Passes	3.11	3.08	3.00	3.14	**3.08**	65%	20

Table 2.3: Results for Test Specimen at 250 m/min cutting speed

250 m/min (Kennametal Inc. Recommended Cutting Speed)							
EDMed Specimen Insert No: 20 Side A	**1st (µm)**	**2nd (µm)**	**3rd (µm)**	**4th (µm)**	**Average (µm)**	**Power Load**	**Machine Time (mins)**
After 5 Cuts/ Passes	2.49	2.60	2.45	2.69	**2.55**	50%	3
After 10 Cuts/ Passes	2.77	2.66	2.79	2.80	**2.73**	53%	6.7
After 15 Cuts/ Passes	3.06	2.23	2.76	3.22	**2.81**	55%	10
After 20 Cuts/ Passes	3.43	3.29	3.87	3.60	**3.54**	50%	13
After 25 Cuts/ Passes	3.90	3.61	3.55	3.05	**3.52**	55%	16
After 30 Cuts/ Passes	3.14	3.29	3.31	3.24	**3.24**	55%	20
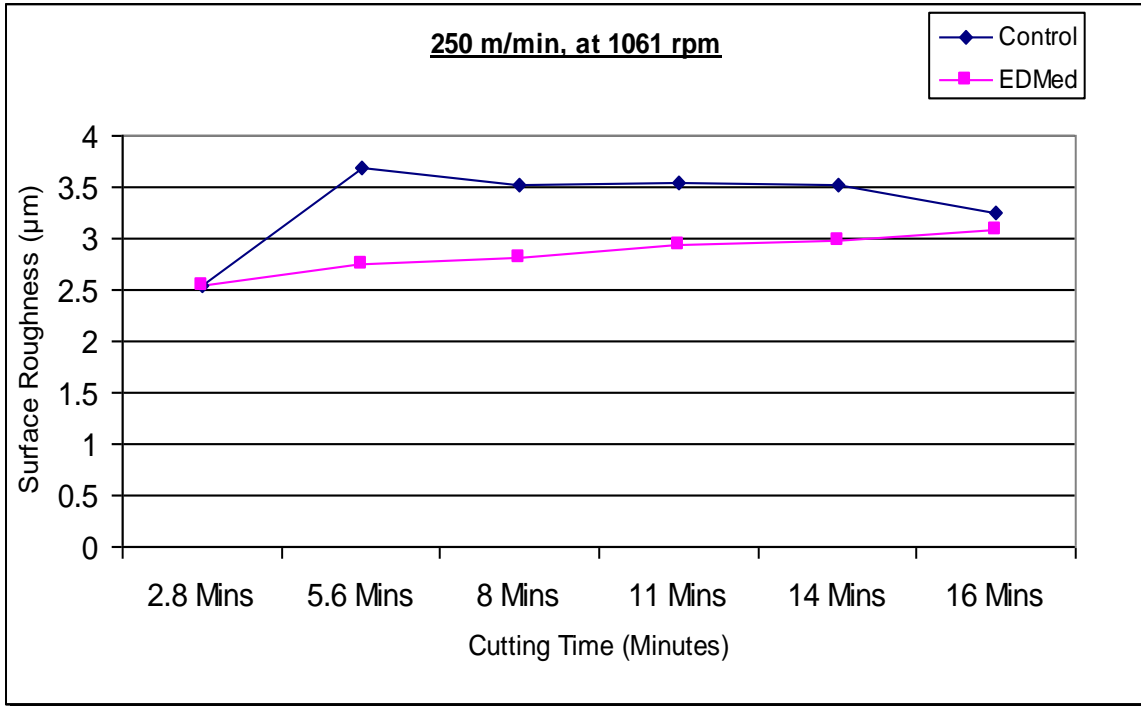
Figure 2.10: Results of cutting at 250 m/min

Table 2.4: Results for Control Specimen at 300 m/min cutting speed

Control Specimen	300 m/min an increase of 20% on the recommended Speed						
	1st (µm)	2nd (µm)	3rd (µm)	4th (µm)	Average (µm)	Power Load	Machine Time (mins)
After 5 Cuts/ Passes	2.39	2.44	3.01	2.41	**2.56**	55%	2.8
After 10 Cuts/ Passes	3.03	2.87	2.84	2.09	**2.70**	55%	5.6
After 15 Cuts/ Passes	2.50	2.73	2.54	2.66	**2.60**	58%	8
After 20 Cuts/ Passes	3.43	4.40	3.89	3.75	**3.86**	60%	11
After 25 Cuts/ Passes	3.67	3.03	2.89	3.71	**3.32**	55%	14
After 30 Cuts/ Passes	3.93	2.99	3.50	3.04	**3.36**	60%	16

Table 2.5: Results for Test Specimen at 300 m/min cutting speed

EDMed Specimen No: 20 side C	300 m/min an increase of 20% on the recommended Speed						
	1st (µm)	2nd (µm)	3rd (µm)	4th (µm)	Average (µm)	Power Load	Machine Time (mins)
After 5 Cuts/ Passes	2.66	2.47	2.63	2.52	2.57	50%	2.8
After 10 Cuts/ Passes	2.66	2.89	2.66	2.71	2.73	53%	5.6
After 15 Cuts/ Passes	3.23	3.48	2.99	2.41	3.02	53%	8
After 20 Cuts/ Passes	2.79	2.86	2.78	2.76	2.79	55%	11
After 25 Cuts/ Passes	2.72	2.89	3.01	3.09	2.92	50%	14
After 30 Cuts/ Passes	3.24	2.95	3.00	3.42	3.15	53%	16
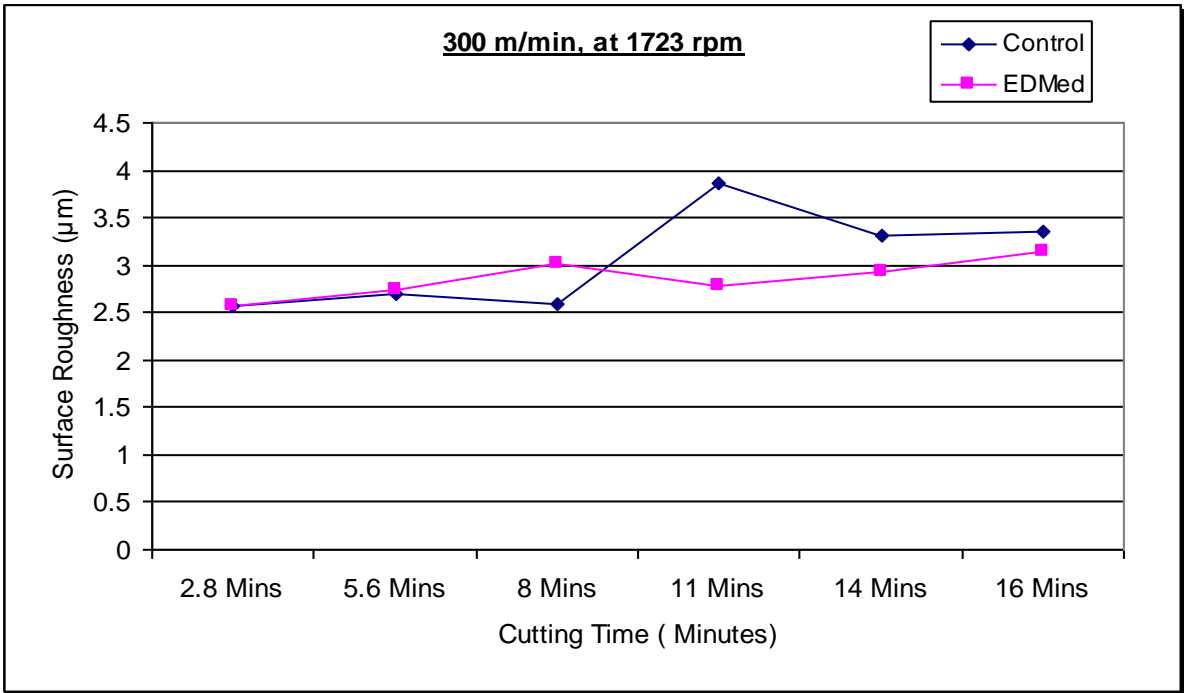
Figure 2.11: Results of cutting at 300 m/min

Table 2.6: **Results for Control Specimen at 325 m/min cutting speed**

Control Specimen	325 m/min an increase of 30% on the recommended Speed						
	1st (µm)	2nd (µm)	3rd (µm)	4th (µm)	Average (µm)	Power Load	Machine Time (mins)
After 5 Cuts/ Passes	2.49	2.49	2.90	2.72	**2.65**	55%	2.5
After 10 Cuts/ Passes	2.89	2.89	2.70	2.74	**2.80**	60%	5
After 15 Cuts/ Passes	3.39	3.50	3.89	3.28	**3.51**	63%	7.7
After 20 Cuts/ Passes	2.88	2.85	3.16	3.18	**3.01**	55%	10
After 25 Cuts/ Passes	3.13	3.08	3.37	2.78	**3.09**	60%	12.9
After 30 Cuts/ Passes	3.37	2.57	3.43	3.52	**3.22**	65%	15.5

Table 2.7: Results for Test Specimen at 325 m/min cutting speed

EDMed Specimen Insert No: 32 Side B	325 m/min an increase of 30% on the recommended Speed						
	1st (µm)	2nd (µm)	3rd (µm)	4th (µm)	Average (µm)	Power Load	Machine Time (mins)
After 5 Cuts/ Passes	2.47	2.67	2.50	2.24	**2.47**	50%	2.5
After 10 Cuts/ Passes	2.48	2.07	2.07	2.97	**2.39**	53%	5
After 15 Cuts/ Passes	2.63	3.62	2.55	2.94	**2.94**	53%	7.7
After 20 Cuts/ Passes	2.40	2.13	3.08	3.89	**2.86**	55%	10
After 25 Cuts/ Passes	3.00	2.04	2.03	4.09	**2.79**	50%	12.9
After 30 Cuts/ Passes	2.40	2.43	2.50	2.44	**2.44**	53%	15.5
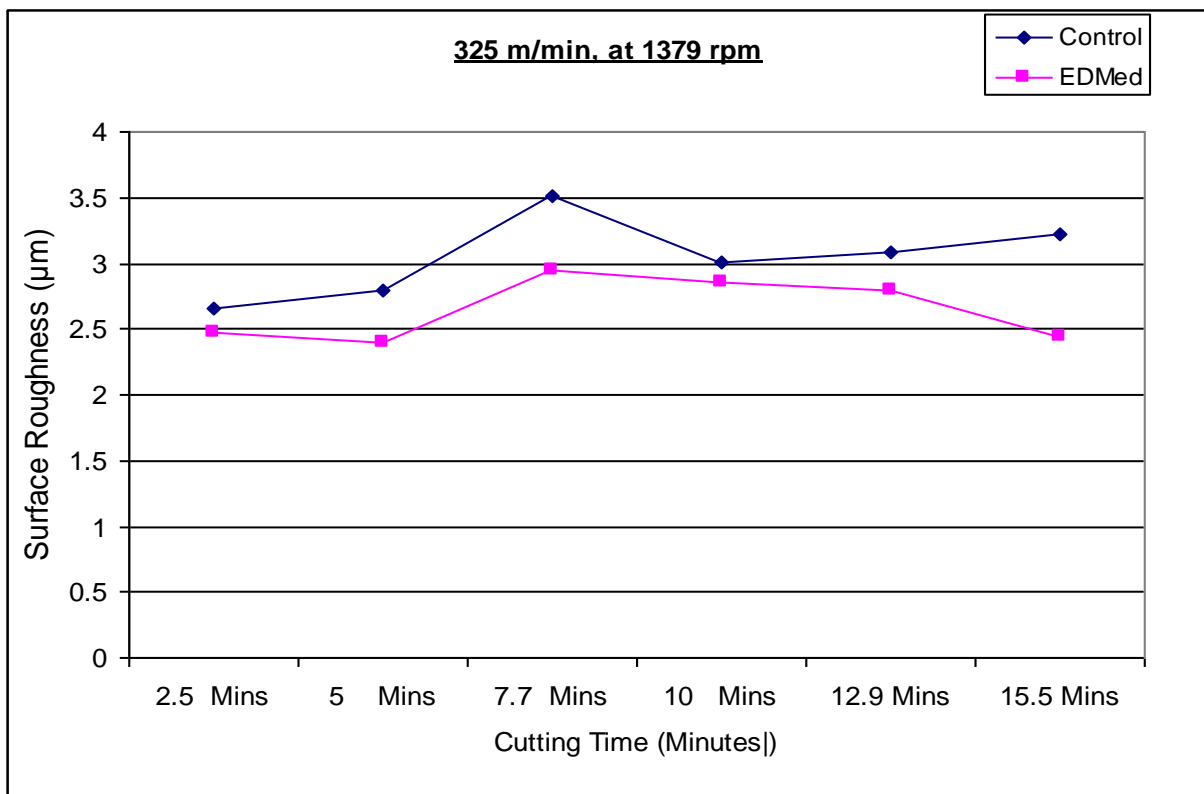
Figure 2.12: Results of cutting at 325 m/min

Table 2.8: Results for Control Specimen at 350 m/min cutting speed

350 m/min an increase of 40% on the recommended Speed							
Control Specimen	1st (µm)	2nd (µm)	3rd (µm)	4th (µm)	Average (µm)	Power Load	Machine Time (mins)
After 5 Cuts/ Passes	3.40	2.63	3.14	3.13	**3.07**	60%	2
After 10 Cuts/ Passes	3.30	2.87	2.88	2.89	**2.98**	60%	4.8
After 15 Cuts/ Passes	3.51	3.12	3.26	3.19	**3.27**	60%	7
After 20 Cuts/ Passes	3.34	3.06	3.57	2.79	**3.19**	63%	9.6
After 25 Cuts/ Passes	3.25	3.45	3.38	3.30	**3.34**	63%	12
After 27 Cuts/ Passes	**7.30**	**7.40**	**7.22**	**7.31**	**7.30**	**70%**	**12.9**

Table 2.9: Results for Test Specimen at 350 m/min cutting speed

350 m/min an increase of 40% on the recommended Speed							
EDMed Specimen Insert No: 24 Side A	1st (µm)	2nd (µm)	3rd (µm)	4th (µm)	Average (µm)	Power Load	Machine Time (mins.)
After 5 Cuts/ Passes	2.41	2.42	2.39	2.42	**2.41**	50%	2
After 10 Cuts/ Passes	2.42	2.54	2.30	2.18	**2.36**	50%	4.8
After 15 Cuts/ Passes	2.84	2.39	2.55	2.58	**2.59**	53%	7
After 20 Cuts/ Passes	2.62	2.83	3.01	3.23	**2.92**	55%	9.6
After 25 Cuts/ Passes	2.47	2.66	2.65	2.75	**2.63**	50%	12
After 30 Cuts/ Passes	2.30	2.14	2.71	2.41	**2.39**	53%	14
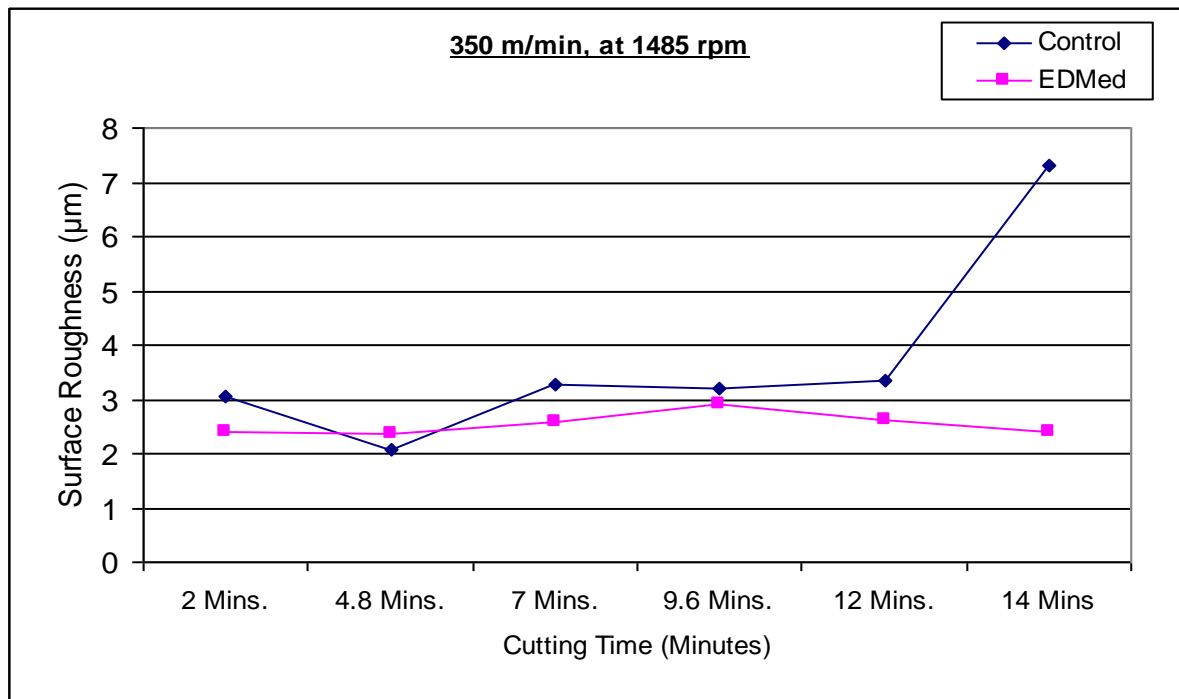
Figure 2.13: Results of cutting at 350 m/min

2.8.0   Repeat Tests for 350 m/min Cutting Speed and tool chipped

Since the control specimen for the 350m/min failed by chipping at the 27th cut a repeat experiment was done. Again, the results of the second tests saw the failure of the control specimen by chipping at 28th cuts. Whereas, the EDMed specimen maintained a good surface finish of 2.59 m after 35 cuts. Furthermore, the power reading for the EDMed specimen was consistently lower than the control specimen was. At this point, it was decided to carry out yet another repeat test at 350 m/min.
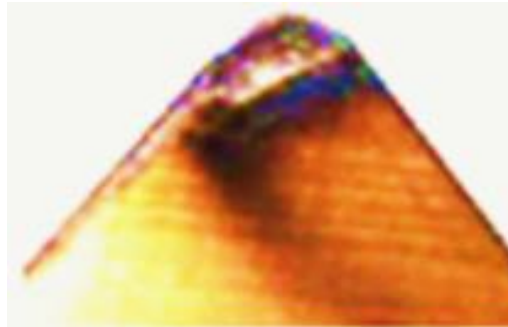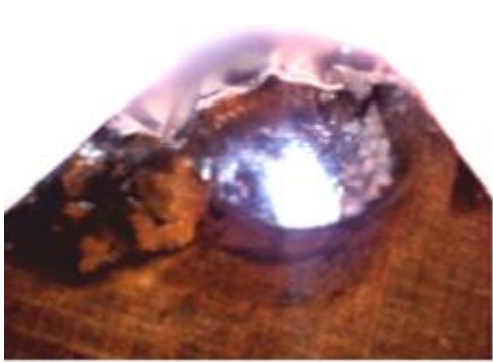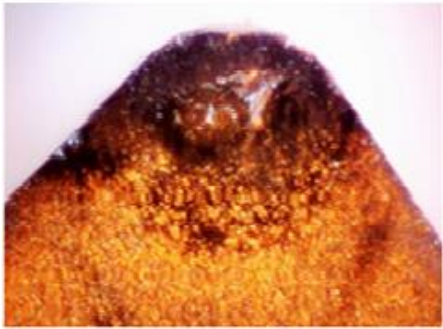
Figure 2.14: Microscopic Picture of Chipping on control Specimen
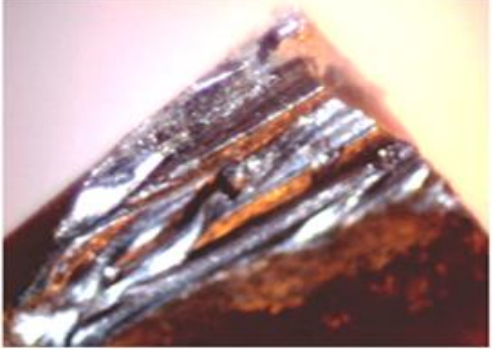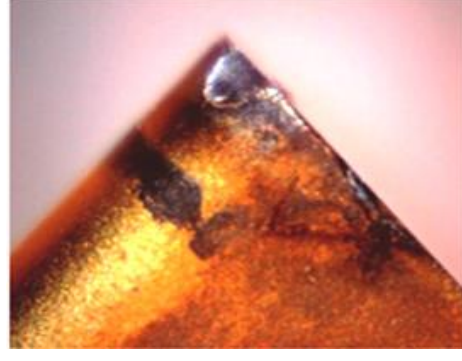
2.8.1   Repeat Tests Results

1st)   In the initial cutting test the control specimen failed after 27 cuts/ passes. The first repeat test also had its control insert (specimen) failing after 28 passes, the modified test specimens made upto 35 cuts and could still go on cutting.

Table 2.10: Comparative Results for Repeat Test I showing rake face
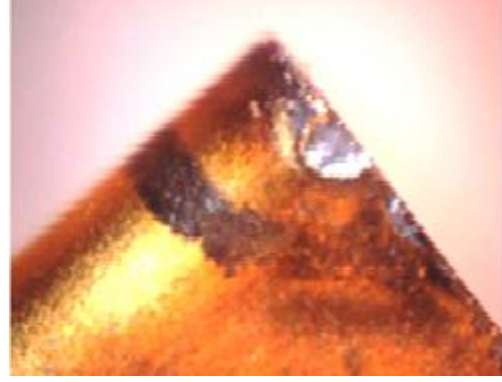
The First Repeat Test with both Control and Modified Test Specimens	
Rake face of Control Specimen	Rake Face of Test Specimen
60x	60x
Power Load = 75%, Tool failed after 28 cuts, work surface measurement = Ra = 5.56 µm, after 13.58 minutes of machining. Diameter 59 mm	Power Load = 54%, Tool cut upto 35 passes, work surface measurement = Ra =2.59 µm, after 14.55 minutes of machining. Diameter 55.02 mm

Table 2.11: Comparative Results for Repeat Test I showing tool Flank

The First Repeat Test with both Control and Modified Test Specimens	
Flank Side of Control Specimen	Flank Side of Modified Test Specimen
60x	60x
Power Load = 75%, Tool failed after 28 cuts, work surface measurement = Ra = 5.56 µm, after 13.58 minutes of machining. Diameter 59 mm	Power Load = 54%, Tool cut upto 35 passes, work surface measurement = Ra =2.59 µm, after 14.55 minutes of machining. Diameter 55.02 mm

2nd) For the second repeat test, the host company whose CNC machine was used had time constraints on their operations, thus; machining test was done using the modified EDMed test specimen only and this again machined upto 35 cuts. However, no control specimen was tested.

Table 2.12: Results for Repeat Test II

The Second Repeat Test with Modified Test Specimen only	
Rake face of test Specimen 2nd Repeat Test	Flank of Test Specimen 2nd Repeat Test
60x	
Power Load = 56%, work surface roughness reading Ra = 2.60 µm, after 35 passes in 17.37 minutes of machining. Diameter 40.1 mm	

The results of the EDMed modified specimens showed low rake face wear, low power consumption and good work surface finish even after 35 cuts. Meanwhile, the failure of the control specimen was observed to be consistent with earlier experimental results. Additional

cutting tests with inserts having EDMed surface but without TiN coating showed conclusively no enhanced wear resistance

2.9.0   Concluding Remarks

The protection that the substrates receive depends on the quality of the fusion between the coating and the tool. TiN and TiC are known for their ability to bond well with the substrates (Kopač, 2004; PalDey and Deevi, 2003). The resulting surface finish of the workpiece may be improved by the presence of a TiN coating on the tool (Jacobson, Wallén and Hogmark, 1987). TiN plays the role of a thermal barrier, by protecting the heat-sensitive tool substrate from thermal softening (Wallén and Hogmark, 1989). The explanation to this is that there is an improved contact condition at the tool–work interface, since a cutting edge is vital for the resultant cutting and thrust forces. They also determine the chip shape and the appearance of the cut surface. About 100% of cutting tool inserts these days come with some sort of coating. The principal coating materials and reasons for their use according to Shaw (2005) are as follows:

- TiN – to lower friction and edge build-up because the coating acts as lubricant and thermal barrier (Dobrzanski *et al.*, 2004; also mentioned in Batista *et al.*, 2002; Cekada *et al.*, 2002; Navinsek *et al.*, 2001),
- TiC – to increase hardness,
- Al_2O_3– to provide a thermal barrier,

The surfaces produced by EDM have been studied, and are found to consist of overlapping crater-like surfaces with deep valleys and peaks.

It can be concluded that the coated EDMed inserts do offer enhanced wear resistance when compared with plain coated control inserts. This enhancement is sustained at speed 40% higher than the recommended, which were sustained upto 35cuts during the cutting tests experiments. This aspect offers the possibility to use tool were compensation to maintain dimensional control thereby prolonging the effective tool life.

Chapter 3

Analysis of Enhanced Wear Resistance of Tools with Undulating Surface Structures

3.0 Introduction

In this study, comparative cutting tests were carried out using Kennametal CNMA-432 cemented carbide tool grade K313 inserts with nose radius (R_ε) of 0.8 mm. The tools' rake faces were modified by EDM processes to a surface roughness 'window' of between 1.4 and 1.8 microns, as discussed in previous chapter This window of roughness was identified in earlier experiments conducted at UEL by the researcher as proof of concepts for the technology and another earlier one done at Imperial College London in 2002. It was acknowledged that the modified inserts would not have enhanced wear resistivity properties if the 'tool surfaces were too smooth or too rough' (Dechjarern, Busso and Hibberd, 2004).

After surface modifications were completed, the tools were coated with TiN to a thickness of approximately 4 µm by PVD in line with BS EN ISO 8503-1 (Appendix VIII, *preparation of substrates before application of paints and related products –surface roughness characteristics of blast-cleaned substrates*. According to Mayrhofer *et al* (2006), the quality of adhesion of the coating depends on the surface topography of the tool. On the other hand, the degree of surface roughness relates to the size of craters as a result of the energy per discharge used during the machining process discussed in chapter 2 under metal removal rate.

3.1.0 Properties of Cemented Carbide Tool Inserts

Attempt to relate the coating of tool materials and their performance was made by Klocke and Krieg (1999). In addition, Bhushan and Gupta (1991) stated that there are four major groups of coating material in use today, and these are:

   a) Titanium-based coating materials such as TiN, TiC and Ti(C,N). The metallic phase is often supplemented by other metals such as aluminium (Al) and chromium (Cr), which are added to improve particular properties such as hardness or oxidation resistance.

52

b) Ceramic-type coatings, an example of which is Al_2O_3 (alumina oxide).

c) Super-hard coatings, for example diamond coating by CVD.

d) Solid lubricant coatings such as amorphous metal-carbon, MoS2 or MoS2/Ti. Solid lubricant in self-lubricating tools by the formation of an in-situ tribological film system between workpiece material and tool during dry cutting processes (Deng *et al* 2012, Aizawa *et al* 2005; Renevier *et al*, 2000) is widely used for low speed machining especially of cast iron steel.

Bhushan and Gupta (1991) discuss the effectiveness of various coatings on cutting tools. It is well documented that coating metal cutting tools considerably improves tool life and boost the performance of carbide tools in all forms of machining. Whether it be in high volume productivity, high speed machining and high-feed cutting or in dry machining. In addition to processing of difficult to-machine materials (Adachi and Hutchings, 2003; Atkins and Liu, 2007; Bayer, 1994; Bhushan, 1999; Davim and Astakhov, 2008; Kato and Adachi, 2001; Siniawski *et al*., 2007; Stachowiak and Batchelor, 2005). Carbide inserts are good for all types of coating, especially with coating materials such as TiN, TiAlN, TiCN, inclusive of solid lubricant coatings (Deng *et al*, 2012) and multilayer coatings for the following reasons:

a) to provide increased surface hardness, for greater wear resistance,

b) to increase resistance to abrasive and adhesive wear, and flank and crater wear,

c) to reduce friction coefficients to ease chip sliding, reduce cutting forces, prevent adhesion to the contact surfaces, reduce heat generated due to chip sliding, etc.,

d) to reduce the portion of the thermal energy that flows into the tool,

e) to increase corrosion and oxidation resistance,

f) to improve crater wear resistance, and

g) to improve the surface quality of finished parts.

3.2.0 Factors that Influence Tool Wear

Generally, many factors influence the wear of cutting tools, and these are;

    i. the tool material

    ii. tool geometry,

    iii. workpiece materials,

    iv. cutting parameters (cutting speed, feedrate and depth of cut),

    v. type of cutting fluids and

    vi. Machine-tool conditions (machine with worn out bearings and poor alignment are susceptible to vibrations) can affect tool life or performance.

3.2.1 Properties of a Tool Material

Different types of tool material, ranging from high-carbon steels to ceramics and diamonds, are used as cutting tool materials in today's metalworking industry with varying degree of application and properties. Davis, (2005) states that the three prime properties of a tool material are:

a) **Hardness Property**

Material hardness is defined as the resistance to indenter penetration. According to Isakov (2004) it directly correlates with the strength of the cutting tool material and it is its ability to maintain high hardness at elevated temperatures or hot hardness.

b) **Material Toughness**

Material toughness is defined as the ability of a material to absorb energy before fracture. The greater the fracture toughness of a tool material, the better its ability to resist shock load, chipping and fracturing, vibration, misalignments, and other imperfections in the machine tool which could lead to self-induced vibrations. Well, self-induced vibrations are a function of cutting speed, machine resonance and cutting forces. These functions individually or in combination can affect the toughness of the tool and hence causes wear. A major trend in the development of tool materials is to increase their toughness while maintaining hardness. For carbides, the toughness measurement is common, as described in the ASTM standard B771-87(2001) on the fracture toughness of cemented carbides.

c) **Resistivity Property**

Tool wear resistance is defined as the attainment of acceptable tool life before cutting tips need to be replaced. Tool wear is a result of intricate physical, chemical, and thermo-mechanical occurrences due to the various mechanisms of wear (adhesion, abrasion, diffusion, oxidation, etc.) acting simultaneously with a predominant influence of one or more of them in different situations.

d) **Tool Wear Process**

Normally, tool wear is a gradual process and in this particular research work an emphasis is placed on the two basic zones of wear in cutting tools: crater wear and flank wear. The reasons for this interest in crater and flank wear is based on the fact that they are the most important measured forms of tool wear, with direct impacts on tool life and work surface finishes. Flank wear is most commonly used for wear monitoring. According to the standard ISO 3685 (1993) on wear measurement, the

major cutting edge is considered to be divided into four regions, as shown in Figure 3.1 below.

SECTION A-A

KF = crater front distance
KB = crater width
KM = crater center distance
KT = crater depth
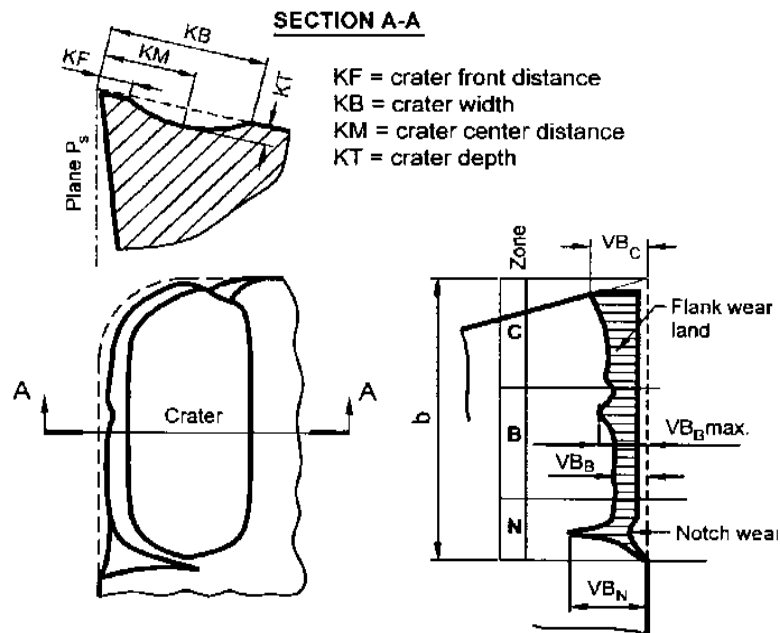
Figure 3.1 Division of Major Cutting Edge

Key:

i.   *Region A* is the quarter of the worn cutting edge length *b* farthest away from the tool,

ii. *Region B* is the remaining straight part of the cutting edge in zone C,

iii. *Region C* is the curved part of the cutting edge at the tool corner,

iv. *Region N* extends beyond the area of mutual contact between the tool and workpiece for approximately 1 – 2 mm along the major cutting edge. The wear is of notch type.

Tool wear is normally measured using a toolmaker's microscope (with video imaging systems and a resolution of less than 0.001mm) or a stylus instrument similar to a profilometer (with ground diamond styluses). Figure 3.2 illustrates the different types of tool wear which occur during metal machining.
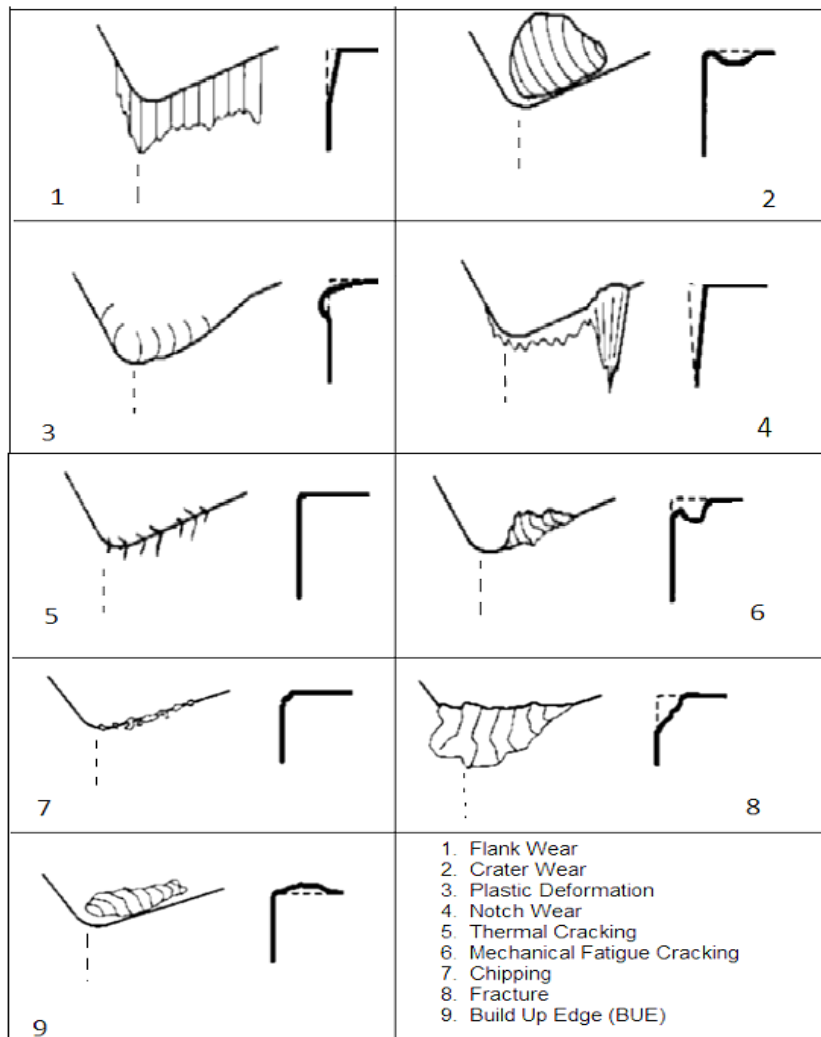
Figure 3.2 Different Types of Tool wear growth During Metal Cutting
(Adopted from Sandvik Coromant, 2008)

3.3.0 Experiment Details on CNC

In order to evaluate the wear characteristics of the modified tools (tools with undulating topographies), cutting experiments were carried out in a laboratory environment. Tools manufacturers recommend that most carbide cutting tips have tool life of between 15 to 20 minutes for machining mild steels provided the manufacturer's guidelines on cutting speeds, use of lubricants (coolants), work materials and depth of cut are followed.

Thus, for this project a minimum of 15 minutes of cutting was set as the baseline for each cutting tip of the inserts used. To ensure consistency in data collection, after every 5 cuts (passes), the tool wear profiles of the inserts were examined under a microscope and pictures taken in order to monitor the progressive wear on the rake face and on the flank of the insert. At the same time the work billet was removed from the machine and the surface roughness

measurement (R_a value) was taken and the cut-off length (λ) set at 0.8 mm. The power load was monitored for each cut using an on-board meter on the lathe.

3.3.1 Cutting Process Information

a) Coolant supply was set at a maximum jet stream 100m/sec and kept constant throughout.

b) An angle was machined at the end of the cut to facilitate easy clearance of the swarf.

c) Swarf was cleared by hand after each cut/pass.

d) Any loose build up on the edge was cleared prior to photography.

e) Diameter of the workpiece was measured after every 5 cuts/passes.

3.3.2 CNC Machining

3.3.3 G-Codes and Modal Program

The cutting tests were done on a 30 HP Hitachi Seiki Computer Numerical Control (CNC) Turning Centre. The programme was written in a language commonly referred to as G and M-Codes. To give an insight into the machining process, a brief explanation is given below on the application and use of G and M-Codes in the next paragraph.

G-codes and M-codes were simple instructions, which made the machine behave in a certain way as designed by the operator. In fact, the program address G identifies a preparatory command, often called the G-Code. This address has only one objective, to prepare the control system to follow a certain desired condition, or to perform a certain operation. For example, the address G00 presets a rapid motion mode for the machine tool. G01 tells the machine to make a linear feed move to a location say X45.9, and M08 instructs the machine to turn the coolant on while M09 tells the machine to turn the coolant off. The term preparatory command indicates the meaning of a command of a G-Code for the machine control system to accept the programming instructions by following the G-Code in a specific way.

The word Modal is based on the word 'Mode' and means that the specific command remains in this mode after it has been used in the program once. It can only be cancelled by another modal command of the same group. Without this feature, for example, a program using linear interpolation in absolute mode with a feedrate of 0.28 mm/rev would contain the absolute command G90, the linear motions command G01 and feedrate F0.28 in every block. With the modal values, the programming output is much shorter. Virtually all controls accept modal commands (Smid, 2003)

3.3.4 Comparative Cutting Tests

Comparative cutting tests using control specimens with no EDM surface structures and tests specimens with EDM crater-like surfaces were carried out on mild steel grade EN-3. The tool manufacturer (Kennametal Inc.) recommends a cutting speed of 250 m/min for this type of material and tool. For this study, various cutting speeds up to an increase of 40% of the recommended speed were investigated. Two sets of experiments were carried out, first to test the tool wear and secondly the work surface finish.

3.3.5 Test Experiments

In the first set a tool-based wear criterion was used (flank wear), and in the second test a work-based wear criterion was used (work surface finish). Test specimens (EDMed modified inserts coated with TiN) were selected from within the 'operating window', and were first used at the Kennametal Inc. recommended cutting speed of 250 m/min, and then a speed increment was implemented. Cutting speeds investigated were as follows:

(a)   250 m/min which was the recommended cutting speed for the particular type of insert to machine mild steel.

(b)   300 m/min, an increase of 20% of the recommended cutting speed.

(c)   325 m/min an increase of 30%.

(d)   350 m/min an increase of 40%.

3.3.6 Experimental Plan

At the outset cutting tests were conducted to verify/prove that the TiN-coated tool with undulating surface structures exhibited evidence of enhanced performance. In this case only three speeds were investigated, the 250 m/min which is the tool manufacturer's recommended speed, 325 m/min and 350 m/min, which was the highest speed achieved in the first set of comparative cutting tests. The investigations centred on flank wear criterion (tool-based wear) and a work-based wear criterion (work surface finish). All cutting parameters were 1 mm depth of cut, 0.28 mm/rev and various cutting speeds.

Table 3.1 Experimental Plan for CNC

Cutting Speed(m/min)	Spindle Speed(rpm)	Number of Cuts in Approx. 15 mins of Cutting
250	1061	23
300	1273	27
325	1379	29
350	1485	32

The following parameters remained unchanged for all speeds investigated:

- Feed rate = 0.28 mm/rev
- Length of cut = 200 mm
- Length of billets = 300 mm
- Depth of cut = 1 mm.

3.4.0 Coated and Un-Coated Inserts

Two sets of tool insert were used for the cutting tests. They were all Kennametal K313 tungsten carbide made of a hard, low binder content, unalloyed W_C/Co fine-grained grade, bearing commercial code CNMA-432 Cemented Carbide. The plain unmodified ones were used as control specimens for the experiments. The test specimens (inserts) had crater-like surfaces on the rake face, as explained in preceding chapters. Figures 3.3 and 3.4 are of the same insert before and after coating.

Figure 3.3 Carbide K313; CNMA-432, Uncoated EDMed Insert	Figure 3.4 Carbide K313; CNMA-432 EDMed Modified and TiN-Coated Insert by PVD process
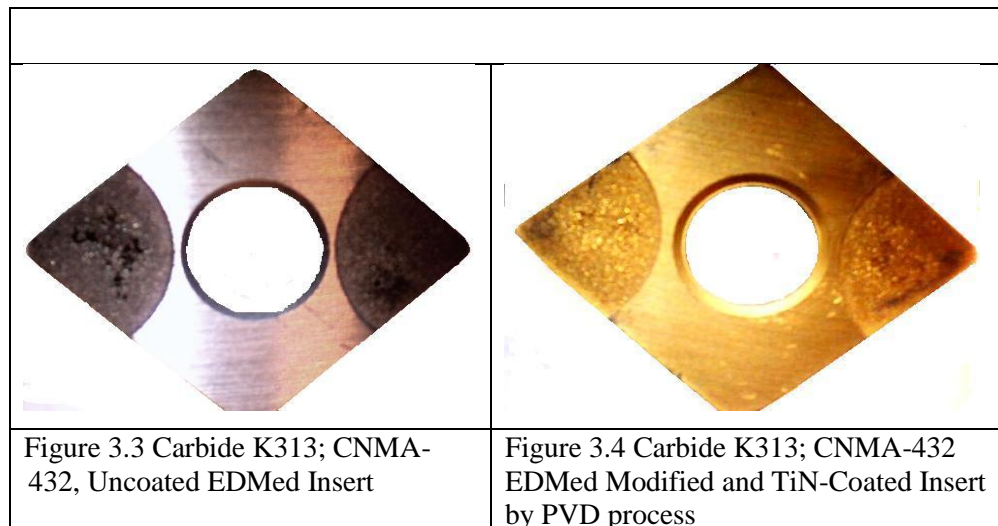
3.5.0 Power Requirement

In physics we know that power consumed in machining is a product of force and velocity (speed of machining), since power input during cutting is expressed as F_cV, where F_c is the cutting force and V is the cutting speed.

therefore

$$Power = F_cV$$ Equation 3.1

During machining, the tool sheared the workpiece material at the tool–chip interface known as the friction zone. At the friction zone power was dissipated. Power load or readings were taken from a monitor on board the CNC lathe. Knowledge of the forces and power involved in cutting operations was important for the following reasons:

a) Power requirements must be known to enable the selection of a machine tool with adequate power.

b) Data on cutting forces is required:

   i. for the mathematical modelling of the cutting process in this research,

   ii. to determine, in advance, the capability of the work for actual production, whether the workpiece is capable of withstanding the cutting forces without excessive distortion,

   iii. for the proper selection of machine tools for the job to maintain the desired tolerances for the finished part, tooling and tool-holders including work-holding devices.

3.6.0   Expressions for Surface Roughness in Turning

The machined component could be seen under microscope as showing the tool profile etched on the machined surface (Figure 3.5), bearing in mind that the geometry of feed marks depends on feedrate, side-cutting edge angle, nose radius and end-cutting edge angle.
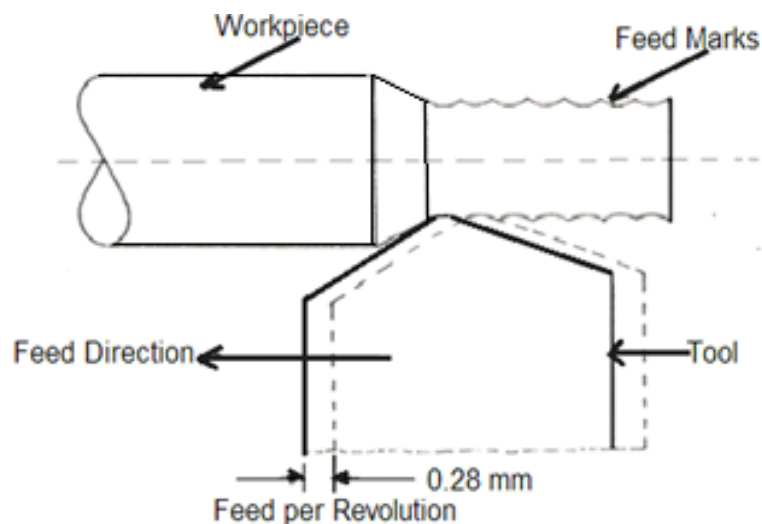
Figure 3.5 Feed Marks Etched on the Work during Machining Operations

It is well known that cutting fluid has some indirect effect on tool life during machining operations. The right type of coolant for machining mild steel was used in the experiment. The lubricant worked as a coolant and reduced tool wear by keeping the cutting edge lubricated during the process. It therefore acts as a lubricant, and tends to reduce friction between the sliding surfaces of the tool, work and chip; thus, these properties tend to improve to a limited extent the surface finish of the machined surface. In the absent or application of the wrong type of coolant the followings could have occurred;

- friction increase at the chip-tool and work-tool interfaces thus the tool energy rises.

60

- temperature rise resulting in high tool wear /deformation due to the high heat.
- the shear energy in the primary zone increases.
- surface finish is likely to deteriorate.
- Tolerances may be difficult to maintain because of the increased temperature and expansion of the workpiece during machining.

3.7.0 Tool Numbering Function for CNC Turning Lathe

CNC lathes require the programming of the selected tool by its tool number, using the T address for the tool function. This function is more extensive and calls for additional information on the actual tool change. For example the rough turn tool was number one and was defined as T01 in the program and was mounted in the turret station number 1, a tool defined T20 must be mounted in turret station number 20, etc. The format for the turning system is T4, or more accurately T2+2. The first two digits identify the turret station number and geometry offset; the last two digits identify the tool wear offset number for the selected tool station see Figure 3.6 below. Geometry offset identifies the position of the tool from program zero, and tool wear was used for fine-tuning dimensions.

The TXXYY format represents tool station XX and wears offset number YY. For instance T0606 will cause the turret to index to tool station number 6 (first two digits) which will become the working station (active tool). At the same time, the associated tool wear offset number (the second pair of digits) will also become effective. The selection of the tool number (the first pair of digits) also selects the geometry offset on modern CNC lathes. In that case, the second pair of digits will select the tool wear offset number.
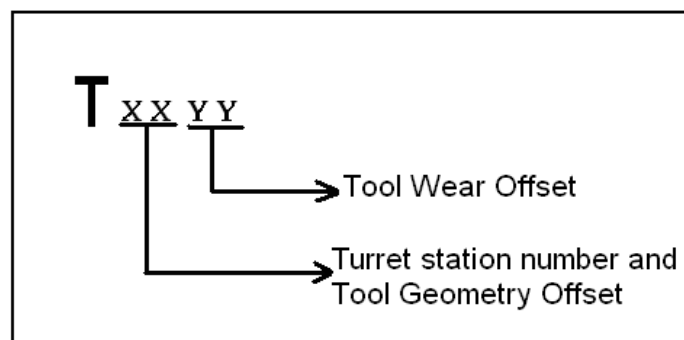
Figure 3.6 Typical Tool Function Address for CNC Lathes

In this cutting test the tool station selected by the turret station identification was associated with offset number within the available offset range as in most machining applications, only one offset number is active for any selected tool. In this case it was wise to program the offset number to be the same as the tool number, this approach made the operator's job easier.

61
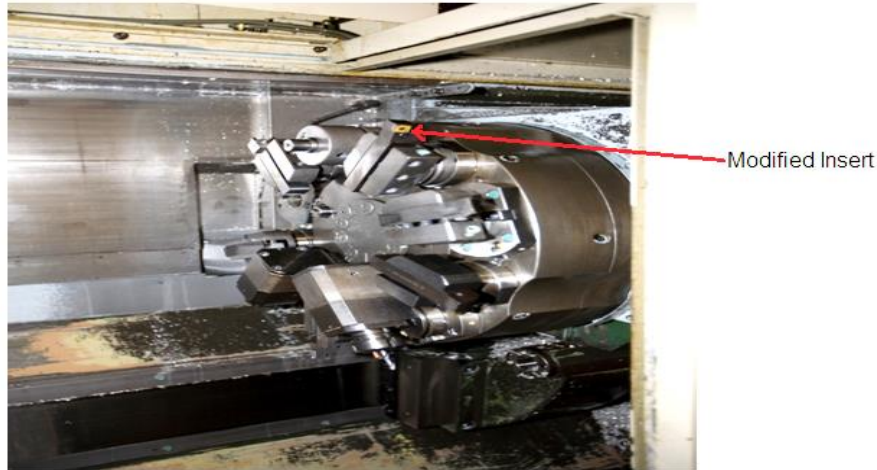
Figure 3.7 Modified Tool on the Turret.

The geometry offset was measured for each tool to establish the actual distance from the tool reference point to the program zero (Z axis distance was stored as a negative value as the X diameter). The CNC programme for the machining processes are in appendix II

3.8.0   Novelty of the Crater-like Topography

In this study, the test specimens (EDMed inserts) showed signs of resistance to wear for a much longer time. The novelty/ reason of the crater-like surface topography exhibiting wear resistivity is that the TiN coating remained trapped longer in the valleys and behind the peaks which considerably 'improve the tool performance by suppressing the mechanisms of the tool edge wear' (Jacobson, Wallén and Hogmark, 1987). Ezugwu *et al* (2001) conducted a comprehensive study of the wear of carbide tungsten (K-313) turning inserts coated to a thickness of 4 µm. They used three different coating materials (TiN, TiC and Al_2O_3) but for the same Cobalt-enriched substrate though two different tool shape (Trigon and Rhomb). Their results showed that the test specimen coated with TiN had superior in terms of removal index. This is probably due to the slightly higher substrate hardness, the greater strength of the 80^0 rhomboid insert over the trigon, and the low friction of the relatively thin TiN outer layer of coating (Shaw, M.C., 2005, Ezugwu, *et al*, 2001). PVD coating of W_C-Co with TiC and TiN enable higher cutting speeds (Shaw, M. C., 2005)

3.8.1   Results collected

The information collected indicates that the cutting tool was exposed to various mechanisms of degradation during the machining process. Chipping and plastic blunting destroyed the tool edges, especially those of the control specimens refer to figure 3.12, which are typical of intermittent metal cutting operations.

62

Söderberg (1986) stated that such tool wear degradation is a result of 'continuous mechanisms such as abrasive, adhesive or continuous wear', and Wellèn (1989) supported that statement. Furthermore, Stephenson and Agapiou (2006) in their book *Metal cutting theory and practice* stated that cutting tools must be made of materials harder than the workpiece material, and that the tool must be able to with stand the heat generated in the metal-cutting process. Stephenson and Agapiou (2006) continued by stating that, ideally, tool materials must have the following properties:

i. High penetration hardness at elevated temperatures to resist abrasive wear.

ii. High deformation resistance to prevent the edge from deforming or collapsing under the stress produced by chip formation.

iii. High fracture toughness to resist edge chipping and breakage, especially in interrupted cutting.

iv. Chemical inertness (low chemical affinity) with respect to the work material to resist diffusion, chemical and oxidation wear.

v. High thermal conductivity to reduce cutting temperatures near the tool edge.

vi. High fatigue resistance for tools used in interrupted cutting.

vii. High thermal shock resistance to prevent tool breakage in interrupted cutting.

viii. High stiffness to maintain accuracy.

ix. Adequate lubricity (low friction) with respect to the work material to prevent BUE, especially when cutting soft or ductile materials.

3.9.0 Observed Outcomes of Chip Rubbing on Rake Face

The cutting tool was subjected to cutting forces that were concentrated over quite a small contact area on the rake face and the flank. Also the chip was sliding over the rake face and this created primary wear mechanism.

Figure 3.8: SEM image showing marks left by chips sliding over tool rake face

During the machining operation, sparks could spatially be seen flying over the contact surfaces, an indication that the temperatures in the cutting zone could be rather high. Each time the tool entered and exited from the cut it was subjected to mechanical as well as thermal shock. The results showed the following; primary wear and progressive wear. Both primary wear development and crater wear mechanism are explained in the next section

3.9.1 Primary Wear Mechanism

The primary wear mechanism was by way of abrasion caused by the chip rubbing against the tool surface. Results showed that at all speeds the EDMed surfaces had a much higher resistance to wear see pictures of specimens in appendices 1A – 1C. Whereas the TiN coating on the rake faces of the control specimens visibly appeared to be worn off after a short duration of cutting. The coating on the EDMed surfaces was visibly held for a much longer duration of cutting. Crater wear is one of the factors that determine the life of a cutting tool. After some duration of cutting, cratering became so severe that the tool edge was weakened and eventually fractured. Crater wear developed on the rake face of the tools. Figure 3.9 illustrates the main manifestations of tool wear: flank wear and crater wear.
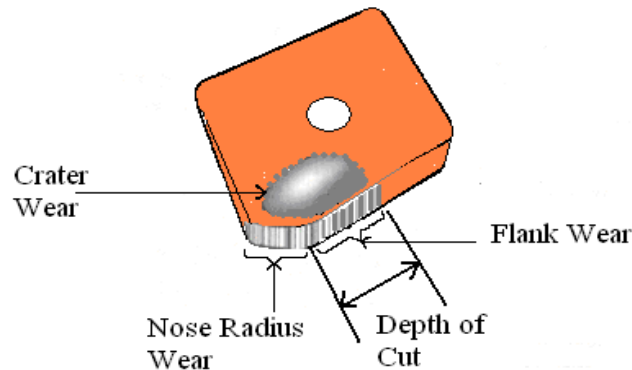
Figure 3.9 Types of Wear on a Single Point Cutting Tool

Wear on the flank caused by friction between the newly machined workpiece surface and the contact area on the tool flank. The wear started to develop around the tool corner radius and progressed along the cutting edge.

3.9.2 Progressive Wear

The progressive wear on the sets of tools took place on the rake face and flank. The wear-land wear, which occurred, can be summarised as crater and flank wear since:

3.9.3 Development of Crater Wear

Wear on the rake face developed as a crater resulting from the friction between the chip undersides rubbing along the tool rake face. It occurred on the rake face of the tool in the form of a pit called the crater. The crater was formed some distance from the cutting edge. Crater wear usually results from temperature-activated diffusion or chemical wear mechanisms (Stephenson and Agapiou, 2006). Although the chips sliding over it has a lower yield stress, it might have become so much work hardened as to be able to exert frictional stress sufficient to cause yielding by shear of the hard tool material on the rake face. It is known that the higher the temperature at the interface, the greater this effect. Figure 3.10 shows how the radius of curvature R_c, the depth of crater d_c, the width of crater b and then distance of the start of the crater from the tool tip a changed with time.   The crater significantly reduced the strength of the tool and led to its total failure. Wear on the rake face took place in the form of a crater away from the cutting edge in a zone where the temperature was the highest.
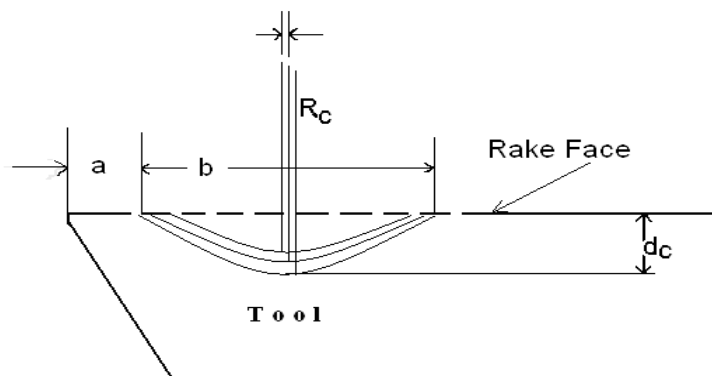
Figure 3.10: Progress of Cratering

3.9.4 Development of Flank Wear

Secondly, wear on the relief face is called flank wear and it developed at a point where a wear-land is formed by the rubbing action of the newly generated workpiece surfaces against the tool cutting point. This wear produced wear-lands on the side and end flanks of the tool on account of the rubbing action of the machined surface. The wear-land developed and grew in size due to abrasion, adhesion, diffusion and shearing.
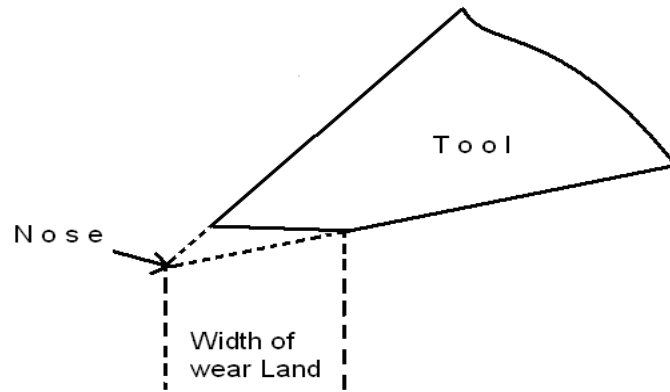
Figure 3.11: Progression of Flank Wear

3.9.5   Chipping of Tool Cutting Tip

Chipping refers to the breaking away of small chips from the cutting edge of a tool or an insert due to the impact of excessive plastic deformation, transient thermal stresses, localised cooling, chatter and excessive cratering and flank wear. When fracture occurs near the cutting edge and results in the loss of only a small part of the tool, it is referred to as edge chipping or fretting. The chipping, which occurred in this experiment, was examined by the appearance of the cutting edge and flank wear-land. The cutting edge appeared too jagged (serrated), and there were cavities showing signs of depression in the wear-land, and this meant that chipping had occurred. It is known that mechanical impact may be caused by intermittent cutting, hard spots in the workpiece, or a sudden change in dimensions of the cut.

Cutting forces of a sufficiently large magnitude may deform the cutting edge so much that the cutting edge fractures. Excess crater wear weakens the cutting edge of the tool and can lead to the deformation or fracture of the tool this was dealt with in chapter 2 section 2.8.0.

3.10 Effect of Coating Material Chemical Properties on Surface Finish

Chemical composition, hardness, micro-structural and metallurgical consistency are known from experience to affect surface finish. TiN has been proven to have excellent chemical stability, and because of this it was mostly used as a diffusion barrier on high temperature resistant alloys in addition TiN also has good resistance properties to oxidation (Navinsek *et al* 2001, Holmberg and Mathews 2009, Stephenson and Agapiou, 2006, Hermann, A. J. M., 2000, Clapa and batory, 2007 and Hedenqvist *et al* 1990). In this research, cutting tests revealed that even when the coating had been partially removed by edge wear, prolonged tool life was still obtained. This fact was explained by Kassman *et al* (1989), when they tried to prove the presence of a '*smearing mechanism*' and assumed that TiN material was

66

continuously transferred from the coated region of the edge on to the uncoated, thereby modifying the contact conditions by atomistic wear process and hence reducing the wear rate

3.10.1 Workpiece Surface Finish Readings

The 'ideal' surface finish is a function of the tool corner radius and the feedrate. The real surface finish is influenced by additional factors such as BUE formation, machine tool vibrations and the 'Sokolowski effect' (sideways extrusion of work material). The surface finish produced by the EDMed inserts was clearly better than those of the control specimens details are discussed in chapter 2.

Results show that, the workpiece suffered intense mechanical stress and localised heating by the tool cutting edge as it locked onto the work. As more heat was generated the tool developed flank wear and the surface of the component gradually deteriorated, because the roughness of a machined workpiece increases in proportion to the damage suffered by the cutting edge (tool flank). Generally, surface finish is influenced by several machining parameters including cutting tool geometry, workpiece geometry, machine tool rigidity, workpiece material, cutting conditions and tool material.

3.11.0 Effects of Speed on Built-up Edge Formation

The high cutting speed in general tends to improve surface finish. The reasons are as follows:

- ☐ At low cutting speeds, the cutting forces are high and the tendency of work material to form a BUE is stronger.
- ☐ Due to an increase in temperature and the consequent decrease in frictional stress at the tool rake face at higher cutting speeds, cutting forces and the tendency towards BUE formation weakens.

Thus as the speed increased from 250 m/min to 300 m/min, conditions became more and more favourable for built-up-edge formation. However, when the cutting speed increased further to 325 m/min, the built-up-edge started to disappear owing to the increased temperature. Finally, at a cutting speed (V_c) of 350 m/min, which was a sufficiently high speed, the built up-edge disappeared altogether and the surface finish became insensitive to cutting speed. Both these effects are beneficial for surface finish as demonstrated in Figure 3.13.
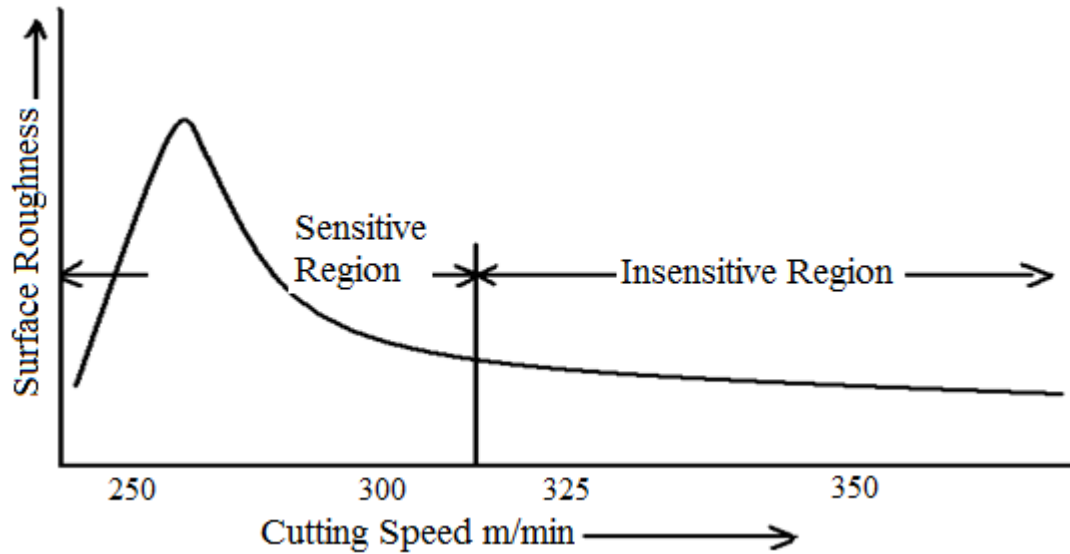
Figure 3.13 Effect of Cutting Speed on Surface Roughness.

For the plain uncoated control specimen in the verifiable comparative test the first insert failed after 4 cuts. Meanwhile, for the second and third inserts the control specimens failed after 5 cuts/passes, while the test specimens (EDMed but uncoated inserts) managed only 5 cuts and the tools developed chipping. In the first set of comparative cutting tests of experiments done at the same cutting speed with TiN-coated inserts, the plain-coated control specimens managed between 26 and 28 cuts/passes, and the test specimen completed 32 cuts/passes and was still capable of doing more cuts.

3.11.1 Effects of Undulating Surface on Tool Performance

The project aimed to study the performance of a TiN-coated tool with undulating surface topography in reducing tool wear. Dechjarern (2002) studied the friction and wear behaviour of a coated cutting tool with different surface topographies, and hypothesised that 'there may be a region of surface roughness, R_a/R_{sm}, where the cutting tool wear resistance is optimum as a result of low contact area, friction and low amount of build-up of wear debris' in the valleys on the tool rake face. To verify this hypothesis during the course of this particular work, experiments were carried out, herein called the 'verifiable comparative test'. From the experiments it was proven that built up and wear debris in the valleys had no effect in resistance to wear, but rather that the TiN coating had an impact because the TiN coating with high hardness acted as a heat barrier and lubricant to the substrates. TiN is typically 3–4 times harder than heat-treated steel, and because the coating exactly follows the shape of the component and the thickness is 4 μm thick it is presumed that the TiN coating continued to provide protection to the substrates. It is known that titanium is a hard ceramic with a high

68

melting point. These properties of the coating material protected the substrates longer by atomising smearing effects (Wallén and Hogmark, 1989). Wallén and Hogmark (1989) stated that 'although the coating is worn off by way of a crater, the remaining coating (along the rim of the wear scar) continues to offer resistance to wear'. To explain this point, Kassman *et al* (1989) tried to prove the presence of a 'smear mechanism'. They assumed that TiN material was continuously transferred from the coated region of the edge to the uncoated, thereby modifying the contact conditions by an atomistic wear process and hence reducing the wear process. This gold-coloured coating offers excellent wear resistance for a wide range of materials, and allows the use of higher feedrates and cutting speeds.
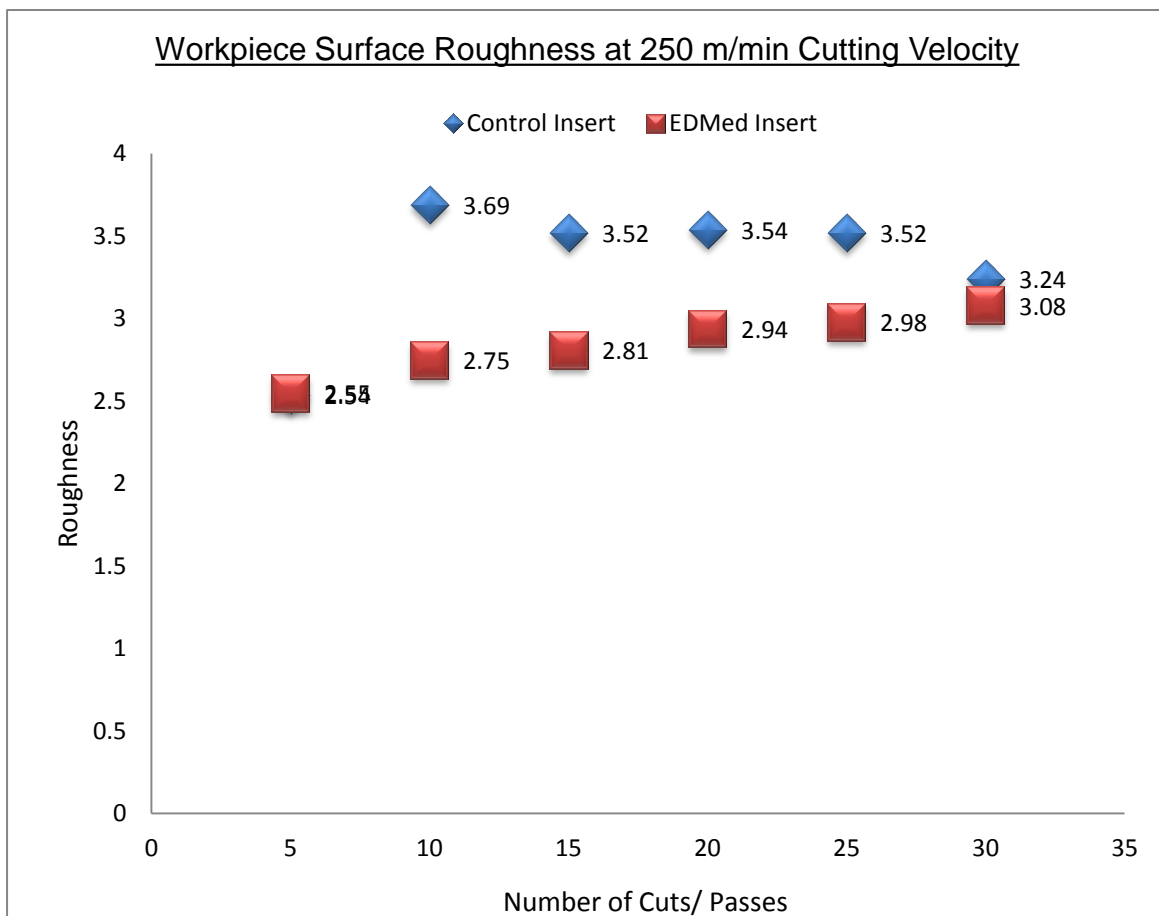
Figure 3.14: Workpiece Surface Roughness Machined at 250 m/min

3.11.2 Behaviour Patterns and Mechanics

The work surface finish readings after 5 cuts for the control specimen was Ra = 2.54 and the test e modified inserts Ra = 2.58. However, after 10 minutes or cutting the reading changed dramatically for the control insert, which registered surface roughness of 3.69 m against 2.75 for the modified insert. Here the tool could have hit some hard spots within the workpiece.
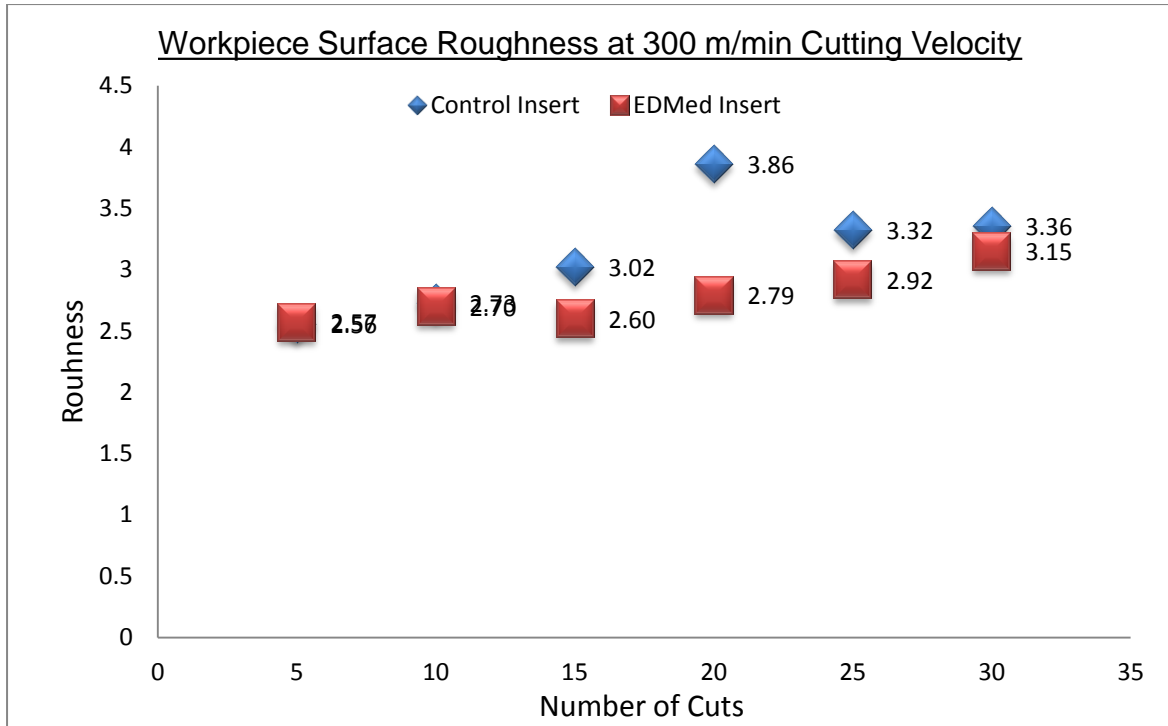
Figure 3.15 Workpiece Surface Roughness Machined at 300 m/min

For the first 10 minutes, the work surface finish readings were similar but there was drastic change in the surface finish reading after 20 minutes of cutting for the control specimen this could be dues to adiabatic cutting conditions at the tool-work interface. Generally, the surface finish of the workpiece machined by the modified tool was better than that machined by the control specimen.
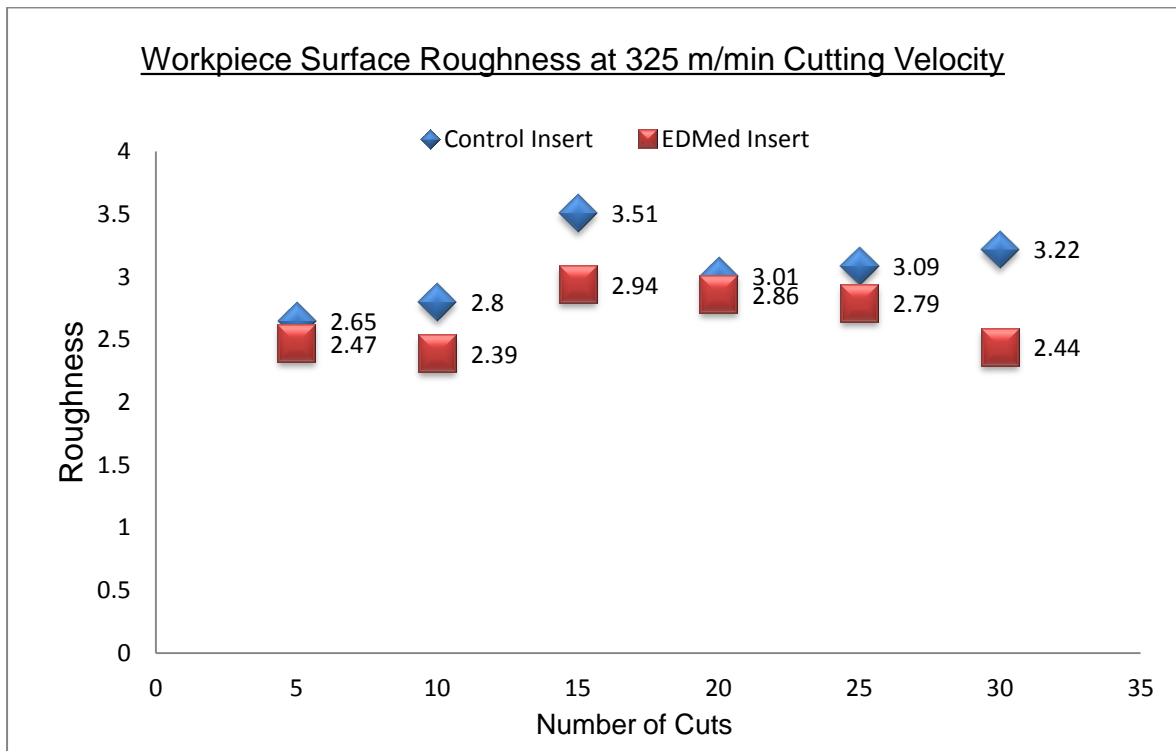
Figure 3.16: Workpiece Surface Roughness Machined at 325 m/min

70

At this cutting speed of 325 m/min the workpiece machined by the control specimen registered surface measurement reading (Ra) value of upto 3.5 µm. Meanwhile, the surface finish produced by the TiN-coated EDMed inserts was clearly better than those of the non-coated specimens.
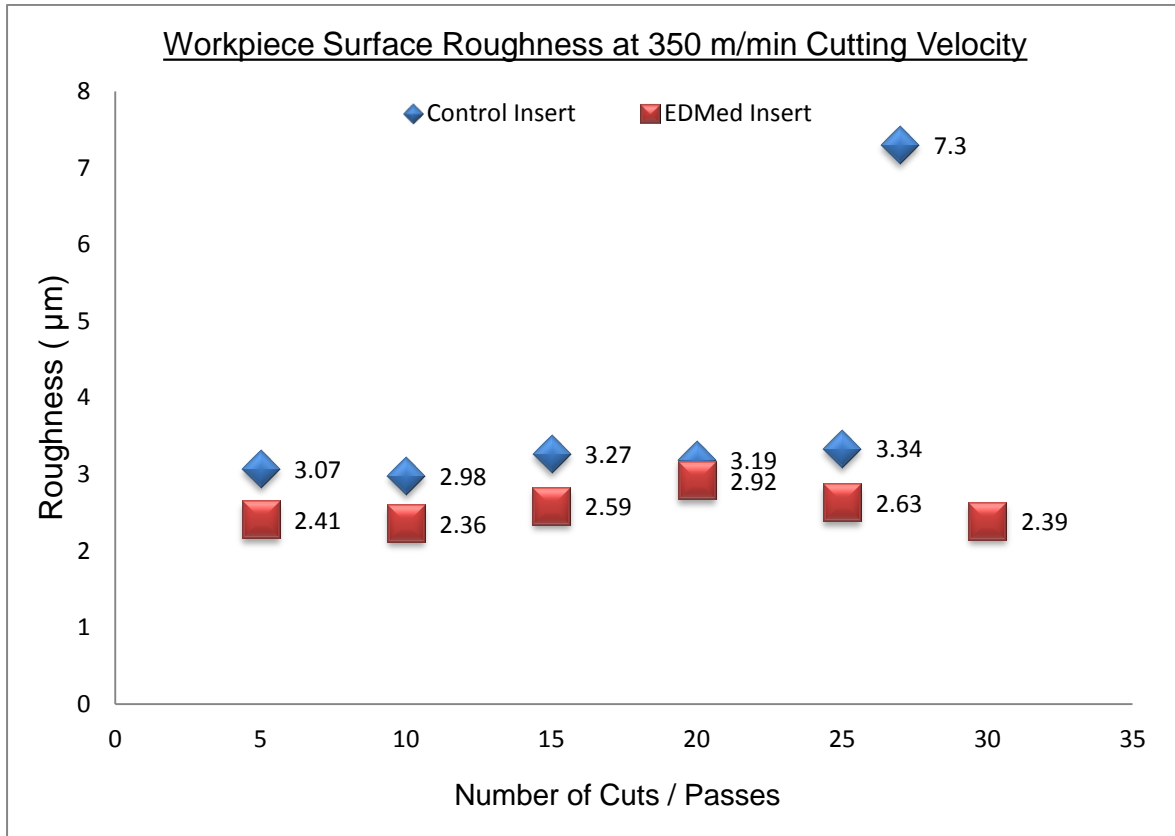
Figure 3.17 Workpiece Surface Roughness Machined at 350 m/min

Here the control specimen failed/ chipped at 27 cuts registering work surface finish of 7.3 µm, but the modified tool could do upto 35 cuts. The graph indicates that the surface finish produced by the non-EDMed inserts was rough as all the readings taken were above (Ra) 3 µm. Meanwhile, the surface finish produced by the TiN-coated EDMed inserts was clearly better than those of the non-coated specimens were. The table in appendix Ia - Ic shows that the EDMed inserts produced low power readings at all speeds investigated. Furthermore, the surface finishes on the work were consistently better for the EDMed inserts

Chapter 4

Field Tests and Tools Performance Characteristics

Two Field-cutting Tests were carried out at Kennics Engineering and Newton Engineering both in Barking, Essex. The components made were standard parts that the companies usually supply to their dedicated customers

4.0   Introduction

Field tests formed part of the objectives of this study. The aim of the trials was to evaluate the performance of the modified tool in a real-world manufacturing environment and make performance comparison between the modified tool and the standard conventional inserts the companies normally use. The comparison was in terms of tool life and for consistency; the companies' tool life criterion was followed. The first field test was carried out at Kennics Engineering and the second test conducted at Newton Engineering Ajax Works. Both these companies are engaged in metal machining producing components for aircraft, automotive and defence industries. Since the components produced were for the companies' dedicated customers, the organisation's quality standard and the customer job specifications were followed.

4.1.0   Field Test Number 1:.Production of Fuel Ring for Armoured Vehicle
This was done at Kennics Engineering –Barking Essex
4.1.1   Aims
To carry out machining operations of stainless steel grade EN-316 on CNC Lathe Machine at cutting speed of 325 m/min using modified TiN coated inserts in order to collect information on the progressive wear-land of the modified tool (test specimens) and then compare the wear characteristics against the company's own conventional tools.

4.2.0   Equipment /Apparatus used

- Hitachi Sehiki, Computer numerical control (CNC) Lathe machine,

- Digital Bresser Microscope for examining the tool wear profiles,

- Tungsten carbide (W_C) rough turn tool inserts, with chip breakers having corner /nose radius ($R_\mathcal{E}$) of 0.8 mm,

- Tungsten carbide (W_C) finish turn tool inserts, with chip breakers having corner /nose radius (R_ε) of 0.6 mm,
- Stainless steel billets 44 mm long and 75 mm (ϕ) diameter,
- Boring tool holder,
- Turning tool holder.

4.2.1 Work and Tool Materials

- The workpiece was Stainless steel grade EN-316 with yield strength of 394 MPa and Brinell Hardness of 200 Bhn.
- The tool inserts used were Kennametal K313 tungsten carbide made of a hard, low binder content, unalloyed W_C/Co fine-grained grade.

4.3.0 Cutting Test Procedure

The company's manufacturing procedures were followed; the followings were the systematic approach, which were taken;

  i.   Visually checked that surface profile of the workpiece was undamaged in accordance with BS EN ISO 8501 (*visual assessment of surface cleanliness*)

 ii.   Workpiece setting. Used probe to input coordinates from a datum position so that the CNC machine controller could work out the angular offsets for all the coordinates accordingly.

iii.   Started up the computer on the lathe machine to recall the CNC part program from the database and the Q-Setter was used to measure the dimensions of the tool inserts.

 iv.   Turn on coolant supply and set it at 50 m/sec so that it was strong enough to wash away debris and lubricate the cutting zone.

  v.   Coolant nozzles where located in directions A (End Clearance angle) and B behind the chip for effective application as illustrated in the figure 4.1 below. Taylor (1907) demonstrated that tool life could be increased by 40% over cutting in air if the coolant nozzle was located and sprayed behind the chip in direction B as seen in the diagram. Meanwhile, Niebusch and Strieder (1951) advised the application from both directions A and B when heavy cuts are taken.
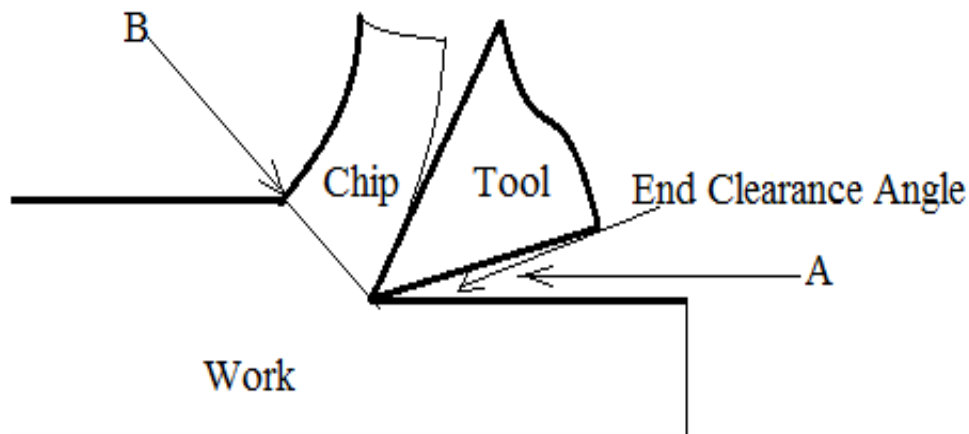
Figure 4.1 Directions of Coolant application during the machining tests

Lauterbach (1952) demonstrated an increase in tool life when the lubricant was introduced in direction A. Pigott and Colwell (1952) supported that analysis. In this machining process, coolant was sprayed in both directions and this is the setup procedure that Kennics Engineering always uses for turning operations.

vi.   Ensured that the doors were closed and started the machine to do the machining process.

vii.   To comply with the company own quality assurance guidelines, one out of every ten components produced were checked for quality and tolerance compliance. The features inspected were;

   a) The workpiece dimensional accuracy. The components had design features with dimensional tolerances. A worn-out tool would produce components outside the design specifications. The frequent checks aimed to eliminate the anomaly.

   b) The work surface roughness measurement (ISO 5436-1: *Geometrical product specifications* appendix IV). The company's requirement was that each workpiece surface roughness must be equal to or less than Ra value of 2.55 μm. Before taking surface roughness measurement, the components were lightly cleaned with a dry fine bristle brush to remove any particle of dust according to ISO 8501 guidelines on surface preparation prior to measurement.

   c) Scratch marks on the machined surface. Scratch marks generated by blunt or worn out tool when blunt tool flank side rubs on the workpiece. Availability of scratch marks would normally make the component be assigned to reject Bins.

viii.   Consistently monitored power load using the on-board computer monitor on the Lathe (machine tool) to ascertain the energy usage for every cut. Increased power load

would be a sign of deteriorating / worn out tool condition that renders the tool unsuitable for use. Worn out tool would produce defective goods.

ix.   Photographs of the tool were taken at various stages/ intervals during the production run to evaluate the tool remaining useful life.

4.3.1   Machining Process Parameters

Cutting velocity (V_c) of 325 m/min was used. This represents a 30% increment on the recommended machining speed for the type of conventional tool and work material. This speed was earlier on used in cutting experiments done under laboratory conditions with the modified tool inserts. Results obtained showed good work surface finish and longer tool life.

The feed rates were set in accordance with the principle that the tool feed-rate must be half the tool nose radius. For this particular carbide tool the nose radius was 0.8 mm for the roughing tool and 0.6 mm for the finish (wiper) insert. The following cutting parameters were used:

* cutting speed (V) = 325 m/min,
* depth of cut (d) = 1 mm,
* rough turn feed-rate (f) = 0.4 mm/rev,
* finish turn feed-rate (f) = 0.3 mm/rev,
* Coolant pressure jet velocity set at 50 m/sec.

4.4.0   Observed Results and the Tool Performance

Each component had a production cycle time of 6 minutes on the CNC machining centre. For the eight and half hour available time for production, 76 components (pieces) were made. There was 30 minutes interlude for lunch. Some minutes were lost during loading of the work billets into the chuck and during tool inspection procedure, which was necessary to monitor the tool progressive wear-land. Tables 4.1 and 4.2 show comparative tool conditions for the modified tool after rough and finish machining operations. Meanwhile, tables 4.3 and 4.4 give comparative results for the company's conventional tools used for rough and finish turn respectively.

Table 4.1: EDMed Modified Tool Inserts Used for **Rough Turn**
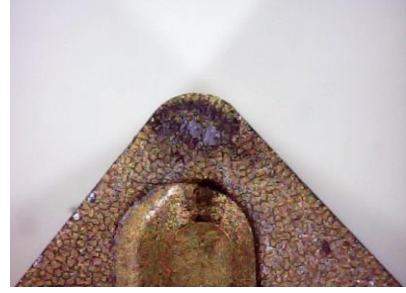
External Diameter Machining	Internal Diameter Machining
20x	20x
• Rake face for the outside diameter for the rough turned tool inserts after **sixteen** components • The tool cutting tips still undamaged	• Rake face for the internal diameter for the rough turned tool Inserts after **sixteen** components • Sign of wear emerging attributed to adiabatic conditions

Table 4.2: EDMed Modified Tool Inserts Used for **Finish Turn**
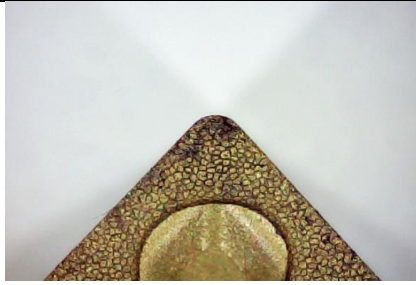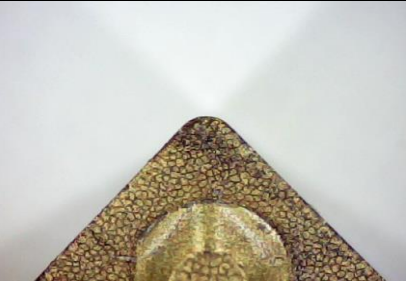
External Finishing Turn Inserts	Internal Finishing Turn Inserts
20x	20x
• Rake face of tip used for external finish turn after **sixteen** components • The tool's Cutting tip unscathed	• Rake face of tip used for internal diameter finish turn after **sixteen** components • Cutting tip unscathed

Table 4.3: The Company conventional/ control specimens used for **Rough Cut**
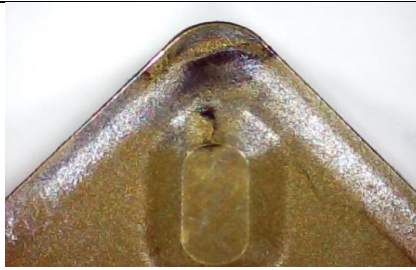
External Diameter Machining	Internal Diameter Machining
20x	20x
Rake face for tool used for rough turn on outside diameter after **six** components	Rake face for tool used for rough turn after three components. Chipping occurred on the **third** component

76

Table 4.4: the Company's conventional control specimens used for **Finish Turn**

External Diameter Machining	Internal Diameter Machining
20x	20x
Rake face of outside diameter finishing tool after **sixteen** components	Rake face of internal diameter finishing tool after **sixteen** components

4.4.1   Components Made

The components produced by both control and modified inserts were tested for design specifications compliance and surface roughness as explained in section 4.3.0 (vii) and all components made by the modified EDMed TiN coated inserts passed the tests.   The components had good dimension accuracy (design specifications) and quality (surface finish) repeatability. Figure 4.2 below is a photographic picture of a few of the swarfs produced and the components are in presented in appendix IX.

4.4.2   Tool Analysis and Swarfs Produced

The performance of both insert types appeared to be comparable for the rough turn machining processes. However, under high magnification, cracking could be seen on the rough turn control insert while the EDMed modified inserts remained undamaged. In tables 4.1 and 4.3 the roughing tool inserts show no sign of wear for the external rough cuts, while for the internal cuts, slight wear developed presumably due to adiabatic conditions at the tool-work and chip-tool interfaces. The chip thickness measurements for the EDMed inserts were taken and found to be 1.43 mm and for the conventional tool inserts, the thickness was 1.53 mm.

Figure 4.2:   Long Shiny Swarfs Generated by EDMed Modified Tool. Chip thickness was 1.43 mm

4.4.3 Presence of Temper Colours on the Chip

The control or conventional inserts produced dark bluish discoloured Swarfs (figure 4.3) evidence of high temperature at the chip tool interface. Available literatures show that temperature of at cutting zone may reach high value particularly when a heavy cut is taken at high speed. This is evident when the work or tool is touched; by the presence of temper colours on the chip, work, or tool (Shaw, M. C., 2005, Stevenson and Oxley, 1970 and Fenton and Oxley, 1970).
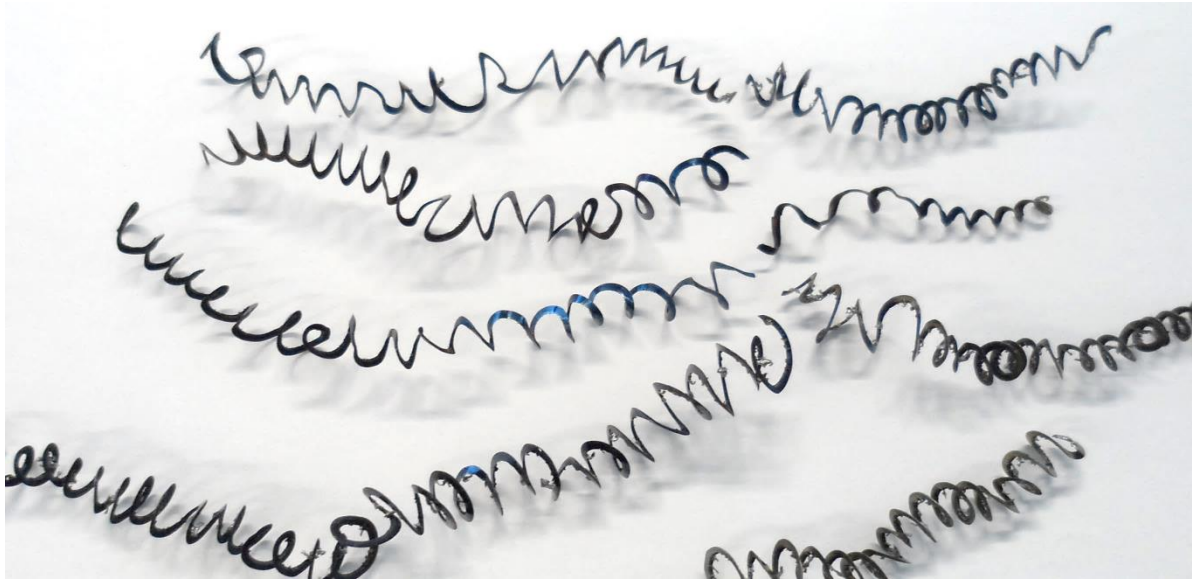
Figure 4.3: showing Heat-affected, discoloured Swarfs produced by Control Inserts. Chip thickness was 1.53 mm

4.5.0 Field Test Number 2: Production of Lift-Hub
This was done at Newton Engineering

4.5.1 Aims: Same as in Test one above but with different grade of work material (stainless steel grade 416)

4.5.2 Equipment/ Apparatus

- Computer numerical control (CNC) lathe,
- Digital microscope for inspecting the Tool inserts after cutting intervals,
- Tungsten carbide (W_C) rough turn tool inserts with chip breakers and having corner/nose radius (R_ε) of 0.8 mm,
- Tungsten carbide (W_C) finish turn tool inserts with chip breakers having corner/nose radius (R_ε) of 0.6 mm,
- Stainless steel billets 100 mm long and 75 mm (ϕ) diameter,
- 10 mm Twist Drill Bit,

4.5.3   Work Material

The work material was stainless steel grade 416 with the following properties:

- Ultimate Tensile Strength of 515 MPa,
- Brinell hardness of 222.
- This material is much harder and more brittle than the grade 316 machined in test one and the free cutting mild steel used in the laboratory work discussed in chapter three.
- The tool inserts used were Kennametal tungsten carbide made of a hard, low binder content, unalloyed W_C/Co fine-grained grade. This tool grade was chosen because of its strength and capability to do the machining process required.

4.5.4   Procedure

a) All process parameters and machining procedures were maintained as in test one section 4.1.0 above except the hole drilling parameters and processes are discussed in the next section.

b) Used chucking reamer to remove 0.2 mm of material from the drilled hole surface to give a fine finish to the drilled hole. (Chucking Reamers are mounted in a chuck and operated by a machine in this case the CNC Lathe machine). Reaming was used to make the hole dimensionally more accurate than could have been obtained by drilling alone and in addition to improve its surface finish.

4.5.5   Drilling Parameters Used

a) Helical twist drill bit to make a 10 mm hole to a depth of 15 mm. By convention depth of drill hole (cut) must be equal to or less than one half of the drill diameter to prevent the drill breaking in the process.

b) Drill speed of 40 m/min and federate of 0.3 mm/rev was used. Cutting speed and feed rates for drilling are normally lower than most other machining operations because of the following reasons;

  i. It is difficult for the drill to eject Swarfs,

  ii. It is difficult to keep the cutting edges cool when they are enclosed in the hole,

  iii. The twist drill is weak compared with other cutting tools.

c) The reamer speeds was one-half (20 m/min) of that for the drill, and three times the feed rate (0.9 mm/rev).

4.6.0   Observed Tool Conditions and Performance

There was no difference in the tool conditions. The performances of both types of inserts were the same. Thus, no further action was taken.

4.6.1 Swarfs Produced in Second Test and Chip Thickness

The swarfs produced in this test were lookalike to those obtained in the first experiment in both colour and length. In all the machining processes, the chip tends to spread sideways, so that the maximum width is always greater than the original depth of cut. For simplification, the irregular cross section of real chips and the chip spread were ignored. A rectangular cross section is assumed. The idealised section normal to the cutting edge of a tool used in orthogonal cutting is shown in figure 4.5 below.
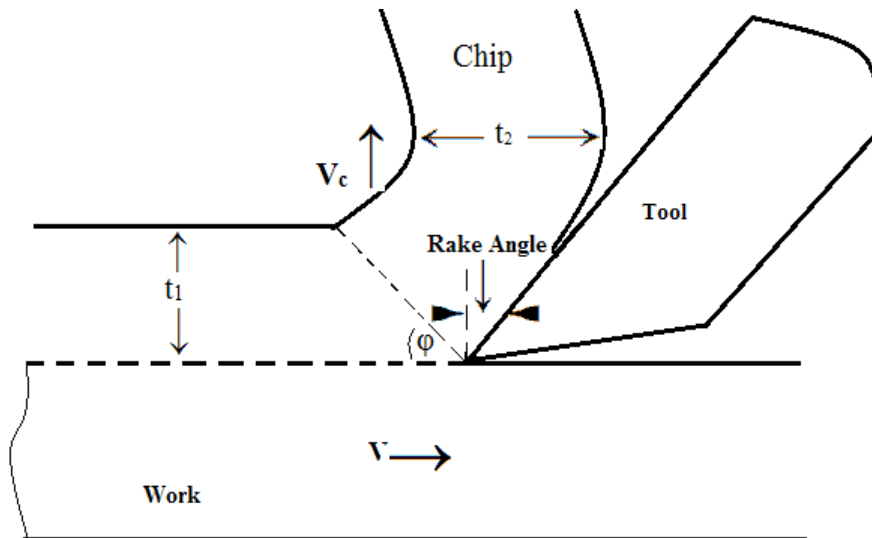
Figure 4.4: Illustration of Orthogonal Metal Cutting Process

It can be seen that the chip thickness ratio t_2/t_1, is geometrically related to the shear plane angle, φ, by the following equation;

$$cot\varphi = \frac{t_2}{t_1} \qquad\qquad \text{Equation 4.1}$$

The chip moved away with a velocity, Vc, which is related to the cutting speed V, and the chip thickness ratio, t_2/t_1, by

$$V_c = V\frac{t_1}{t_2} \qquad\qquad \text{Equation 4.2}$$

From the above equation, it was presumed that the chip thickness ratio depended on the shear plane angle. Further discussion on chip thickness ratio and shear angle relationship is in section 5.1.2 in the next chapter. In a small shear plane angle, the chip thickness ratio was high exhibited in figure 4.8, of the dark bluish Swarfs produced by the conventional tool. On the other hand a large shear plane angle formed a thin, high velocity moving Swarfs exhibited by the long shinny Swarfs

Figure 4.5: showing long shiny Swarfs in a Tray in the machining centre compartment.

Those outside the tray are dark bluish Swarfs produced by conventional tool inserts used by the company earlier during a machining process. The long shiny Swarfs were between 72 to 180 mm long. A few were as long as 350mm. The long twisting Swarfs were presumably produced due to the following factors:

a)   A high positive rake angle on the modified inserts.

b)   A sharp cutting edge of the inserts

c)   Low friction between tool and chip inherent of the TiN coating.

d)   The high cutting speed of 325 m/min
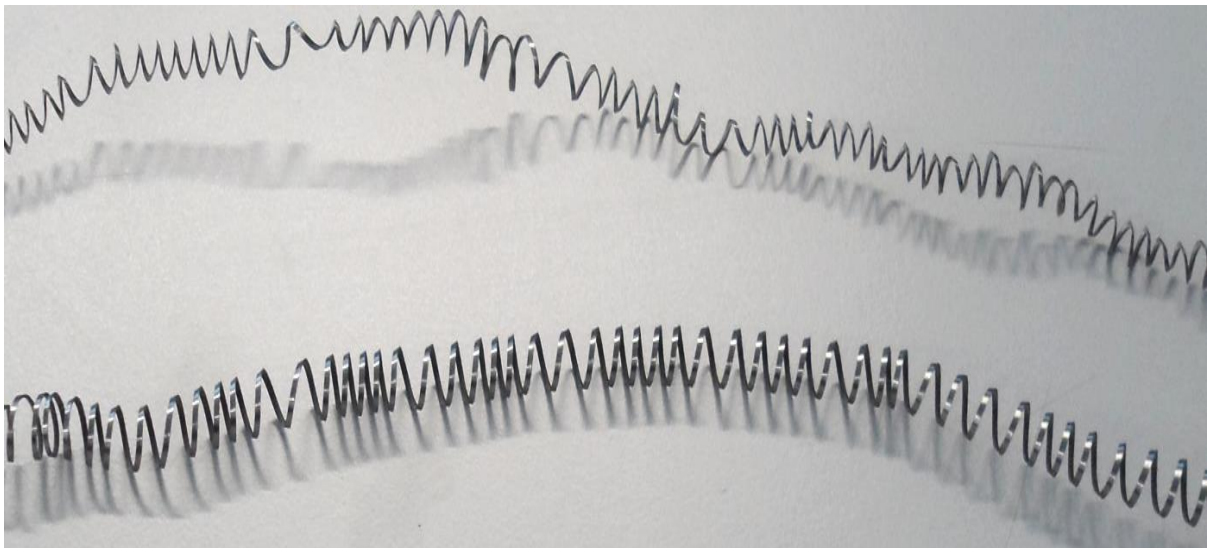
Figure 4.6: Long shiny Swarfs produced by TiN coated surface modified tool

On the other hand the dark-bluish Swarfs were much shorter in length mostly between 72 to 122 mm long but thicker in width (1.59 mm) compared to the shiny ones which measured 1.43 mm in thickness.
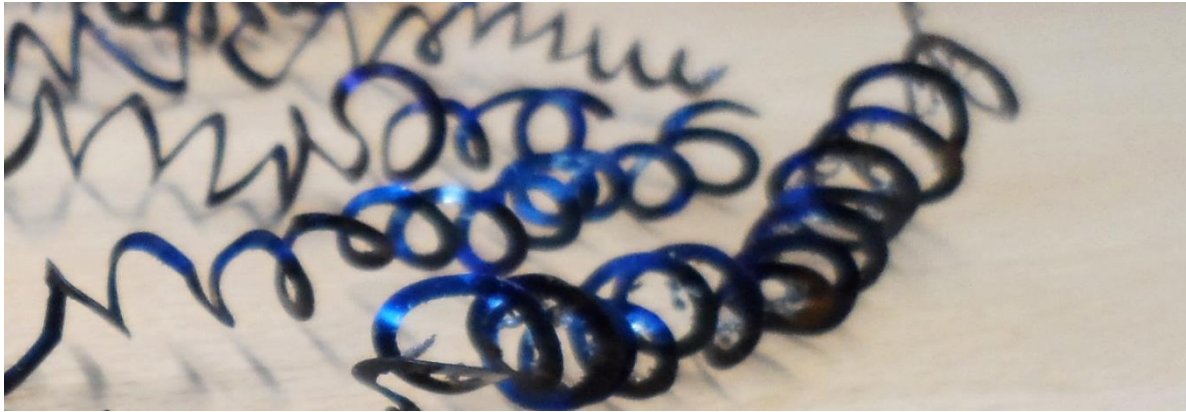
Figure 4.7: Dark-bluish Swarfs produced by conventional tool the company normally uses clearly showing the effects of heat / high temperatures

4.7.0   Components Produced at Field Test 2

During the field test /cutting experiment, 135 components were made over 8 hours of machining. The components made were standard parts the company supplies to a dedicated customer presented in appendix IX.

4.8.0   What is Preventing Heat from damaging the Cutting Tips

The work material stainless steel EN 416 was harder than the grade EN 316 used in the first field test. The modified inserts performed better showing little signs of heat deterioration. The following explanations assumption are arrived at;

a) The modified tools (with crater-like surface topography), though worn out after 65 components, continued to show remnants of the TiN coatings on the tool face which continued to protect the cutting tips as a thermal barrier but also as a diffusion barrier (Astakhov, V. P., 2006, Shaw, M. C, 2005, and Tantatov, N. V, 1992). Tantalov studied the effect of coating tool with TiN and the structure of carbide cutting tips. He proved that coating tool and proper cutting edge preparation improve tool life by reducing the common causes of failure, such as chipping and heat-induced failures.

b) The trapped TiN coating between the valleys and peaks on the modified tool influenced the thermo-conductivity on the tribological conditions at the tool-chip interface in two ways. First it affects the mean contact temperature, and secondly, it affects the temperature distribution over the surface since TiN has thermal barrier properties (Komvopoulos, et al, 1986, Schulz et al 2003, Sue and Troue, 1990). While, the control specimens had their coatings worn out completely. This helps to explain why the control inserts produced dark bluish Swarfs, which is a manifestation of high temperature effects.

4.9.0 Swarfs Generated and Their Characteristics

Characteristically, the Swarfs produced were long, shiny for the EDMed Inserts, and dark-bluish for the company's conventional tools, which leads to the following assumptions;

- Long shiny Swarfs (figure 4.7) produced which indicate that was low heat at the chip tool (EDMed inserts) interface. The long shiny Swarfs is evident of low friction and heat at the chip-tool interface due to the TiN lubricity properties (Shaw, M. C., 2005)

- The long Swarfs produced by the EDMed inserts could be an indication that the chip breakers were operating at a lower efficiency because part of the chip breaker got damaged during the EDM process.

- the high speed machining, caused the Swarfs to soften and deformed faster than the chip breakers could deformed and break them. This is attributed to the presence of titanium nitride coating which enabled higher cutting speeds and lower cutting forces due to action of nitrogen when the coating material is decomposed in the presence of the austenitic surface of the chip (Rao et al, 1978).

4.9.1 Power Load, Energy Consumption and Saving

In cutting mechanics we know that energy consumed during machining P_m is given by

$$P_m = F_c V$$

Where Fc is the cutting force of the tool and V is the cutting velocity. During the field test, the workpiece was sheared by the tool making it deformed plastically. Thus, converting most of the energy into heat as the material was subjected to high strains. However, as the tool was still sharp the heat source remained small and is neglected in this analysis.

The modified tool saved energy as it operated at 18% reduced power load on the 11 KW motor of the Hitachi Seiki CNC lathe. Which means that motor only used 9 KWhr worth of energy to machine the work which represents a saving of 1,980 KWhr

4.10 Remarks on Cutting Conditions Optimisation

From these tests, there is substantiation that resistance to wear of the coated modified substrates was good. The TiN coating lowered the friction coefficient at the chip-tool and work-tool interfaces. As a result, the decrease in friction also reduced the tendency towards adhesive wear. The EDMed inserts operated at 18% reduced power consumption. The reduction in power consumption is good for metal machinists/ industries involved in high volume production because the technology (tool with undulating surface structures) reduces their expenses on energy (electricity).

The high speed machining resulted in lowering the shear strength of the workpiece material at the work-tool interface, as it was deforming faster than the coolant could cool the zone given the fact that the heat had soften the work material and hence resulted in lowering cutting forces. This means that the rate at which workpiece material was softening due to the tearing of chip by the tool, was much higher than the tool deforming rate resulting in higher deformation softening of the chip (Zhan et al., 2000) thereby causing twisting (spiral) Swarfs. The observed results shows that if the tool surface roughness is within the 'operating window' and the coating applied consistently as discussed in chapter 2 the tool will give optimum (fine) service. Evidence from the field tests indicate that making the right choice in tool selection is important for metal machining operations to get the machining processes right with good tool life and product quality. From the above statement, the modified tool performance fits the selection criterion and procedure suggested by Kramer in 1987.

Part configuration and rigidity
Geometry, surface finish, accuracy
Manufacturing practice

Condition and capability of machine tools
Overall part production economics
Tool life end point

INPUTS

Work Material properties

Type of cut (*continuous vs intermittent*)

Published Machinability data

Tool Selection Methodology

Select tools *(based on grade, shape and geometry and physical properties)*

Aim for optimum cutting conditions

OUTPUTS

Data from trade and technical literature

Experience

Vendor information

MECHANISMS

Figure 4.9 Suggested Procedures for Tool Selection and Optimisation of Cutting Conditions; Courtesy of Kramer (1987)

4.11.0   Summary

In the early 1980s the coating of tungsten tools with TiC by the PVD process was introduced whereas TiN coatings came about in 1985, and both types of coatings enabled higher cutting speeds. This study achieved speeds of upto 30% higher than the tool manufacturer recommended speed of 250 m/min for the particular work material.

It is known that the metal machining action produces high temperatures at the tool–work interface, especially when high speeds and/or feed rates are used and when materials with high strengths and high thermal resistances are machined. This was evidenced by the fact

that hot hardness, which is the ability of a cutting tool material to resist, stresses and maintain hardness while cutting efficiently at elevated temperatures, was achieved by the EDMed inserts. The ability of the modified tool to retain hardness (recovery hardness) at room temperature after exposure to elevated temperatures was good.

Chapter 5

Simulation Modelling of the Tool in Turning Processes

This chapter looks at the numerical modelling and simulation of the tool performance in this study. Modelling was done to substantiate experimental results collected earlier in the project. The chapter begins with a literature review of current finite element models of the metal cutting process and the general approaches that need to be understood in computer simulation modelling. The discussion of results and postulations will be presented in the next chapter, using some of the results obtained in this chapter as the prescribed conditions.

5.0 Introduction

The potential that FEM has to accommodate general geometric and materials assumptions has generated interest in the analysis of machining processes. FEM helps in the computing of cutting forces, tool stresses, cutting temperatures and Von Mises stresses, which are difficult to measure. This section focuses on temperature distributions, force and stress modelling to understand how the specimens (tools) deform during metal cutting under loading. In metal cutting, friction between the tool and the chip has some influence on the primary deformation, BUE formation, tool wear and temperature. The simplest way to characterise tool–chip friction according to Stephenson and Agapaiou (2006) is to define an effective friction coefficient, (μ_e) as the ratio of the cutting force P parallel to the tool rake–face to the force normal to the rake face, N:

$$\mu_e = \frac{P}{N}$$
<div align="right">Equation 5.1</div>

μ_e is sometimes converted to a friction angle, β, given by:

$$\beta = \arctan(\mu_e)$$
<div align="right">Equation 5.2</div>

Note that force components N (normal) and P (parallel) can be estimated from cutting force measurements and computed from the equations:

$$N = F_n \cos\alpha - F_z \sin\alpha$$
<div align="right">Equation 5.3</div>

$$P = \frac{F_n \sin\alpha + F_z \cos\alpha}{\cos\eta}$$
<div align="right">Equation 5.4</div>

Where α is the normal rake angle of the tool, measured in a plane normal to the cutting edge, and η is the chip flow angle, defined as the angle between the direction of chip flow and the normal to the cutting edge, measured in the plane of the rake face of the tool. In specific processes, force components are often related to the axes of motion of the machine tool.

5.1.0 Development of Analytical Machining Models

Development of FEA started in early 1970s and continued to gain momentum in the first part of 1990s. In 1993, Lin and Lin worked on a coupled model of thermo-elastic-plastic material under large deformation. In the same year, Moriwaki, Sigimure and Luan (1993) analysed the mechanics of steady state orthogonal machining of copper using a rigid-plastic FEM. In 1991, Komvopoulos and Erpenbeck analysed machining process with a rigid BUE using the 'elastic-perfectly plastic and elastic-plastic material models'. Meanwhile, Strenkwoski and Moon (1990) analysed steady state 2-D cutting in predicting chip geometry and chip–tool contact length.

Many researchers have developed analytical machining models in order to improve their understanding of the metal cutting mechanism and to predict the general trends of the process, pioneered by Merchant in 1945 and who was followed by others like Lee and Shaffer (1951), Boothroyd and Knight (1989), Oxley (1989), Venuvinod (1996) and Jaspers (1999). Many of the models developed in the past were meant to predict cutting forces, residual stresses, and chip shape formation, but a single solution suitable for all of these features and a wide range of cutting conditions has not been found. Dewhurst (1978) made a statement that 'a unique solution does not exist for a particular set of cutting conditions'. Thus, it is right to say that analyses are made which predict only one of a few particular features of metal cutting process conditions. A semi-empirical thermal analysis was developed by Oxley (1989), which gave good results at conventional cutting velocities and was based on a thermo-mechanical model which had emphasis on the temperature property and material characteristics such as strain rate sensitivity and strain hardening.

Merchant made the first quantitative analysis of cutting forces in 1941, based on the upper bound theory (Ernst and Merchant, 1945). A few years later, Lee and Shaffer (1951) proposed a model based on slip-line field theory. Let us look at the two models:

5.1.1 Ernst and Merchant Model

Ernst and Merchant reasoned that the shear plane would take such a position that the shear stress acting upon it would be a maximum (Ernst and Merchant, 1941). In the Merchant model, cutting forces were predicted in view of the fact that a chip forms under shearing along a plane surface originating at the tool edge and inclined with an angle ϕ (the shear plane) with respect to the workpiece surface. The material was assumed to be perfectly rigid plastic. In this model, a Coulomb friction law at the tool–chip interface is assumed with a constant friction of coefficient, but it neglects thermo-mechanical effects. Assuming the shear stress to be uniformly distributed according to Merchant, it states that:

$$\tau = \frac{F_S}{A_S} = \frac{F_R \cos(\varphi + \beta + -\alpha)}{A_S} \qquad \text{Equation 5.5}$$

Where A_S is the area of the shear plane. The optimum was found by differentiating this expression with respect to ϕ and equating the resulting expression to zero. Under the assumption that τ_f and β are independent of ϕ, this leads to:

$$\phi = \frac{\pi}{4} - \frac{\beta}{2} + \frac{\alpha}{2} \qquad \textit{Equation 5.6}$$

This equation gives a simple relation between the shear angle $\emptyset$ and the friction angle β. Combining this equation with the force relationships of the shear plane representation in equations 5.5 and 5.6, the cutting forces can be calculated if ϕ and τ_f are known. Using the geometrical relations of figure 5.1, the shear angle ϕ can be determined if the chip thickness is measured experimentally.

5.1.2   Shear Angle Determination

Determining shear angle in this study was done by means of the cutting ratio (r) convention, which is the ratio of the depth of cut (t) to the chip thickness (t_c). This ratio may be determined by directly measuring t_c. It is known that when metal is cut it is experimentally found that there is no change in density and hence:

$$tbl = t_c b_c l_c \qquad \text{Equation 5.7}$$

Where $t,$ $b,$ and l are the depth of cut, width of cut, and length of cut, respectively, and the subscript C refers to the corresponding measurements on the chip (Shaw, 2005). Thus from equation 5.7 above the cutting ratio (r) is computed as follows:

$$\frac{t}{t_C} = \frac{l_C}{l} = r \qquad \text{Equation 5.8}$$

The relationship between cutting ratio (r) and shear angle (ϕ) may be obtained with the aid of Figure 5.1.
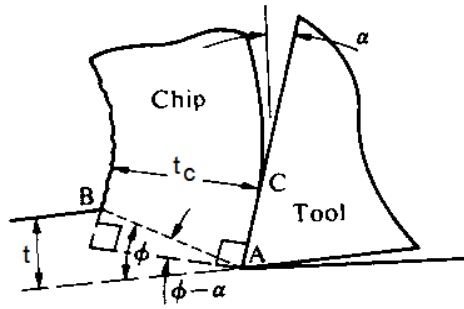
Figure 5.1 Construction for Deriving Relation between Shear Angle (ϕ) and Cutting Ratio
(After Shaw (2005, p. 20))

From this figure 5.1, it can be proved that:

$$r = \frac{t}{t_C} = \frac{AB \, \sin \alpha}{AB \, \cos(\varphi - \alpha)} \qquad \text{Equation 5.9}$$

By solving for ϕ:

$$\tan \varphi = \frac{r \, \cos \alpha}{1 - r \, \sin \alpha} \qquad \text{Equation 5.10}$$

The shear angle (ϕ) can then be read from a Nomograph. A Nomograph is presented in Figure 5.2.
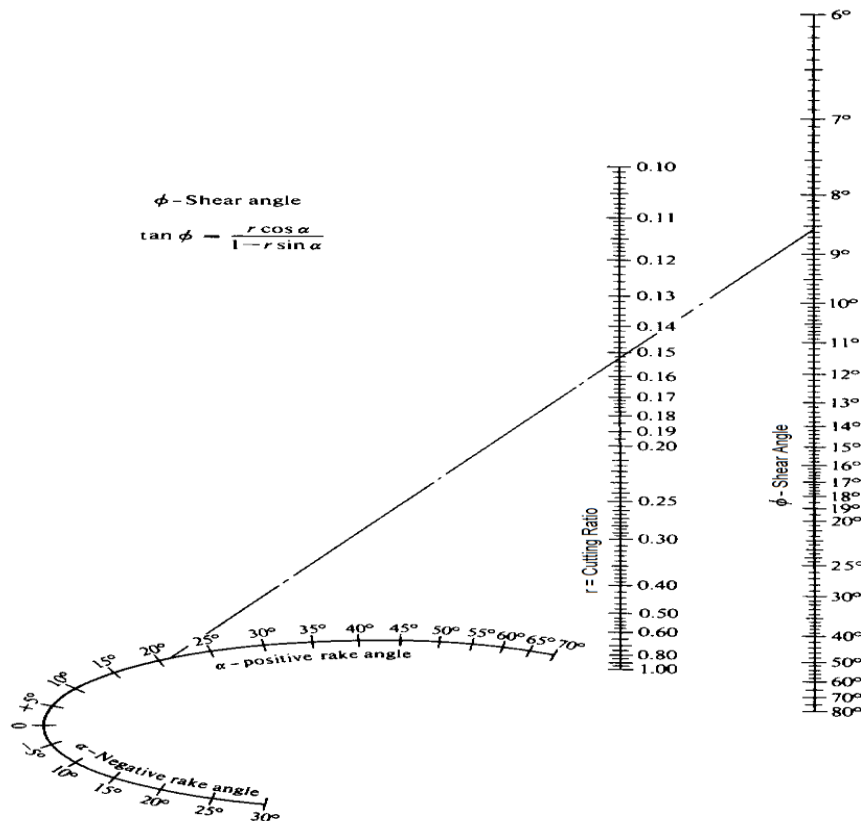
Nomograph for shear angle. (after Merchant and Zlatin, 1945) [Example: Rake angle = 21°, cutting ratio = 0.152, shear angle = 8.55°.]

Figure 5.2 Nomograph for Shear Angle Readings
(After Merchant and Zlatin, 1945; also cited by Shaw, 2005 page 21).

89

5.1.3   Shear Angle Slip-Line Theory

It was Lee and Shaffer who first applied the slip-line theory to find the shear angle solution (Lee and Shaffer, 1951). They considered the workpiece to be a rigid plastic solid without strain hardening or thermal effects. As in the Ernst-Merchant model they assumed the shear plane *AB* to be a direction of maximum stress where all deformation takes place. However, Lee and Shaffer constructed a slip-line field *ABC* in which the material is in a uniform state of stress just below the yield point as shown in Figure 5.3. Since no forces act on the chip after it has passed *BC,* this plane can be regarded as a free surface and has to make an angle of 45° with the shear plane.
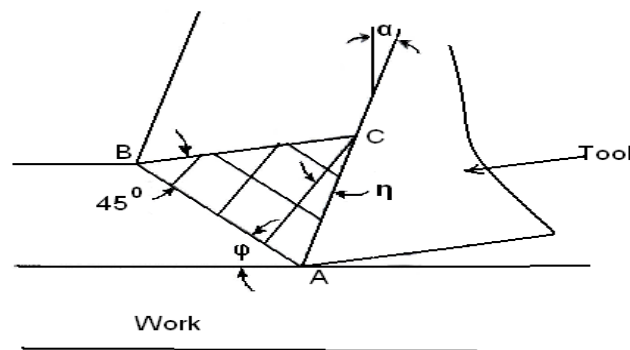
Figure 5.3 Lee and Shaffer's Slip-Line Field Model

At the boundary *AC* they assumed the stress to be uniform and inclined to the tool with an angle β, where $\beta = \frac{\pi}{4} - \eta$. This led to the following equation for the shear angle:

$$\varphi = \frac{\pi}{4} - \beta + \alpha \qquad\qquad \text{Equation 5.11}$$

5.2.0   Assumption of Forces Acting on a Cutting Tool

FEM is used to analyse the possibility of numerically modelling different types of metal cutting problems. One of these problems is tool wear during machining, associated with material transfer between the tool and workpiece. Tool wear is dependent on 'cutting temperature, contact stresses and sliding velocity produced during cutting' (Dechjarern, Busso and Hibberd, 2004). To determine the load (force) to be applied in the finite element model it is important to ascertain the resultant force. When a turning operation is taking place on a lathe there are three perpendicular forces acting on it. These forces are shown diagrammatically in Figure 5.4, where F_z is the vertical cutting force, F_x the feeding force, and F_y the horizontal pressure on the work as shown.
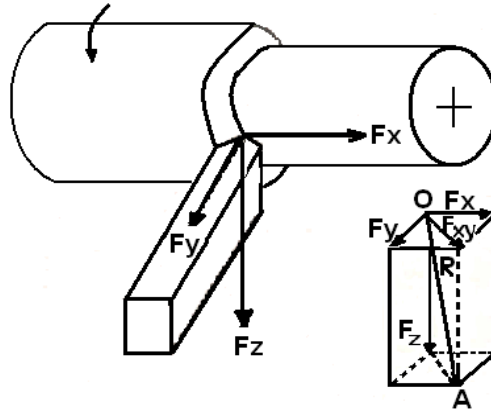
Figure 5.4 Model of Turning Process

The relationships between forces $F_{X^2} + F_{Y^2} + F_{Z^2}$ depend upon the cutting variables, geometry of the tool point, the work material, tool wear and cutting speed. The resultant force (R) is represented in this formula:

$$R = \sqrt{F_X{}^2 + F_Y{}^2} + F_Z{}^2 \qquad\qquad \text{Equation 5.12}$$

Figure 5.4 above is a model of the 'ideal' turning process that completely restrains the concept of inhomogeneous strain by assuming the material to behave in a completely homogeneous fashion. The work-material model in AdvantEdge[TM] V.5.9011 FEA software contains power-law strain hardening, thermal softening, and rate sensitivity Formula in-built in the software are given in appendix XI.

Where $\bar{\sigma}$ is the Von Mises stresses, σ_0 is the initial yield stress, ε^P is the plastic strain, $\dot{\varepsilon}^P$ is the plastic strain rate, $\dot{\varepsilon}_0^P$ is the reference plastic strain rate, $\dot{\varepsilon}_t$ is the threshold strain rate, ε_0^P is the reference plastic strain, m_1 and m_2 are the strain rate exponents, and n is the strain hardening exponent. $\theta(T)$ in equation 5.15 in appendix XI is determined by:

$$\theta(T) = C_0 + C_1 T + C_2 T^2 + C_3 T^3 + \cdots \quad \text{if } T \leq T_{cut} \qquad \text{Equation 5.15}$$

$$\theta(T) = \theta(T_{cut}) - \left(\frac{T - T_{cut}}{T_{melt} - T_{cut}}\right) \qquad if\ T > T_{cut} \qquad \text{Equation 5.16}$$

Where $C_0, C_1, \dots$ are material constants, T_{cut} is the threshold temperature and T_{melt} is the melting temperature. AdvantEdge[TM] software has all the parameters as built-in constants in the material database. The thermal conductivity and heat capacity are assumed to be temperature independent, and are set as 16.4 W/mK and 523 J/Kg^{0}C, respectively. For Hardness, 200 Bhn was chosen and set, and the Young's modulus and Poisson's ratio are 208 GPa, and 0.37 respectively.

The Young's modulus of tungsten carbide (W_C) is 800 GPa, which is four times larger than that of mild steel EN-3. This implies that the deformation of the tool may be less severe. As a result, the W_C tool is assumed perfectly elastic. One coulomb coefficient of friction is used across the whole rake face to model the friction at the tool–chip interface.

The modelling was based on the assumptions that:

   i.   the tool is perfectly sharp and there is no contact along the clearance face,

   ii.   the shear surface is a plane extending upward from the cutting edge,

   iii. the load applied is uniformly distributed,

   iv.   the work moves relative to the tool with uniform velocity,

   v.   a continuous chip is produced with no BUE,

   vi.   the shear and normal stresses along the shear plane and tool are uniform (strength of materials approach).

5.3.0   Finite Element Method

Generally, FEM has the potential to accommodate more general geometric and material assumptions in order to analyse machining processes, and this has generated a great deal of interest in its application. During metal cutting, the material undergoes high plastic deformation and transformation due to temperature and stress changes. This results in chip flow and heat localisation, creating deformation bands of intense shear during the metal cutting process.

5.3.1   Simulations and Modelling Setup

Figure 5.5 shows the initial 3D finite element mesh using a tool with a nose radius of 0.8 mm.
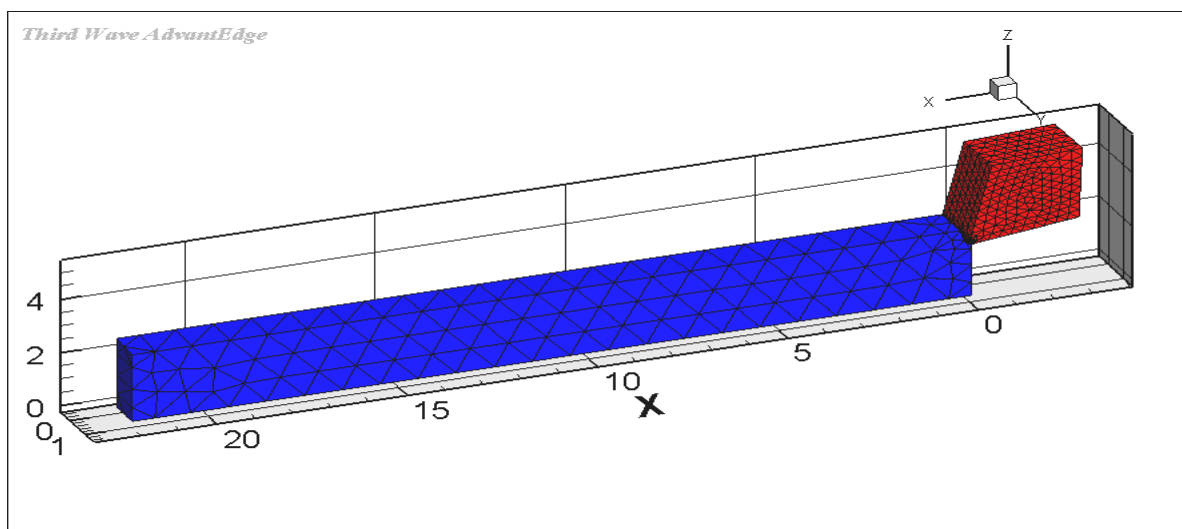
Figure 5.5 Initial 3D Finite Element Mesh

The 4-node, 12 degree-of-freedom tetrahedral finite element was used to model the work and tool. The top and back ends of the tool were fixed in all directions. The workpiece was constrained in the vertical (Z) and lateral (Y) directions on the bottom surface and move at a cutting speed of 325 m/min in the horizontal direction (-X) toward the stationary tool.

The software enabled the comparison of simulation results for different cutting conditions (temperature, cutting pressure, strain rate, plastic strain rate) and tool geometries to find optimal results and provided the following:

i.   analysis of temperature distributions and stress profiles by gauging wear of the TiN-coated EDMed tool due to its ability to withstand high temperatures,

ii.   solutions to problems such as chip formation, curling, strain hardening, effects of temperature and heat impacts on both workpiece and tool,

iii. appraisal of force plots to lower cutting forces and power consumption in metal machining operations during modelling.

5.3.2 AdvantEdge^{TM} FEM Components

AdvantEdge^{TM} FEM has three main components:

(a)   the simulation setup interface for setting up the entire simulation, including defining tool geometries, material conditions and machining parameters,

(b)   the AdvantEdge^{TM} engine performs all the calculations from the setup inputs,

(c)   the results viewer (Tecplot) function is for the extraction of the necessary simulation results, including cutting forces, tool temperatures, Von Mises stresses, strain rate, plastic strain rate, etc.
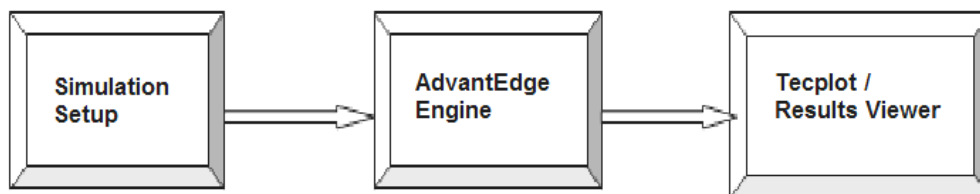
Figure 5.6 AdvantEdge Software Compositions

5.3.3 Modelling Formulations

Direct measurement of tool temperature during cutting experiments was not possible. The finite element simulation could provide a quick and accurate prediction of the tool temperature under various cutting conditions. The cutting conditions and parameters for the machining experiments were entered as inputs. The effect of cutting speed on tool temperature was investigated. The effect of tool edge radius on cutting forces, chip thickness and

93

maximum tool temperature was analysed. There were four main steps to setting up simulation job for this study:

a) choosing the process,

b) the workpiece material,

c) the tool definition, and

d) process parameters.

In this study, discussion about finite element modelling of machining is based on the following areas:

i. the formulation, which determined what problems the model would best serve,

ii. the tool and workpiece material assumption, their thermal property assumptions and physical properties.

In computer modelling there are two basic formulations in modelling machining processes: Lagrangian and Eulerian. In Lagrangian formulations, the user/modeller imagines that the workpiece is fitted in space and the tool is fed into it, imposing displacement boundary conditions, which drive plastic deformation. This approach is suited to incipient and transient analysis, and to the study of chip breakage and burr formation. According to Eu-Gene and Aspinwall (2002) the advantage of using the Lagrangian formulation method lies in the fact that 'the tool can be simulated from some initial state to steady state cutting and the chip geometry together with workpiece residual stress can be predicted'.

5.3.4   Simulation Modelling System

For this study the Eulerian formulation was adopted because of the ease its application and its functionality. Whereby the tool is viewed as being fixed in space and the work material is treated as a fluid flowing through a control volume in front of it. The beauty of this process was that it eliminated the need to integrate from the incipient stage to obtain steady state results, thus reducing the computational load. This study agrees with Strenkowski and Moon (1990) who proposed a steady-state metal cutting technique based on an Eulerian formulation. They used the technique to predict chip geometry and temperature distribution.

5.3.5   Steady State Metal Cutting Models

The finite element (FE) model by Usui and Shirakashi (1982) focussed on steady state metal cutting based on empirical data and assumed rate-independent deformation behaviour. Meanwhile, the effect of friction between the chip and the tool rake face was investigated by Iwata, Osakada and Terasaka (1984). Though their work was limited to very low cutting

94

speeds and strain rates, they assumed rigid-plastic deformation. Strenkowski and Carroll (1988) used the general-purpose FE code NIKE2D and employed an updated Lagrangian formulation to model the orthogonal metal cutting process. They developed a technique for element separation in front of the tool tip and proposed an element-separation criterion based on the magnitude of plastic strains. Their technique simulated the cutting process from the initial stage to the steady state in predicting cutting force, chip geometry, plastic deformation and residual stress in the workpiece.

5.3.6 Specific Cutting Power

According to Stephenson and Agapiou (2006), the specific cutting power, u_s, is also called the unit cutting power, specific cutting energy, or unit cutting energy, and it is the power required to machine a unit volume of the work material. It is easily computed from measured cutting forces and is often used to compare the machinability of different materials, especially when comparative tool life data are unavailable.

However, only the torque or tangential force on the rotating element of the system is considered in computing u_s, because the rotational speed is much larger than the feed speed (Agapiou, 2006) but this has not been of interest in this research.

5.4.0 Oblique Model in Perspective

The majority of metal machining processes are oblique in nature, and the model for this study is 3D oblique turning. Scores of literature now discuss tool wear and cutting processes, though the majority and this particular study discuss plastic and elastic deformations of tools and work surfaces. Friction exists in metal cutting processes and is responsible for the power requirement, but importantly contributes a great deal to the quality of the workpiece surface finish. To give some insight, Komvopoulos and Erpenbeck (1991) carried out a simulation of chip separation by using the 'distance tolerance' criterion. While Tyan and Yang (1992) used an Eulerian reference coordinate system to describe the steady state motion of a workpiece relative to the tool to analyse the orthogonal metal cutting process based on a limit analysis theorem. Meanwhile, Dechjarern (2008) used a 3D model to study the effect of the tool rake face on the cutting mechanism at different speeds, with a FE simulation of a cutting operation from the incipient state to steady state with TiN-coated tungsten carbide (W_C) cutting tools. In order to predict the chip separation and the form of the fractured surface during the cutting process, consideration was paid to fracture initiation and propagation. The results of the Dechjarern (2008) tests showed that 'cutting forces decrease with the increase in rake angle

for all cutting speeds investigated'.

Shih and Yang (1993) conducted a combined experimental and numerical investigation of the orthogonal metal cutting process and the effects of large strain, high strain-rate and temperature. The chip separation criterion they used was based on the distance in the cutting direction between the tip of the cutting tool and the FE nodal point located immediately ahead of the tool tip.

Shi, Deng and Shet (2002) discussed the effect of friction on chip formation, contact length, shear angle, cutting force, and maximum temperature. Their findings were based on FE simulation solutions assuming modified Coulomb friction law. In the simulations processes, they used four coefficient of friction values (0.0, 0.2, 0.4, and 0.6) and four rake angle values (15^0, 20^0, 25^0, and 30^0). They concluded that 'when the rake angle takes the small value of 15^0, the coefficient of friction varies only between '0.0 to 0.4'. At the higher coefficient value of 0.6, they found that the friction force is too large and the cutting operation could not proceed (Shi, Deng and Shet, 2002). Shi, Deng and Shet then stated that 'the shear angle, which is the angle between the cutting direction and the primary shear zone originating from the tool tip, also depends quite strongly on the friction coefficient and the rake angle'. According to them, 'for a fixed rake angle, the shear angle decreases as the friction coefficient increases, and for a fixed friction coefficient, the shear angle increases as the rake angle increases'. On the other hand, 'the normal force across the tool–chip interface becomes larger for the same amount of cutting force' (Movahhedy, Gadala and Altintas., 2000). Movahhedy, Altintas and Gadala (2002) further used a FE model to study the effect of a blunt or chamfered edge of a tool on cutting forces during the machining process. The approach combined an Eulerian-Lagrangian model and a tool–workpiece contact algorithm (Lin and Lin, 1992) for sliding-sticking friction conditions based on a relation such as:

$$\tau_{f=}\,\tau.\left[1 - e^{-\mu_\tau^\sigma}\right]$$

Equation 6.18

Where τ_f is the friction stress, σ is the normal stress, τ is the shear flow stress, and $\mu = 1$ based on experimental force measurements.

5.5.0   Coefficient of Coulomb Friction

In mechanical engineering friction effects at the tool and chip interface are described by a constant coefficient of Coulomb friction μ_f (Astakhov, 2006), and

$$\mu_f = \frac{F}{N}$$

Equation 6.19

Where N is the normal force and F is the frictional force at the tool chip interface. Coulomb law states that the friction forces are propositional to the normal load. This implies that the coefficient of friction is constant and independent of the apparent or geometric area of the sliding interface, and where the actual and apparent contact areas have the same contact pressures the numerator and denominator of equation 6.19 can be divided over the tool–chip contact area A_c. Recalling that the mean normal stress at the interface is $\sigma_c = N/A_c$ and the mean shear (frictional) stress at the interface is $\tau_c = F/A_c$, this equation is obtained:

$$\mu_f = \frac{\tau_c}{\sigma_c}$$

Equation 6.20

This indicates that there is constant friction coefficient at the tool–chip contact zone which means that the ratio of the shear and normal stresses is the same along the whole contact length (Dieter, 1976). In the case of sticking friction, where there is no relative motion between the chip–tool interface, the shear strength should be equal to the flow stress in shear, k_c and the normal stress to the yield stress of the work material σ_y (Astakhov, 2006). Therefore using the Von Mises yield criterion, the coefficient of friction under sticking conditions is:

$$\mu_f = \frac{k_c}{\sigma_y} = \frac{\sigma_y/\sqrt{3}}{\sigma_y} = 0.577$$

Equation 6.21

By and large, the coefficient of friction for sliding surfaces remains constant within wide ranges of the chip relative velocity, the apparent area of contact and load, while in metal cutting it varies with respect to load, the apparent area of contact and relative velocity (Astakhov, 2006). Below is a list of various μ_f obtained by different scholars through experiments and modelling. Finnie and Shaw (1956) suggested that the ratio of the real to apparent area of contact might be approximated as follows:

$$\frac{A_R}{A} \equiv 1 - e^{-BP}$$

Equation 6.22

Where B is the constant for a given material combination and P is the applied load. This explains why the coefficient of friction in metal cutting is so variable.

Table 5.2 Values of Coefficient of Friction Used by Researchers in Past Studies

Researcher Name and Year	μ_f Value	Particulars
Armarego and Brown (1969)	0.8–2.0	Obtained these experimentally
Endres, De Vor and Kappor (1995)	0.05, 0.10,	
	0.25 and 0.5	In simulations of metal cutting
Finnie and Shaw (1956)	0.88–1.85	Obtained these experimentally
Hill (1954)	0.5–1.0	Experiment on Merchant model
Zorev (1966)	0.6–1.8	Obtained these experimentally
Komvopoulos and Erpenbeck (1991)	0.0–0.5	In simulations of metal cutting
Kronenberg (1966)	0.77–1.46	Obtained these experimentally
Lin and Lin (1992)	0.001	In simulations of metal cutting
Lin, Pan and Lo (1995)	0.074	In simulations of metal cutting
Olovsson, Nilson and Simonsson (1998)	0.1	In simulations of metal cutting
Strenkowsky and Carroll (1985)	0.3	In simulations of metal cutting
Wu (1989)	0.3	Assumed it to be constant
Strenkowsky and Moon (1990)	0.2	In simulations of metal cutting
Usui and Takeyama (1960)	0.4–2.0	Obtained these experimentally

Source: data collected and compiled for this research from published work of the authors cited in Column 1 in the table.

5.5.1 Coulomb Friction Coefficient in this Study

There are various types of friction experiment that can be used to measure friction and surface damage. Williams (1992) used a block-on-cylinder method consisting of two rectangular flats loaded perpendicularly to the axis of rotation or oscillation on a disk. The drawback with this method is that it only provides information when the two surfaces are in contact repeatedly for long periods of time. A modified pin-on-cylinder rig by Olsson and Hedenqvist (1988) was found to give an excellent reproduction of the contact conditions in the machining processes because it is universally agreed that an important feature of a wear test for the simulation of cutting tool wear is the continuous introduction of a fresh counter material surface that has not previously been in contact with the test pin/tool.

In this study, chip flow over the tool rake face was simulated using commercially available FEM software AdvantEdge[TM] V.5.9011, to obtain friction coefficients of machining mild steel EN3 using a TiN-coated modified carbide tungsten cutting tool. The modelling approach was used to evaluate both the average and instantaneous cutting force coefficients. For this

work, the tool specimens for the cutting tests experiment had a cutting edge radius of 0.8 mm. Information on the edge radius is very crucial in modelling turning process using FEA.

5.5.2   Procedure for Determining the Coulomb Friction Coefficient

The procedure of determining the Coulomb friction coefficient for simulation modelling in this study involved a 2D cutting model with a tungsten carbide (W_C) tool having zero rake angle, cutting mild steel according to Eulerian formulations.
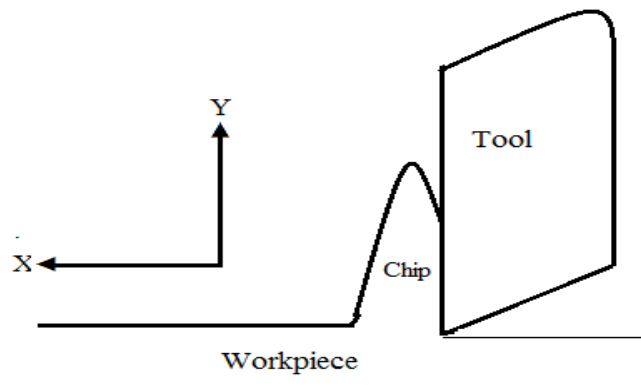
Figure 5.7: Showing a 2-D cutting model with a tool having zero rake angle
for determining Coulomb friction coefficient

Inputs of both material and physical properties of the work (mild steel grade EN-3) and tool were entered. The parameters were: 1 mm depth of cut, 0.4 mm/rev feed rate and cutting velocity of 300 m/min. The results were viewed in Tecplot v.360-2011R2. The numerical force data for Fy (thrust force) and Fx (cutting force) were exported to Excel spreadsheets and interpreted. Then by calculation, $\mu = Fy/Fx$, the Coulomb friction coefficient for this work was determined. See Appendix XIV for data of *Fx* and *Fy* collected from modelling.

In simulating, the model there was continuous introduction of fresh Swarfs material on the rake face of the tool over a long distance that had not previously been in contact with the tool rake face, thereby generating an excellent reproduction of the friction/contact conditions in the machining process.
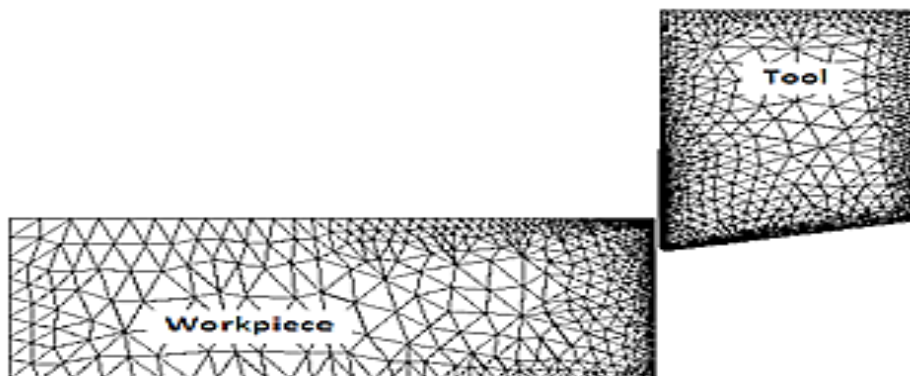
Figure 5.7 Model Mesh for tool with Zero Rake Angle, used in calculating μ

99

Table 5.3, shows the Coulomb coefficients of friction for the two tool structures and work materials.

Table 5.3 Lists of Coefficients of Friction from Modelling with Zero Rake Tool

Tool Type	Material Type	Coefficients of Friction (μf)
TiN-Coated Tungsten carbide (WC) plain surface	Mild Steel Grade EN-3	0.5
TiN-Coated Tungsten carbide (WC) Undulating Surface	Mild Steel Grade EN-3	0.45
TiN-Coated Tungsten carbide (WC) plain surface	Stainless Steel Grade 316	0.9
TiN-Coated Tungsten carbide (WC) Undulating Surface	Stainless Steel Grade 316	0.8

5.5.3 Rake Face Components Effect of Friction Coefficient

The tool face components where chip flows over are of importance since they enable the coefficient of friction on the tool rake face to be determined ($\mu = \tan \beta$ where β is the friction angle as shown in Figure 5.9 on the next page– which is of a free body diagram of a chip).

The coefficients of friction were determined by simulating a 2D model of metal cutting with a tool with zero rake angle, as explained above, based on this equation:

$$\mu = \frac{F_C}{N_C} = \frac{F_P \sin \alpha + F_Q \cos \alpha}{F_P \cos \alpha - F_Q \sin \alpha} = \frac{F_Q + F_P \tan \alpha}{F_P - F_Q \tan \alpha} \qquad \text{Equation 6.23}$$

Here two forces were considered- the force between the tool face and the chip (R) and the force between the workpiece and the chip along the shear plane (R') presumably, these must be equal for equilibrium (R = R') rule. This means that the forces R and R' are conveniently resolved into three sets of components as shown in the free body diagram on figure 6.8 below.

      1st.   along and perpendicular to the tool face, F_C and N_C

      2nd.   in the horizontal and vertical direction, F_P and F_Q

      3rd.   along and perpendicular to the shear plane, F_S and N_S

The friction coefficients obtained for the modified tool were used in the final simulation model of the tool's performance.
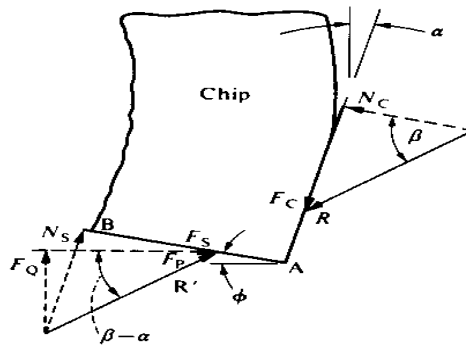
Figure 5.9 Free Body Diagram of Chip
(Courtesy of Shaw (2005, p. 17))

Each surface roughness gave a different friction coefficient. A study of the effect of friction coefficient on the chip formation process and its effect on the contact length, shear angle, contact pressure and maximum temperature could reveal the effect of each surface roughness on the cutting tool performance. Appendix XIV provides tables of friction coefficients of different surfaces obtained by simulating different tool surface roughness at the same depth of cut (chip thickness).

5.5.4   Chip Thickness and Sliding Speed Effects on Friction Coefficient

In turning operations the chip tends to spread askew, causing the maximum width to become wider than the original depth of cut. For consistency the irregular cross-section of chips produced were measured. The chip generated by the modified tool with undulating surface structures was measured and found to be $t_2 = 1.43$ mm, and for the conventional tool the chip thickness was $t_2 = 1.53$ mm. While the depth of cut ($t_1 = 1$ mm) in both cases according to convention t_1 is the chip thickness before cut. It could therefore be seen that the chip thickness ratio, t_2/t_1, is geometrically related to the shear plane angle, ϕ, by the following equation:

$$\cot \emptyset \ = \ \frac{t_2}{t_1} \qquad\qquad Equation\ 6.24$$

The chip moved away with a velocity V_c, which is related to the cutting speed, V, and the chip thickness ratio, t_2/t_1, by equation:

$$V_C \ = \ V \frac{t_1}{t_2} \qquad\qquad Equation\ 6.25$$

5.5.5 Laws of Friction and Bearing on Coefficient of Friction

It is a well-known fact that friction is independent of the apparent area of contact of the two bodies involved, and that the friction force *F* is proportional to the normal load, *W*– Amonton's laws of 1699.

$$\text{Thus} \qquad F = \mu W \qquad\qquad\qquad \textit{Equation 6.26}$$

Where, μ is the constant of proportionality, known as the coefficient of friction. These laws are known as Amonton's laws, named after the French engineer who first presented them in 1699. Coulomb (1785) proposed a third law, that the kinetic friction is almost independent of the speed of sliding. In order to apply Amonton's laws in this project it was important to examine the two laws by making the following assumptions:

i. During sliding, the resistive force per unit area of contact is constant, so that:

$$F = A.s \qquad\qquad\qquad\qquad\qquad \textit{Equation 6.27}$$

Whereby *F* is the friction force, *A* is the real area of contact and *S* is the friction force per unit area.

ii The real area of contact, *A*, is proportional to the normal load, *W* which means

$$A = q.W \qquad\qquad\qquad\qquad\qquad \textit{Equation 6.28}$$

Where, *q* is the constant of proportionality. Eliminating *A* from these two equations gives

$$F = q.s.W \qquad\qquad\qquad\qquad\qquad \textit{Equation 6.29}$$

Thus from the above, equations 6.23 and 6.24 proved that the friction force depends upon the real area of contact and that this is independent of the apparent surface area.

According to the Merchant force model, cutting force (F_c) and thrust force (F_t) components can be transformed to normal (*N*) and friction (*F*) components applied on the tool face as follows:

$$F = F_c \text{Sin}(\alpha) + F_t \text{Cos}(\alpha) \qquad\qquad\qquad \text{Equation 6.30}$$

$$N = F_c \text{Cos}(\alpha) - F_t \text{Sin}(\alpha) \qquad\qquad\qquad \text{Equation 6.31}$$

In which (α) is the normal rake angle. According to Coulomb law, the apparent coefficient of friction on tool–chip interface becomes:

$$\mu = \left[\frac{F}{N}\right] = \left[\frac{F_c \sin\alpha + F_t \cos\alpha}{F_c \cos\alpha - F_t \sin\alpha}\right] = \left[\frac{\tau}{\sigma}\right] \qquad\qquad \text{Equation 6.32}$$

where (τ) and (σ) are the friction shear and normal stress at the tool–chip interface respectively. This implies that the Coulomb friction model gives a constant coefficient of

friction (μ), or that the frictional stress (τ) on the rake contact region is directly proportional to the normal stress (σ).

5.6.0 Aspects of Heat Generation in Metal Cutting

5.6.1 Zorev Model

The Zorev (1966) model illustrates the sticking and sliding regions in the metal cutting process with a single point cutting tool. The stress distributions at the chip–tool interface are based on Zorev's model, where the force is greater at the stiction region and low at the sliding region. Heat generation and transfer in this chip–tool interface zone obey the second law of thermodynamics. A discretized weak form of the first law is given by these thermal equations:

$$CT_{n+1} + KT_{n+1} = Q_{n+1} \qquad\qquad \text{Equation 6.33}$$

A lumped capacitance matrix   is used to eliminate the need for any equation solving.

$$CT + KT = Q \qquad\qquad \text{Equation 6.34}$$

Where **T** is the array of nodal temperatures,

$$C_{ab} + \int_{Bt} c\rho\, N_a N_b\, dV_o \qquad\qquad \text{Equation 6.35}$$

is the heat capacity matrix,

$$K_{ab} = \int_{BO} D_{ij} N_{a.i} N_{b.j}\, dV \qquad\qquad \text{Equation 6.36}$$

is the conductivity matrix, and

$$Q_a = \int_{Bt} sN_a dV + \int_{B\tau q} hN_a\, dS \qquad\qquad \text{Equation 6.37}$$

is the heat source array, with **h** having the appropriate value for the chip or tool.

5.6.2 Uniformly Distributed Load

In a uniformly distributed load, the total weight is assumed to be in the centre of the distributed load. We know that the total force (F_w) is given by $Fw = \int_a^b m \lg dx$, or $Fw = mlgl$ where l is the length of the chip. While the total force F_w may be assumed to act on a rigid body so that the moment of this force about any point is the same as the moment due to the distributed load, this point is presumed to be a distance X_g from the left-hand end of the chip A. Thus, the moment of the equivalent force F_w about A must be equal to the sum of the moments of the weights of the individual elements of the distributed load. Mathematically given as:

$$x_g = \frac{\int_a^b mlgx\; dx}{\int_a^b mlg\; dx} = \frac{l}{2} \qquad\qquad \text{Equation 6.38}$$

The approach combines both Eulerian-Lagrangian models and the tool–workpiece contact algorithm (Lin and Lin, 1992) for sliding-sticking friction conditions based on this relation

$$\tau_f = \tau \left[1 - e^{-\mu \frac{\sigma}{\tau}} \right]$$
Equation 6.39

Where τ_f is the friction stress, σ is the normal stress and τ is the shear flow stress, and $\mu = 1$ based on experimental force measurements.

5.6.3   Simulating the Model Systems

AdvantEdge^{TM} V.5.9011 machining simulations package integrates FE numerics and material modelling appropriate for metal machining. Following the description in section 6.5.4, the workpiece moved with velocity *V*. The cutting tool is parameterised by rake and clearance angles, and a cutting edge radius. In the plain strain case the depth of cut into the plane is considered to be large in comparison to the feed. A schematic representation of the cutting conditions is demonstrated in Figure 5.10.
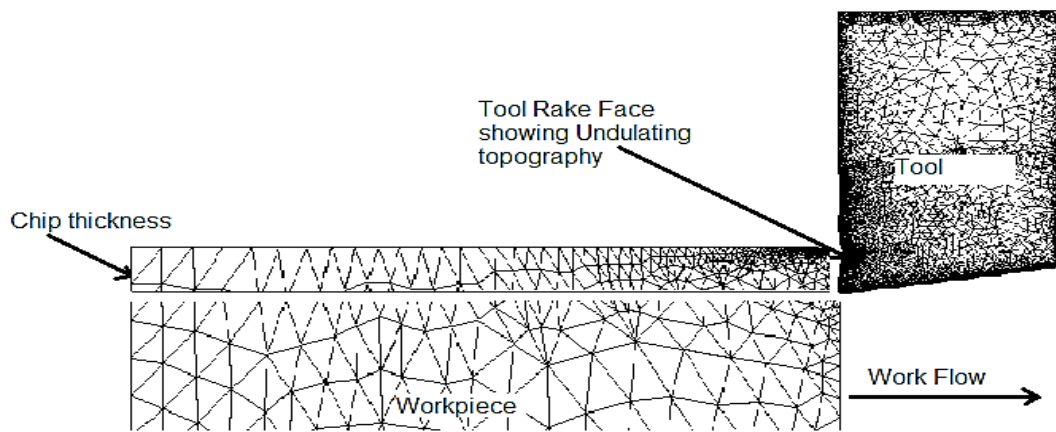
Figure 5.10: Schematic Presentation of the Cutting Conditions

When the simulation model was submitted for processing, the cutting tool initially indents the workpiece as shown in Figure 5.11, and the chip begins to form as seen in Figure 5.12 Figure 5.13 indicates how the chip will curl round and hit the workpiece.
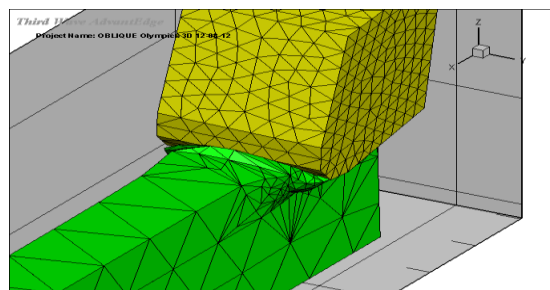
Figure 5.11: The Cutting Tool Initially Indents the Workpiece

The balance of linear momentum is written as:

$$\sigma_{ij,j} + \rho_{bi} = \rho_{üj}$$
Equation 6.40

The weak form of the principal of virtual work becomes:

$$\int_B V_i \sigma_{ij,j} + V_i \rho b_i \, dV = \int_B \rho V_i \ddot{u}_i \, dV \qquad\qquad \text{Equation 6.41}$$

Integration by parts and rearranging terms provides:

$$\int_B \rho v_i \ddot{u}_i \, dV + \int_B v_{i,j} \sigma_{ij} \, dV = \int_{\partial B} Vi\sigma_{ij} \, n_j \, d\Omega + \int_B V_i \rho b_i \, dV \qquad \text{Equation 6.42}$$
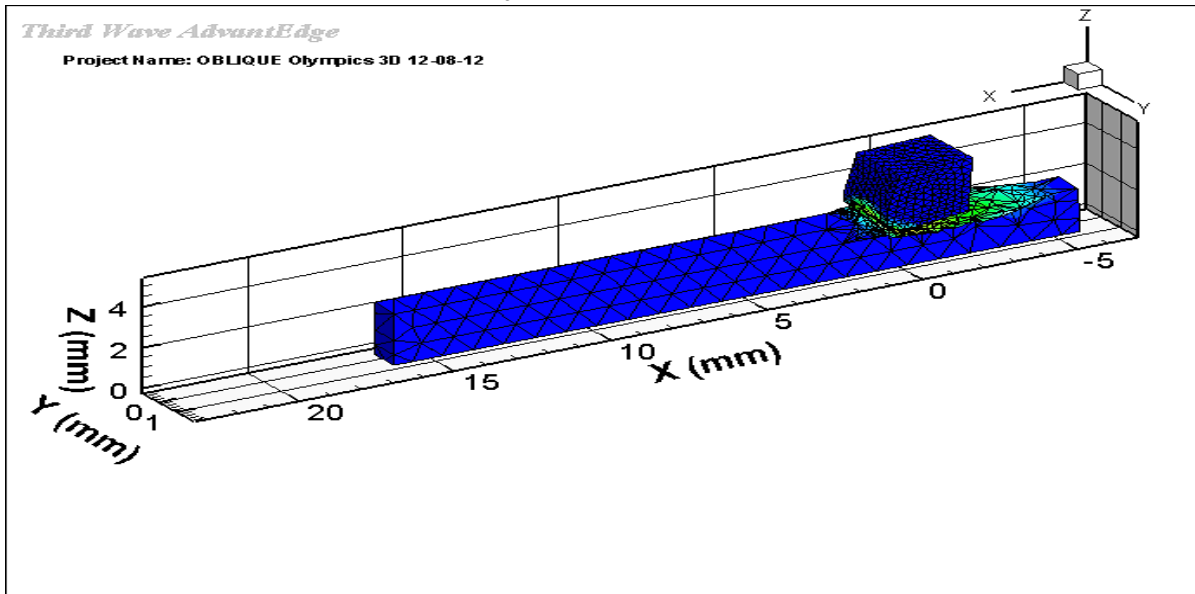
Figure 5.12: The Chip Begins to Curl
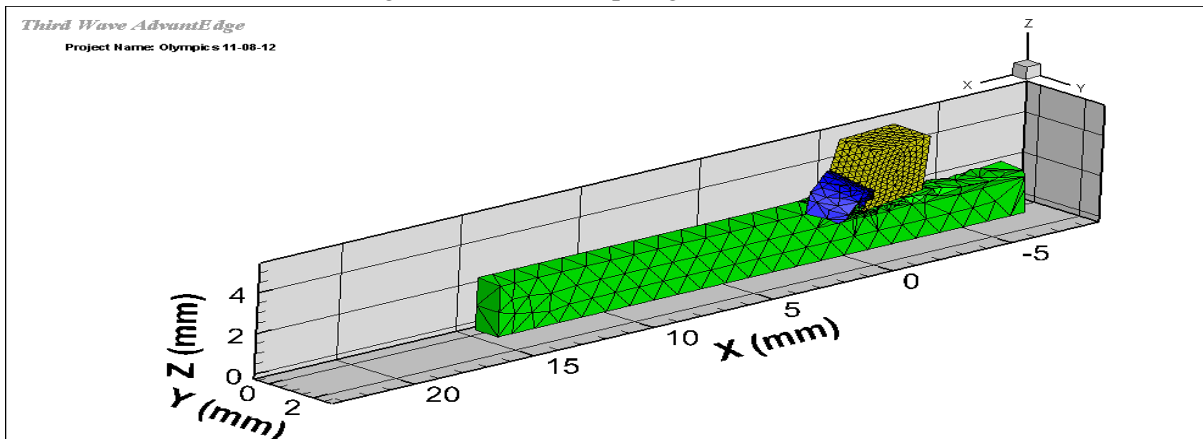
Figure 5.13: Chip Curls Round and Hits the Workpiece.

Which can be interpreted as:

(Inertial Terms) + (Internal Forces) = (External Forces) + (Body Forces)

FE discretisation provides:

$$\int_B \rho N_a N_b \ddot{u}_{ib} dV + \int_B N_{a,j} \sigma_{ij} \, dV = \int_{\partial B} N_a \tau_i \, d\Omega + \int_B \rho N_a \, b_i \, dV \qquad \text{Equation 6.43}$$

In matrix form:

$$M_a + R_{n+1}^{int} + = R_{n+1}^{ext} \qquad\qquad \text{Equation 6.44}$$

Where:

$$M_{ab} = \int_{BO} \rho_0 \, N_a N_b dv_0 \qquad\qquad \text{Equation 6.45}$$

is the mass matrix

$$R_{ia}^{ext} = \int_{BO} b_i N_a \, dV_O + \int_{\partial B0\tau} \tau_i \, N_a d\Omega_O \qquad \text{Equation 6.46}$$

Which is the external force array and:

$$R_{ia}^{int} = \int_{BO} P_{ij} N_{a,j} \, dV_O \qquad \qquad \text{Equation 6.47}$$

is the internal force array.

In the above expressions, N_a, a = 1, ..., numnp are the chip shape functions, repeated indices imply summation, and a comma (,) represents partial differentiation with respect to the corresponding spatial coordinate, and P_{ij} is the first Piola-Kirchhoff stress tensor, analogous to the engineering or nominal stress.

5.6.4   Linearly Increasing Load Assumption

Since tool wear is dependent, on 'cutting temperature, contact stresses and sliding velocity' produced during metal cutting, and by applying Amonton's laws of friction, the following assumptions are arrived at:

i. During sliding, the resistive force per unit area of contact is constant which means $F = A.s$ where F is the friction force, A is the real area of contact and s is the frictional force per unit area.

ii. The real area of contact, A is proportional to the normal load, W which means that $A = q.W$ where, q is the constant of proportionality.

Eliminating A from these two equations gives $F = q.s.W$ which confirms that the friction force is proportional to the normal load when the contact is plastic, regardless of the surface topography, and also whenever the contacting surfaces have exponential asperity height distributions, and regardless of the mode of deformation.

For the linearly increasing load $m_l = \dfrac{x}{l} \, m_A,$

since $a = 0$ and $b = l,$ the equation becomes:

$$F_w \;=\; \int_a^b mlg \; dx \qquad \qquad \text{Equation 6.44}$$

Which becomes $Fw \;=\; \int_0^l \dfrac{x}{l} mAg \; dx$

$$= \; \frac{mAg}{l}\left(\frac{x^2}{2}\right)\frac{l}{0} \; = \; \frac{mAgl}{2} \qquad \qquad \text{Equation 6.45}$$

The result for F_w is equal to the area of the loading X_g. This value X_g is equal to the distance to the centroid of the area of loading which means that equation

$$F_w X_g \;=\; \int_a^b mlgx \; dx \qquad \text{or}$$

$$X_g \;=\; \frac{\int_a^b mlgx \; dx}{\int_a^b mlg \; dx}$$

106

$$\text{becomes } X_g \;=\; \frac{\int_0^l (mAg/l)x^2\,dx}{mAg\,(l/2)} \;=\; \frac{2}{3}l \qquad\qquad \text{Equation 6.46}$$

Taking m_l = mass of the load per unit area and length (l) is constant.

Thus (force) $F_w \;=\; mlg\ dx$

$$F_{w=} \int_a^b mlg\ dx \qquad\qquad \text{Equation 6.47}$$

5.7.0   Observed Simulation Results

The following outputs were observed from the simulation.

Table 5.4: Outputs of the Simulation Modelling

Factors	Maximum Output	Units
Temperature	924	^0C
Von Mises Stress	1000	MPa
Plastic Strain	1000	/sec
Heat Rate	12500	W/mm

5.7.1   Output Result Discussions

Several observations may be made concerning the data of table 6.4 above.

5.7.2   Temperature:

The maximum temperature appears on the rake face as a result of the frictional heat and the temperature distribution on the workpiece showed that the deformation concentrated at the primary and secondary shear zones. The temperature (924 ^0C) reached is low, compared to results from cutting experiments with conventional tools. The low temperature could be due to the lubricity and thermal barrier properties of Titanium nitride and the availability of adequate coolant. Ample supply of coolant into the cutting zones (chip-tool and work-tool interfaces) gave an increase in chip curl due to cooling effect and this result was identified by Sharma *et al*. (1971) when they injected cutting fluids directly into the chip-tool interface through a small hole in the tool and this gave an initial in chip curl due to cooling. With a sharp tool, the increased curl that accompanies chip cooling shifts the maximum tool-face temperature closer to the cutting edge and this may give rise to more heat flow into the workpiece.

5.7.3   Von Mises Stress:

The Von Mises stress is used to predict yielding of materials under any loading condition from the results of simple uniaxial tensile tests. In this experiment, the Von Mises stress satisfies the property of two stress states with equal distortion energy of 1000 Mpa.

According to Nadai (1950), a material is said to start yielding when its Von Mises stress reaches a critical value known as the yield strength (σy) in this case was 1000 MPa.

5.7.4 Plastic Strain:

The plastic strain distribution of the workpiece shows that the deformation concentrates at the primary and secondary shear zone as well as the temperature explained above. The distribution of normal stress and shear stress on the tool rake face surface agrees well with the experimental results reported by many researchers. At steady state chip formation, strains were high and there is evidence that strain-hardening materials tend to undergo some fracture even when chips are in the form of continuous ribbons such as was experienced in the field tests and seen in the simulation results. The strain distributions varied with friction coefficient.

5.7.5 Heat Rate:

The heat rate distribution at 12500 W/mm was greater at the tool cutting tip zones along the flank where the tool flank rubbed against the machined surface and at the rake face where the swarf was rubbing at the chip-tool interface. There was also high heat rate distribution at both the primary and secondary shearing zone as the chip begin to deform into a curl.
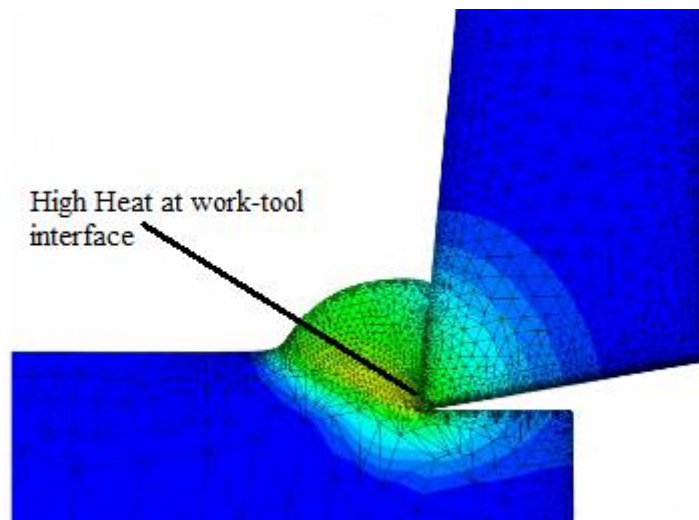
Figure 5.14: Showing Heat Rate Distribution

5.8.0 Summary of Findings in the Modelling

The cutting forces increased until reached the steady state, at which point the cutting force no longer increases. The steady state cutting forces were compared with the experimental data obtained. It could be seen that in the model the chip formed into a long spiral Swarfs, which was similar to those, obtained in the cutting experiments. Presumably, due to the adiabatic conditions assumed in the FEA model. The adiabatic condition leads to a higher

chip temperature being generated, for that reason the chip was softening and less cutting force was needed to deform it.

i.   The model of the modified tool exhibited low temperature, which could be attributed to low friction at the tool-work interface due to coating effect, which remained on the EDMed tool surface longer.

ii. The value of friction coefficient is dependent on presence of TiN coatings on the tool surface, which continued to provide lubricity.

iii. It is presumed that the low temperature is due to the lubricity properties of the TiN coatings on the tool surface roughness (Ra) and its load-bearing ratio (T_p) ability. The value of friction coefficient is dependent on presence of TiN coatings on the tool surface.

iv. As could be seen in the mesh the coated EDMed inserts retained the coating longer in the valleys because of improved adhesion of the coatings onto the tool which helped to reduce friction or heat generation

Chapter 6

Discussion of Results, Postulations and Contributions to Knowledge

An investigation into the performance characteristics of metal cutting tools with undulating surface topographies is complete. The tools' novel surface structure was modified by the EDM process to a surface roughness of between 1.4–1.8 μm and coated with one layer of TiN to a thickness of 4 μm. The modified tools were subjected to cutting tests at various cutting speeds in order to assess the tools' performance and the possibility of using this study to improve future tool design and cutting capability. In order to achieve this goal, during machining experiments the tool wear was monitored by scrutinising tool flank wear and work surface finish. Data from the observed results have been used in the computer simulation and modelling of the tool performance to authenticate experimental findings.

6.0   Interest in Tool-Wear

For manufacturing industries involved in metal machining; their production engineers and planners are interested in predicting the life span of tools for every component produced. The reason for this interest is because tool life estimation and its economic benefits are essential in manufacturing 'process planning and component machining optimisation' (Ee *et al.*, 2003). When machining with flat-faced tools, either the flank wear or the crater wear is often considered as a measure of tool life (ASME: B94.55M, 1985; Colding, 1959; ISO 3685, 1993; Rubenstein, 1976; Usui *et al.,* 1984). The Usui wear model was used in the simulation model based on equation 6.1 for wear characteristics as proposed by Usui *et al.* (1984). This provides a simple relationship that relates the wear rate with the normal stress and the temperature field on a flat faced tool, but it is rather complicated for tools with a crater-like surface topography because of the intrinsic complex geometry.

$$\dot{w} = K.e\left(\frac{Alpha}{T+273.15}\right).p.v \qquad \text{Equation 6.1}$$

Where the constant *K* has units (1 Pa or 2E-9) and *Alpha* (3000) are material constants which are both dimensionless, $\dot{w}$ represents the wear model (volume loss per unit area per unit time), *T* represents the steady state temperature of the tool with a given amount of wear, *v* is the sliding velocity, and *p* is the pressure.

The basic requirement for the efficient machining of steel is a tool material that exhibits the toughness of the tungsten carbide while giving the superior wear resistance of TiC coatings (Boothroyd and Knight, 1989). Eventually, when the coating is worn off by abrasion, Boothroyd and Knight stated that the tool wear rate becomes the same as that for the uncoated conventional tool. Successes have been reported with coatings of tool substrates with TiC (Suh and Sanghvi, 1971), titanium dioxide (Feinberg, 1971), and TiN (Dobrzanski *et al.,* 2004). Up till now, it is assumed that the best results would be obtained with a TiN coating on a solid tool because the main characteristics of titanium are high strength, low density and high corrosion resistance to acid, alkali and chlorine (Jaharah *et al*., 2010). These special characteristics of titanium made it the first choice in chemical, bio-material, and military industries, and for shipping and marine applications (Nuawi *et al.*, 2007; also cited by Jahara *et al.*, 2010).

6.1.0   Hard Coatings Analysis

Among the many hard coatings available today, TiN and TiC are the most widely used ceramics coatings in the metal cutting industry, and this is due to their hardness and high wear resistance, low coefficient of friction, high temperature strength and chemical stability (Bhushan and Gupta, (1991); Jahara *et al.*, (2010); Kickel *et al.*, (2000); also cited by Zenghi and Hashmi, (2004).

According to Zenghi and Hashmi (2004), the application of TiN and TiC by CVD or PVD processes to tool steel substrates reduces tool wear by up to six times. Sundqvist, Sirvio and Kurkien (1983) proposed that an 'increase in the wear resistance of tool life coated with TiN can be expected only when the roughness of the surface is less than the coating thickness'. Thus, for this particular study the coating applied to the tungsten carbide inserts was 4 μm thick and the tools' surface roughness is in the range of between 1.4–1.8 μm, which is in agreement with Sundqvist, Sirvio and Kurkien (1983).

6.1.1 Analysis

<u>Test on Coated EDMed Specimens and Plain-Coated Inserts</u> The results show the following:

6.1.2 Wear on Rake Face

Wear on the rake face took place in the form of a crater away from the cutting edge, in a zone where the temperature was highest due to friction and normal loads. The primary mechanism was by way of abrasion caused by the chip rubbing against the tool surface. Results showed that at all speeds, the EDMed surfaces investigated have a much higher resistance to wear. The TiN coating on the rake faces of the control specimens visibly appeared to be worn off after a short duration of cutting. Meanwhile, the coating on the EDMed surfaces was noticeably held for a much longer duration of cutting. However, although the coating was worn off by way of a crater, the remaining coating continued to offer resistance to wear. This phenomenon of wear resistance due to coating was also noticed earlier by Holmberg and Mathews (2009); Wallén and Hogmark (1989); and also cited by Smith *et al*. (1988); Stjernberg (1985); and Sundqvist, Sirvio and Kurkien (1983). Furthermore, the coating was capable of carrying the full load of the chip without collapsing. Wallén and Hogmark (1989) compared the profile of wear scars produced on uncoated and TiN-coated cylinders in a crossed-cylinder wear test. They found that the presence of the TiN rim produced a concave wear scar, while the scar on the corresponding uncoated specimen was flat. In regard to the EDMed surface, it can be postulated that the sliding friction is likely to be reduced, as islands of residual TiN coating are likely to remain for longer in the 'valleys' of the undulating surface topography. During the cutting tests, consistent lower power readings for EDMed specimens indicate lower friction forces at the tool–workpiece interface. Considering the cutting speed of the 350 m/min test results, whereas wear was visible after a short time of five cuts/passes (which equates to 2 minutes) on the control specimen, wear became visible after 15 cuts (which equates to 7 minutes) on the TiN-coated EDMed test specimen. Interestingly, after 27 cuts (which equates to 12.9 minutes) the control specimen fails possibly due to excessive crater wear on the rake face, which can be explained mathematically by equation 6.2 below. Although there was no visible wear on the rake faces of the EDMed test specimens after five cuts, the surfaces on the cutting zone appeared to be 'mottled'. Figure 6.1 below is a demonstration of how excessive crater wear developed on the tool's rake face.
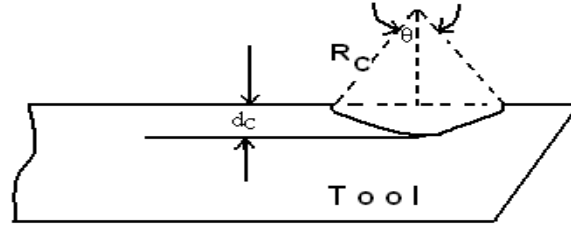
Figure 6.1 Illustration of the Development of Crater Wear
(After Juneja, Nitin and Sekhon, 2003)

Mathematically, let us Take R_c to be the radius of curvature of the crater and θ as its included angle in radians ($\theta < 1$) in order to calculate the tool rake face wear volume.

$$W = \frac{1}{2}bR^2(\theta - \sin\theta) = \frac{1}{2}bR^2\left[\theta - \left(\theta - \frac{\theta}{6} + ...\right)\right] = \frac{1}{12}bR^2\theta^3 \qquad \text{Equation 6.2}$$

By assuming that the rate of wear is proportional to the contact area we have:

$$\frac{dW}{dt} = \kappa_4 bR\theta \qquad \text{Equation 6.3}$$

Where κ_4 is a constant of proportionality.

$$\text{Thus} \quad \frac{d}{dt}\left(\frac{1}{12}bR^2\theta^3\right) = \kappa_4 bR\theta \qquad \text{Equation 6.4}$$

Now both R_c or simply R and θ are functions of time. Differentiating the LHS, we obtain:

$$\frac{bR\theta^3}{6}\frac{dR}{dt} + \frac{bR^2\theta^2}{4}\frac{d\theta}{dt} = \kappa_4 bR\theta$$

$$\frac{R\theta^2}{6}\frac{dR}{dt} + \frac{R^2\theta}{4}\frac{d\theta}{dt} = \kappa_4 R$$

Multiplying both sides by $8R^{-2/3}$

$$\frac{d}{dt}\left(\theta^2 R^{4/3}\right) = 8\kappa_4 R^{1/3}$$

$$\theta^2 R^{4/3} = 8\kappa_4 \int R^{1/3} dt + C \qquad \text{Equation 6.5}$$

Where the constant of integration C is zero. The radius of curvature of the crater decreases with time according to exponential law.

$$R = at^{-n} \qquad \text{Equation 6.6}$$

Where a and n are positive constants.

Substituting (7.6) in (7.5), we get:

$$\theta^2 a^{4/3} t^{-4n/3} = 8\kappa_4 \int a^{1/3} t^{-n/3} dt$$

113

$$\theta^2 = \frac{8\kappa_4 t^{1+n}}{a\left(1-\dfrac{n}{3}\right)}$$

$$\theta = \sqrt{\frac{8\kappa_4}{\left(1-\dfrac{n}{3}\right)}}\, t^{(1+n)/2} = \kappa'_{ad}\, t^{(1+n)/2}$$

<div align="right">Equation 6.7</div>

The depth of crater d_c is given by the relationship:

$$d_c = R\left(1-\cos\frac{\theta}{2}\right) \cong R\left[1-\left(1-\frac{1}{2}x\frac{\theta^2}{4}\right)\right]$$

$$= \frac{R\theta^2}{8} = \frac{at^{-n}}{8}\, x\left(\kappa'_{ad}\right)^2 xt^{1+n} = \frac{a(k'_{ad})^2}{8}\, t$$

$$d_c = \kappa_5 t$$

<div align="right">Equation 6.8</div>

Where κ_5 is a constant $= \dfrac{a(\kappa'_{ad})^2}{8}$

Accordingly, this proves that the depth of crater wear increases linearly with time.

6.1.3 Flank Wear

Wear on the tool leading flank started to develop around the tool corner radius and progressed along the cutting edge. Flank wear is considered as a criterion for tool life and it is attributable to rubbing against the machined work surface through diffusion of the constituents of the tool material occurring at the contact length at the flank and the contact length at the chip–tool interface, as illustrated in Figure 6.2.
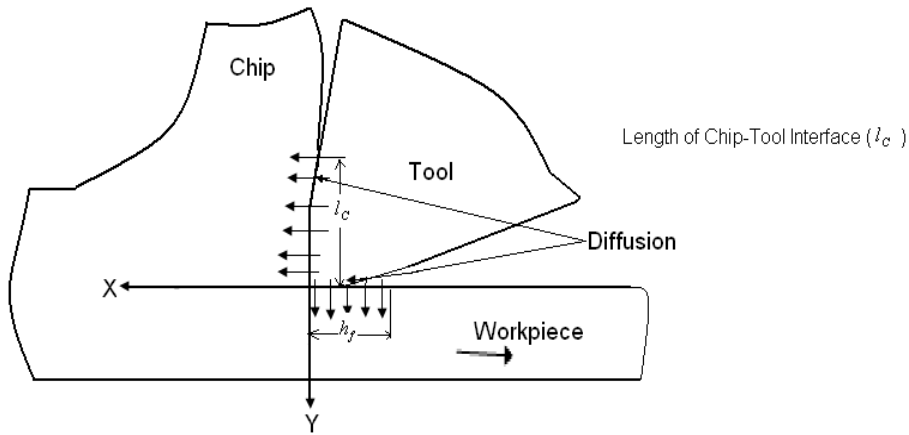
Figure 6.2 Illustrative Analysis of Diffusion Wear

The diffusion of the constituents of the tool material occurred according to Fick's second law, which predicts how diffusion causes the concentration field to change with time. The rate of change concentration $\dfrac{dc}{dt}$ of the diffusing constituents is proportional to the mass input in

the direction of diffusion across the wear-land at the flank. Mathematically, the law is expressed as follows:

$$\frac{dc}{dt} = D\frac{\delta^2 C}{\delta y^2}$$

Equation 6.9

Where D is called the diffusion coefficient in dimensions of (length^{2}time^{-1}), as in this example $\left(\frac{m^2}{S}\right)$, and t is the time in seconds, D is temperature dependent such that:

$$D = D_0 e^{-Q/RT}$$

Equation 6.10

Where D_o is a constant, Q is the activation energy for the diffusion process, R is the universal gas constant and T is the absolute temperature, assumed constant over the flank length h_f. On solving the above equation, the expression for concentration C of the diffusing constituents gives equation 6.11 with respect to time t.

$$C = C_0\left[1 - erf\left(\frac{y}{2\sqrt{Dt}}\right)\right]$$

Equation 6.11

Where C_0 is the concentration of the diffusing constant at the interface $y = 0$, and the error function $erf\left(\frac{y}{2\sqrt{Dt}}\right)$ is given by:

$$erf\left(\frac{y}{2\sqrt{Dt}}\right) = \frac{2}{\sqrt{\pi}}\int_0^{y/2\sqrt{Dt}} e^{-\alpha^2}dx$$

Equation 6.12

Let J_y denote the diffusing mass per unit area per unit time in the y-direction. Applying Fick's law, we have the diffused mass in time τ_f across the flank face as:

$$J_y = -D\left(\frac{\delta c}{\delta y}\right)_{y=0}.x\tau_f$$

Equation 6.13

By differentiating equation 6.11, it becomes

$$\left(\frac{\delta c}{\delta y}\right)_{y=0} = \frac{-2C_0}{\sqrt{\pi Dt}}$$

$$(Jy)_{y=0} = 2C_0\sqrt{\frac{D}{\pi\tau}}$$

Therefore, the diffusion mass M_f across the flank face in time τ_f is given by:

$$M_f = 2C_0 h_f b\sqrt{\frac{D\tau_f}{\pi}}$$

Equation 6.14

115

from equation 6.10, we get

$$M_f = 2C_0 h_f b \sqrt{\frac{D_0 \tau_f}{\pi}} \chi \exp\left(-\frac{Q}{2RT_f}\right)$$

Equation 6.15

From equation 7.15 it can be interpreted that if the values of flank wear-land h_f, width of the cut b, time τ_f and flank face temperature T_f are high, then there is bound to be a greater amount of the diffused mass, which agrees with Fick's second law.

Fick's second law predicts how diffusion causes the concentration to change with time:

$$\frac{d\emptyset}{dt} = D \frac{\partial^2}{\partial x^2}$$

Equation 6.16

Where:

- Φ is the concentration in dimensions of [(amount of substance) length^{-3}],

- t is time [s]

- D is the diffusion coefficient in dimensions of [length^2 time^{-1}], e.g. $\left(\frac{m^2}{s}\right)$

- x is the position [length], e.g. m

from Fick's First law and the mass conservation in the absence of any chemical reactions:

$$\frac{\partial \emptyset}{\partial t} + \frac{\partial}{\partial x} J = 0 => \frac{\partial \emptyset}{\partial t} - \frac{\partial}{\partial x}\left(D \frac{\partial}{\partial x} \emptyset\right) = 0$$

Equation 6.17

Assuming the diffusion coefficient D to be a constant, then exchanging the orders of the differentiation and multiplying by the constant:

$$\frac{\partial}{\partial x}\left(D \frac{\partial}{\partial x} \emptyset\right) = D \frac{\partial}{\partial x} \frac{\partial}{\partial x} \emptyset = D \frac{\partial^2 \emptyset}{\partial x^2}$$

Equation 6.18

and thus we reach the form of the Fick's equations as stated above.

As a rule of thumb, flank wear around the tool corner radius will affect the surface finish and dimensional accuracy of the work. Results showed that flank wear on both the control and the EDMed specimens was similar, though different in magnitude.

However to consider diffusion at the rake face, let T_C be the average rake face temperature, l_C the length of the chip–tool interface and τ_C the time during which diffusion takes place.

Then following equation 6.15, the diffused mass M_C may be expressed across the chip–tool interface by the equation:

$$M_C = 2C_0 l_C b \sqrt{\frac{D_0 \tau_C}{\pi}} \exp\left(-\frac{Q}{2RT_C}\right)$$

Equation 6.19

Equation 6.19 is an approximation because the temperature varies rather sharply over the length of the chip–tool interface as well as with time. In addition this analysis only gives loss of tool material through diffusion, and it does not include the loss through post-diffusion adhesive wear, which is difficult to quantify.

6.1.4   Surface Finish

The 'ideal' surface finish of a turned component is a function of the tool corner radius ($R\mathcal{E}$), which is 0.8 mm for the inserts in this study, and the tool feed rate. The real surface finish is influenced by additional factors such as BUE formation, machine tool vibrations and the 'Sokolowski effect' (*sideways extrusion of work material*). The surface finish produced by the EDMed inserts is clearly better than those of the control specimens, which could be attributed to the smooth characteristics of titanium.

6.2.0   Scrutiny and Postulations

6.2.1   Cutting Tests for Both Uncoated EDMed and Non-EDMed Inserts

The overall performance of uncoated inserts for both EDMed and non-EDMed was on the whole poor. It was evident that after only 2 minutes of cutting, which equates to 5 cuts/passes, a substantial wear-land became visible on the rake face and the flank of both the control specimens and the uncoated EDMed test specimens. This observation was consistent for all pairs of specimens tested. The surface finish on the workpiece machined with these uncoated inserts was consistently bad. Another observation noted was that the wear on the uncoated EDMed test specimen was marginally higher, which can be attributed to the higher friction generated by the rough EDMed surface. This result is in contrast to the results obtained for coated EDMed surfaces, and strengthens the 'residual islands' hypothesis in relation to the key role of the TiN coating.

6.2.2   Friction Force on the Chip–Tool Interface

Coatings are widely used to control friction and wear in all kinds of contact. This is reinforced by a large amount of experimental experience about the behaviour of coated surfaces in tribological contact and can be of much use in tool design and manufacture.

Generally contact in-between two coated surfaces with differing parameters which affect the tribological contact process can be characterised as:

i. coating to substrates hardness relationship,

ii. the film thickness of the coating,

iii. the surface roughness of the coating contour,

iv. the debris in the contact area.

This therefore implies that the interrelationship between these dimensions for each real case can be considered to have a dominating effect on both friction and wear at the macroscale. Friction and wear are governed by the shear force taking place at the top surface of the workpiece and in the deformed surface layer, and by the elastic, plastic and fracture behaviour both at the tip and within the deformed surface layer. A thin coating is typically a part of this deformed surface layer. In addition, surface degradation may take place due to tribolo-chemical and fatigue processes (Holmberg and Mathews, 2009) that influence the surface strength and the ability to withstand loaded conditions. Accordingly, Holmberg and Mathews state that the most crucial material parameters to consider in a modelling approach are the elastic modulus, the hardness, shear strength and the fracture toughness on the top surface, in the coating, at the coating–substrate interface and in the substrate under the coating. It was essential to investigate the interaction between the cutting tool and the chip to obtain good, practical simulation results for the cutting tests completed in this project. It is known that friction force is strongly influenced by cutting speed, contact pressure and cutting temperature. Zorev's (1963) model reveals two distinct regions on the chip–tool interface, these are the sliding region and sticking region. The normal and frictional shear stress distribution at the chip–tool interface is shown in Figure 6.3. It can be seen that from the tip of the tool up to a point, frictional stress is considered constant in a sticking region. After this point, frictional stress decreases on the tool rake face in the sliding region where Coulomb's friction law can be applied. This can be represented as follows:

$$\tau_f = \mu\sigma_n \text{, when } \mu\sigma_n < k_{chip} \text{ (sliding)} \qquad \text{Equation 6.20}$$

$$\tau_f = \kappa \text{, when } \mu\sigma_n \geq K_{chip} \text{ (sticking)} \qquad \text{Equation 6.21}$$

Where τ_f is the frictional stress, σ_n is the normal stress, μ is the coefficient of friction, and k_{chip} is the shear flow stress of the material.
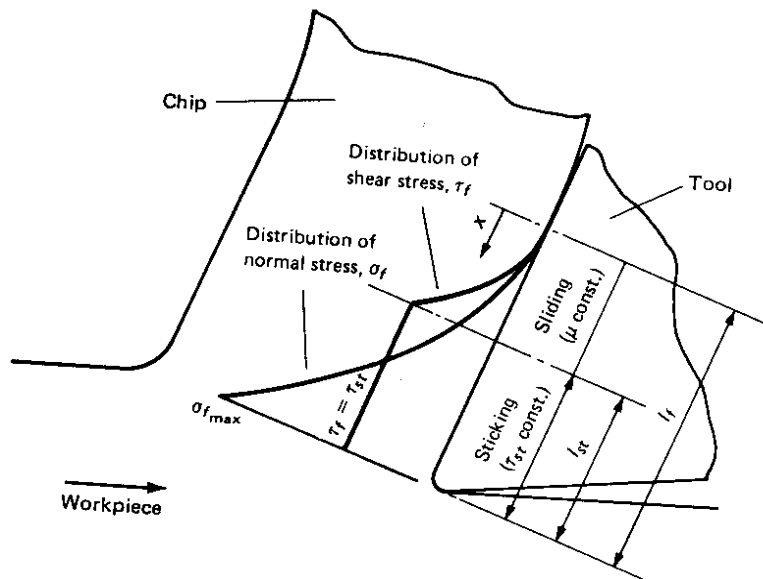
Figure 6.3 Curves Representing Normal (σ_n) and Frictional Stress (τ_f) Distribution on the Rake Face. (Adopted from Zorev (1963) page 42)

Simulation modelling of the cutting process using TiN-coated insert was completed and the mean coefficient of friction (μf) was determined by sampling 3,600 data of nodal μf in a sample size of 200 per set. The following were the results of the variance of the mean coefficient of friction from the incredibly high normal pressures that existed at the chip–tool interface: μf = 0.5, 0.4, 0.3, 0.2, 0.3, 0.3, 0.3, 0.3, 0.3, 0.3, 0.3, 0.2, 0.4, 0.3, 0.2, 0.2, 0.2, 0.0. This gave a mean coefficient of friction of 0.3. The results are plotted onto a graph and presented in Figure 6.4.
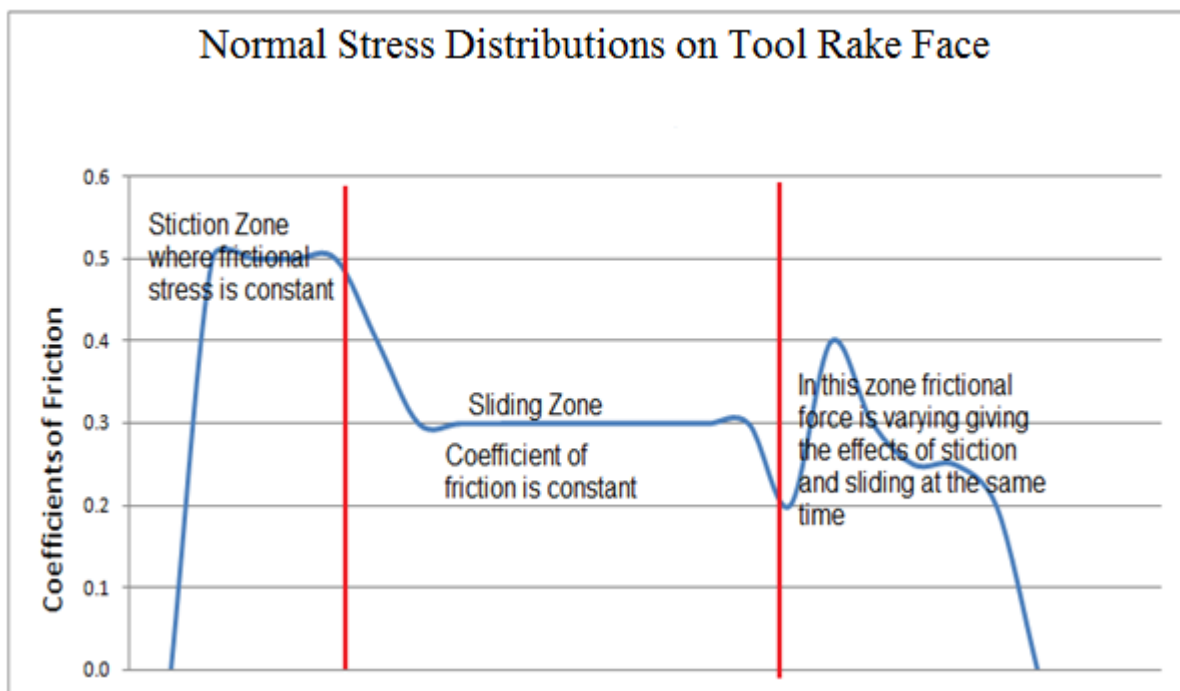
Figure 6.4: Normal and Frictional Stress Distributions on the Tool Rake Face

119

6.2.3   Stress Distribution on Tool Rake Face Explained

During, metal cutting it was observed that the mean coefficient of friction between the chip and the tool varied considerably and was affected by changes such as the cutting speed, rake angle, cutting fluid and materials property (Boothroyd and Knight, 1989). This variance of the mean coefficient of friction resulted from the very high normal pressures that existed at the chip-tool interface exhibited in the graph as stiction zone in figure 6.4 above. Zerov (1963) explained that when steel is machined, these normal pressures can be as high as 3.5 GN/m^2 and can cause the real area of contact to approach, or become equal to the apparent contact area over a portion of the chip-tool interface (i.e. $A_r/A_0 = 1$) as discussed in the last chapter, section 5.5.0. Thus under these circumstances A$_r$ has reached its maximum value and is constant as is demonstrated by the sliding action seen in the graph. At this point / zone, the coefficient of friction was constant.

6.3.0   Discussion of Results

Crater and flank wear as well as the chipping of the cutting edge affected some of the tools' performances in this study. It is known that cutting forces are normally increased by tool wear.   Nonetheless, crater wear under certain circumstances may reduce forces by effectively increasing the rake angle of the cutting tool.

Bhushan (1999) defined wear as the volume or mass of material removed per unit time or per unit sliding distance, and it is a complex function of time. Accordingly, looking at the coated tools, it could be seen that the cutting forces were lower than those of the uncoated inserts. This could be due to a number of reasons; the first may well be that there is decrease in friction between the chip and tool, and chip and work, and secondly the impact of the TiN coating acting as a thermal barrier.

6.3.1   Finite Element Simulations

The values for the coefficient of friction used in the tool performance modelling were obtained from simulations done with AdvantEdge V.5.9011 software as explained in section 5.5.2 in the previous chapter.

6.4.0 TiN Coating

Coating was applied to the tool surfaces to increase the tool's wear resistance. From observations the EDMed TiN-coated surface demonstrated lower wear than the plain-coated inserts as there was less coating material loss from the EDMed specimens compared to the plain-coated inserts. Though chips rubbing against the tool surface caused primary wear by abrasion, the EDMed surfaces still have a much higher resistance to wear. Results also show that the TiN coating on the rake faces of the control specimens appeared to wear off after only

a short duration of cutting, whereas the coating on the EDMed surfaces noticeably held for a much longer duration of cutting. This study agrees with Holmberg and Mathews (2009) who stated that the increased wear resistance of the tool was achieved by the high hardness of the TiN coating (2000 to 2500 Hv) which has good resistance to abrasive wear and chemical stability, resulting in a high resistance to solution wear.

From the results achieved so far and in addition to studies by other researchers there are indications that TiN has the following advantages:

a) Tough resistance to wear because oxidation of the TiN surface is slow at temperatures below 600 ^{0}C.

b) High chemical stability since it has high melting point, excellent thermal and chemical stability thus excellent wear and oxidation resistant properties at high temperatures.

c) Excellent lubricity and tribological properties, with a coefficient of friction as low as 0.15 to 0.3 and very low wear (Hbig, 1990; also mentioned by Franklin and Beuger, 1992).

d) Good friction stability and resistance to galling (Podgornik *et al.*, 2006).

e) High hardness of TiN coating, between 2000 and 2500 Hv, and good adhesion to substrates, which can inhibit interfacial cracking even when the substrate is plastically deformed due to surface stresses.

The resulting surface finish of the workpiece was improved by the presence of a TiN coating on the tool (Usenius *et al,* (2004); Jacobson, Wallén and Hogmark, (1987); Smith *et al.*, (1988). Usenius *et al.* (2004) noticed an improvement of 20% in reduced rake face wear when cutting spruce with HSS TiN-coated tools compared with uncoated tools. This is explained by the improved contact conditions causing smaller or fewer BUE fragments to be deposited on the cut surface, and partly by the fact that the lower forces obtained reduce the tool vibrations, which lead to deterioration in the surface finish (Hedenqvist, Olsson and Söderberg, (1988).

6.4.1 Benefits of Coated Tool Having Undulating Surface

6.4.2 Increased Production Rate

In many cases it is beneficial to increase the rate of production and maintain the same tool life. Similarly, knowledge gained in this study on improved properties of the cutting edge can be used to increase the cutting speed, feed and depth of cut or any combination of these parameters, in order for industries to obtain production at a higher rate.

6.4.3   Reduced Power Reading

The low power reading is beneficial, primarily because it demands less motor power of the cutting machine, while a reduced thrust force aids in lowering the demands for machine stability.

6.4.4   Load Carrying Capacity of the Surface

The explanation is that the remaining coating continues to oppose wear and is furthermore capable of carrying the full load of the chip without collapsing. It is thought that low and localised loads may be carried by the coating itself, with no need for support from the substrate; hence the relevant hardness would be inherent of the coating.

6.5.0   Effects of Undulating Surface Topography on Workpiece

In this work it has been established that there is unique adhesion of TiN to EDM crater-like surface topographies. The coating was 4 microns thick and the substrates had a roughness of between 1.4–1.8 μm. The overall work surface roughness measurements of components machined by EDMed TiN-coated inserts was particularly better for the 325 and 350 m/min cutting speeds giving work surface finish of 2.44 and 2.39 μm after 30 passes. This study indicates that after 2.5 minutes of cutting, a substantial wear-land became visible on the rake face of the control specimen, whereas after 7.7 minutes of cutting there was still no visible wear-land on the EDMed rake face of the test specimens. This is significant because it indicates the possibility of a longer tool life by way of tool wear compensation. Furthermore, the EDMed inserts operated at up to 18% reduced power consumption. This is beneficial to metal machinists because they can have reduced energy costs compared to a machinist using conventional tools who might be using upto 100% motor power for the same job.

6.5.1   Graph Explained for the 325 m/min cutting velocity

By comparison, the work surface finish, machined by the control specimen was rough ranging between 3.22 and 3.51 *μm*. On the other hand the workpiece machined by the EDMed modified and TiN coated insert revealed low Ra values of between 2.44 to 2.94 *μm*. The following assumptions can be deduced from figure 6.5 below.

- After five cuts the tools (inserts) both control and modified still sharp cutting tips with EDMed inserts leaving work surface roughness finish at 2.47 μm and conventional tool leaving Ra of 2.65 μm
- After ten passes, the control specimen started to abrade giving surface finish of 2.8 μm while the modified insert registered only 2.39 μm.
- After fifteen passes, there were mark changes in both work surface readings done by two inserts as the control insert registered 3.51 μm and the modified insert generated surface roughness of

2.94 μm. Giving an increase in work surface readings of 0.71 μm for the control and 0.55μm for the modified tool. These big changes could have occurred due to adiabatic conditions at the work-tool interface.
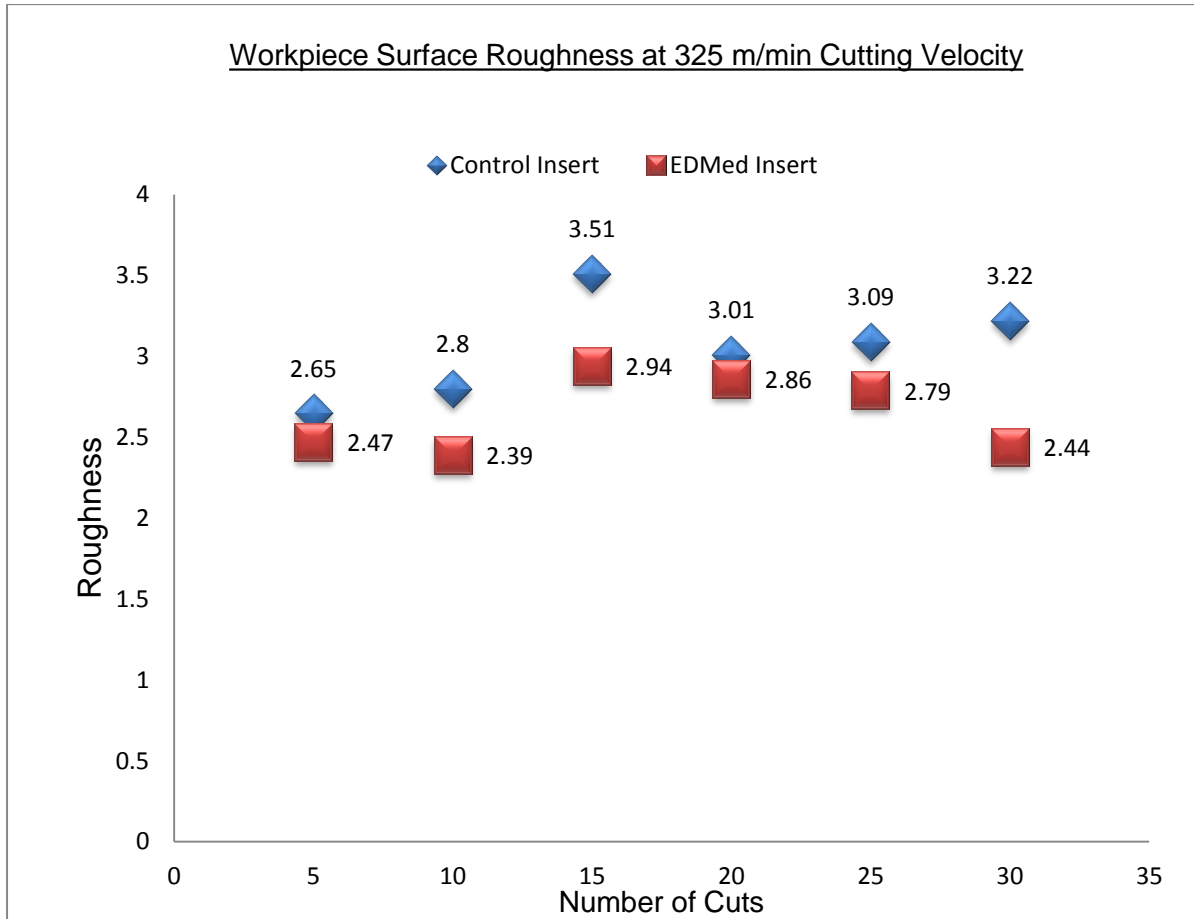
Figure 6.5: Work surface finish readings compared for the 325 m/min cutting velocity

- After this point surface roughness readings for the control insert kept on deteriorating ending up with Ra = 3.22 μm after 30 passes. Meanwhile, for the EDMed modified insert the work surface finish continued to improve and got better ending with Ra = 2.44 μm for the same number of (30) passes.
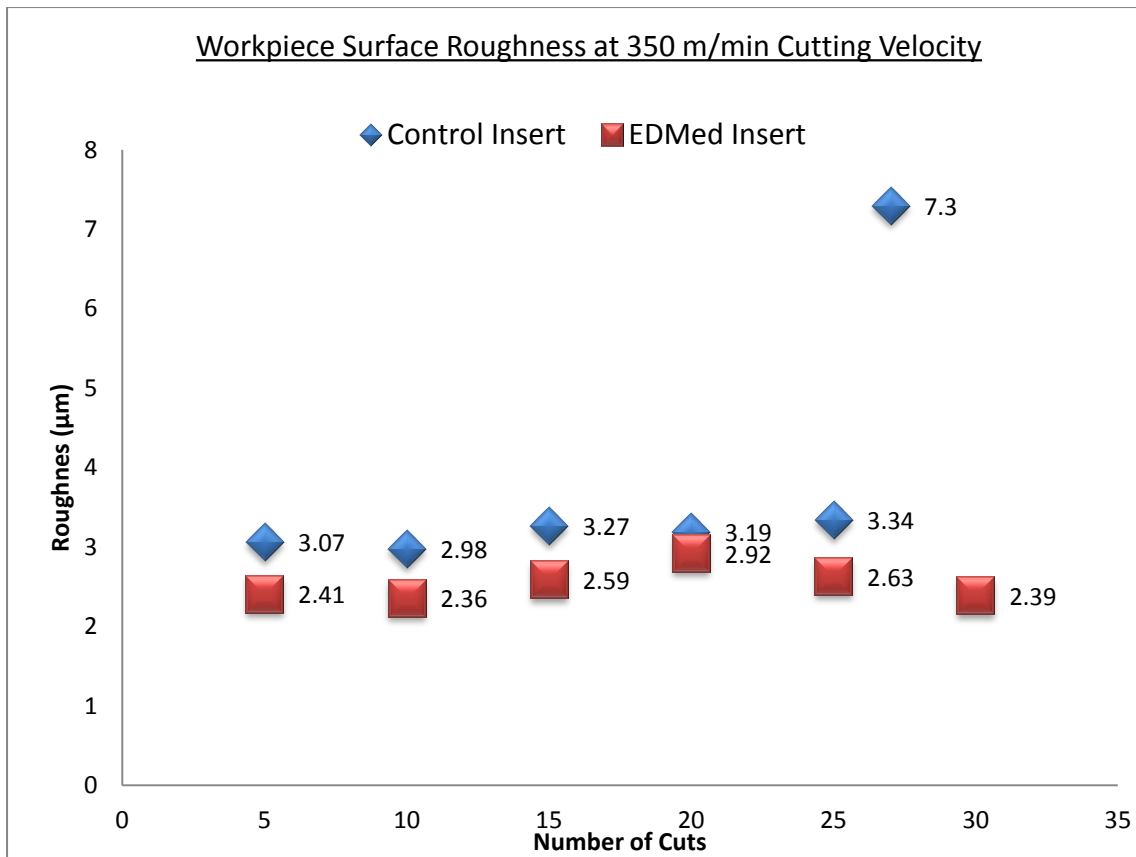
Figure 6.6: Work Surface finish compared for the cutting speed of 350 m/min

6.5.2 Graph Explained for the 350 m/min Cutting Velocity

By comparison, the performances of both tools were very contrasting. The Control Specimen left work surface finish readings of between Ra = 3.07 to 7.3 *μm*. These readings were clearly rougher than those of the EDMed modified insert Ra values of between 2.36 and 2.92 *μm*. Practical results show that machining at higher speeds generated smoother surface finish and this experience has been proven in the 350 m/min cutting speed. The 350 m/min cutting speed is very high by current standard in metal machining. The following assumptions can be deduced from figure 6.6 above.

- After five (5) passes the difference in surface roughness readings between the two inserts is 0.66 μm, with the modified insert reading at Ra = 2.41 μm, while the control Ra = 3.07 μm

- After ten (10) passes the difference in surface roughness readings between the two inserts is 0.62 μm, with the modified insert reading at Ra = 2.36 μm, while the control Ra = 2.98 μm

- After fifteen (15) passes the difference in surface roughness readings between the two inserts is 0.68 μm, with the modified insert reading at Ra = 2.59 μm, while the control Ra = 3.27 μm

124

- After twenty five (25) passes the difference in surface roughness readings between the two inserts is 0.71 µm, with the modified insert reading at Ra = 2.63 µm, while the control Ra = 3.34 µm

- The control specimen failed at 28 passes leaving work surface reading Ra= 7.5 m. while the modified tool registered Ra values of 2.39 m at both 30 and 35 passes. It never failed and was still capable of going further.

The lower power readings observed resulted from less heat generation and consequently lower edge temperatures. Thus, the temperature-dependent tool wear condition was decelerated with the TiN coating, and even after the coating was locally worn through by crater wear, the remnants still protected the substrate. The explanation is that the remaining coating continues to lubricate the tool surface and oppose wear, as the sticking region of the tool still had the coating, which reduced the friction coefficient.

Results from the simulation modelling of the tool with an undulating surface showed that the temperature at the tool–chip interface reached 734 ^{0}C, which was comparatively low. While, simulation results for the conventional tool varied between 1120 ^{0}C to 1300 ^{0}C. The low temperature effects allowed the tool to last longer with reduced friction between the tool flank and newly machined surface.

This explains why plain-coated inserts showed crater wear immediately after five cuts, yet the EDMed inserts showed no visible crater wear until after fifteen cuts. With the Digital Blue (5X) microscope under high magnification it could be seen that crater wear on the EDMed inserts began after 10 cuts, but was resisted by the coatings over the peaks and valleys on the tool rake face. The wear became apparent when it reached the bottom of the valleys. For this particular research, the tool substrate was coated with TiN by the PVD process to a thickness of 4 µm. It is documented that 'PVD coating techniques make it possible to extend tool life by 50% ' (Usenius *et al.*, 2004; also mentioned by Batista *et al.,* 2002; and Li *et al.*, 2001).

a) Through an atomistic wear process, TiN material is assumed to be continuously transferred from the coated region of the edge onto the worn out region, thereby modifying the contact conditions and reducing the wear rate.

b) This experiment proved that the tool can cut at very high speed (up to 40% higher than the manufacturers' recommended cutting speed).

c) The resulting surface finish of the workpiece was better due to the presence of a TiN coating on the tool which partly improved the contact conditions. Also partly by the

fact that the lower forces obtained reduce tool vibrations, which lead to deterioration in the surface finish in the case of using conventional tools (Smith *et al.*, 1988).

6.6.0 Statement Leading to Contributions to Knowledge

An investigation into the cutting characteristics of EDM surface-modified cutting tool inserts coated with TiN has been conducted. Comparative cutting tests on mild steel using control specimens with no EDM surface structures and cutting test specimens with EDM surface structures both coated with TiN to a thickness of 4 μm were carried out. Various cutting speeds up to an increase of 40% of the recommended speed of 250 m/min were investigated. The results showed that the EDMed inserts have enhanced wear characteristics at all speeds investigated. Furthermore, the surface finishes on the work were consistently better for the EDMed inserts.

The resistance to wear was observed at even greater speeds than the tool manufacturer's recommendation. In this study, the cutting speed was increased by up to 40%. Many papers have been presented which all show that TiN coatings often yield decreased wear rates and usually reduced friction coefficients in lubricated contact (Ajayi, *et al.*, 2003; Boving *et al.*, 1983; Jacobson and Hogmark, 2001; Iliuc, 2006; Liu *et al.*, 1991; Mabuchi *et al.*, 2004; Podgornik *et al.*, 2003; Ronkanien *et al.*, 1998). Batista *et al.* (2002) stated that 'in addition to enhanced abrasion resistance, TiAlN coatings can also provide wear and oxidation resistance, especially at high temperatures'.

6.6.1 Contributions to Knowledge

With respect to the above statement, the final results showed that the EDMed modified and TiN-coated tool inserts have properties which are resistant to wear during machining, and this phenomenon leads to the following contributions to knowledge:

(a) Provide technique of designing tool with roughened surface comprising of peaks and valleys covered in conformal coating with a material such as TiN, TiC etc which is wear-resisting structure with surface roughness profile compose of valleys which entrap residual coating material during wear thereby enabling the entrapped coating material to give improved wear resistance.

(b) Provide knowledge for increased tool life through wear resistance, hardness and chemical stability at high temperatures because of reduced friction at the tool-chip and work-tool interfaces, which leads to reduced heat generation.

(c)   Provide knowledge of coating a wear-resisting surface structure for application in contact surfaces and structures in metal cutting and forming tools with ability to give wear-resisting surface.

(d)   Undulating surface topographies on cutting tips tend to hold coating materials longer in the valleys, thus giving enhanced protection to the tool and the tool can cut faster by 40% and last 60% longer than conventional tools on the markets today.

6.6.2   Hypothesis

It can therefore be hypothesised that:

   i.   Coating metal cutting tools with undulating surface topographies to a thickness greater than the substrates surface roughness with hard materials like TiN or TiC permits higher cutting speeds and feeds, which may result in superior quality machining.

  ii.   The crater-like surface topography holds the coating in the valleys longer, thereby enhancing both the tool's performance and its operational life.

Chapter 7

Conclusions and Recommendations

The objective to investigate the performance of cutting tools with undulating surface topographies coated with TiN is complete. The specimens were subjected to cutting tests at various cutting speeds in order to assess the tool's performance and the possibility of using this study to improve tool design and cutting capability.

7.0 Observations

This study developed the experimental procedures for assessing the modified tools' performance and designed turning models to predict the tool's performance and resistance to wear including temperature distributions during machining. The cutting models showed that the highest temperature (950 ^{0}C) on the tool occurred in the tool–chip and tool–work interfaces under all cutting conditions and speeds investigated. It was presumed that the supply of cutting fluid helped prevent premature tool failure, which could have happened due to high temperature and other, unpredicted adverse conditions.

It was noted that there was increase tool life in the study. The increased tool life obtained by the TiN anti-wear coatings on the tool surfaces was due to chemical bonding to the tool's surfaces and valleys, which protected the substrates' from oxidation and excessive overheating. Since EDMed surfaces have peaks, troughs, the TiN particles entrapped in the valleys offered extended protection to the tool until when the peaks began to wear out.

7.1.0 Weaknesses of the Study

Though the project reached successful conclusions at the end, the research had many challenges right from the start to the end. The weaknesses in the study were;

    a) Lack of equipment at the University of East London, namely; Electrical discharge machine (EDM), Microscope, CNC Lathe machine and surface measuring machine. This prompted the need to sourcing the electrical discharge machine from Newport

Engineering in Harlow Essex on payment of over £1,000 (one thousand pounds sterling) for ten days of work at the company.

b) Meanwhile, for the initial laboratory cutting experiments on mild steel which needed a CNC Lathe machine, the work was done at Kennics Engineering Limited for a total fee of £1,200 (one thousand two hundred pounds). The cutting experiments were spasmodically done (i.e. *done occasionally on weekends, public holidays and weekdays*) and lasted over 30 days in all.

c) Lack of equipment for friction experiments that could be used to measure friction and surface damage. This was solved by simulating a 2-D turning/ cutting process with a tool having zero rake angle in the AdvantEdge[TM] software. This was discussed in detail in section 5.5.2, procedure for determining the Coulomb Friction Coefficient.

d) Absence of the right simulation software at UEL for the project modelling tasks presented a big setback for the project. This solved when a copy of AdvantEdge[TM] V.5011 was secured by Kyambogo University –Uganda at a price of US \$4,000 with a one-year License. Kyambogo University, gave part scholarship for the whole research.

7.2.0 Conclusions

The 3D FEA simulation of oblique turning was validated by comparing the coefficient of frictions and peak temperatures. It was noted that the contact conditions at the tool–chip interface were severe, as the cutting pressure was high (1000 MPa) and this caused heating at the interface, which affected the friction conditions and tool life. Since tool life is temperature dependent at the tool–chip and tool–work interfaces. The adverse effects of high cutting speed on tool temperature and tool wear around the cutting edge radius were reduced for the EDMed TiN coated test specimens presumably due to the TiN lubricity property as discussed in sections 4.8.0 – 4.10 and in the previous chapter section 6.5.0.

During the modelling, it was noticed that the steady state contact length and cutting force behaved in a way which suggested that the steady state was reached within the simulation time. In the AdvantEgde[TM] v.5.011 Simulation Software it was possible to compute steady state forces and stresses over a length of cut set at 200 mm for this study and this gave the cutting conditions just before the end of the cut based on analysis of heat transfer centred on heat generation. Good agreement was obtained between machining experiments and numerical results of cutting forces at 325 and 350 m/min cutting velocities as the simulation

results were in the range ±10% of the experimental results because adiabatic condition was assumed in the finite element model. The plastic strain and temperature distribution of the workpiece (see figure 5.1.4) shows that the deformation was greater at the primary and secondary shear zones because the adiabatic condition made the chip to soften thereby requiring less cutting force.

From the discussions presented in the preceding chapters on the characteristics of the modified TiN-coated tool, it can therefore be concluded that:

i. TiN coating substantially reduced the wear rate of inserts in the study as the coating remained on the EDMed surface, which composed of peaks, and valleys that provided pockets, which entrapped TiN coating layer /material, this gave improved wear resistance.

ii. The improved wear resistance of the TiN-coated inserts was due to the high wear resistivity and low friction coefficients of the TiN's outstanding properties of lubricity that remained on the tool rake face and consequently the contact temperature was also reduced due to the TiN chemical bonding onto the substrates and lubricity property.

iii. Peaks of the roughened EDMed surface with heights greater than the height of coating in the valleys gave wear-resistance for some duration while entrapped coatings in the valleys continued to lubricate the chip-tool contact zone by atomicity (Hedenqvist, P., *et al* 1990). The entrapped coatings provided good resistance to abrasive and adhesive wear as was evident on the workpiece surfaces despite the high temperature of 950 ^{0}C reached.

iv. Roughened contact surface comprising of peaks and valleys coated with a coating material (TiN) provided wear-resisting properties as the coatings were entrapped in the valleys and reduced friction at the chip-tool interface.

Furthermore, results showed that the EDMed coated tool inserts had properties that resisted wear during machining and even in cases where there were signs of wear still some remnants of the coatings remained visible by microscope in the wear scars, which continued to provide resistance to wear. The resistance to wear was observed at even higher speeds than the tool manufacturer's recommendation. In this study, the cutting speed was increased by up to 40% of the tool manufacturer's (Kennametal Inc.) recommendations. Many papers have been presented which all show that TiN coatings often yield decreased wear rates and generally reduced friction coefficients (Navinsek *et al* 2001, Holmberg and Mathews 2009, Stephenson and Agapiou, 2006, Hermann, A. J. M., 2000, Clapa and batory, 2007 and Hedenqvist *et al*

1990). In the course of cutting experiments/ tests, it was noticed that there was a unique adhesion of TiN to the EDM crater-like surfaces, which no one had previously identified.

7.2.0 Suggestions for Further Work

This work focussed on the study of the 'performance characteristics of a surface-modified cutting tool' for turning operations. Consequently, the study identified several future research avenues. To avoid going off track, the following suggestions are recommended for further study:

i. The work surface finish produced by the EDMed inserts is clearly better than those of the control specimens were. It was noticed that as the tool begun to wear the workpiece surface finish improved for sometime before deteriorating. It was also evident that the tool cut at a reduced power requirement of 18%, and that the work surface finish was better. This aspect warrants further investigation into the phenomenon.

ii. There should be some research to develop new tool-life relationships for machining operations by considering the tool's undulating surface structures. To establish a link between cutting conditions, tool coatings, work surface roughness, for all work materials (Aluminium, Brass, Stainless Steel etc.).

iii. The use of EDM to create the crater-like surfaces used in these experiments was not economical as it was slow and cannot be used for high volume production. Also the edges of the tool /inserts were weakened by the process, which resulted in ''mottled'' edges. Therefore, it would be useful to conduct research to determine the best way to create the crater-like surface topographies on the rake face of the inserts.

iv. During the cutting process, it was realised that the rake face of the EDMed specimen after five cuts appeared to be 'mottled'. It is therefore suggested that further investigation using SEM should examine the effect on the surface topography in this zone.

REFERENCES

Adachi, K. and Hutchings, I. M. 'Wear-mode mapping for the micro-scale', *Journal of Wear,* Vol.255 (2003), pp. 23- 29.

AdvantEdge^{TM} v.5.9011 Simulation modelling software. http://www.*Thirdwavesys.com 2012*

Agapiou, J.S., Steinhilper, E., Gu, F., and Bandyopadhyay, P., Modelling machining errors on a transfer line to predict quality, *SME J. Manuf. Processes, Vol.5,*(2003) pp1-12

Ajayi, O. O., Kovalchenko, A., Hersberger, J. D., Erdemir, A., Fenske, G. R., Surface damage and wear mechanisms of amorphous carbon coatings under boundary lubrication conditions, *Journal of Surface Engineering*, Vol.19(2003) pp447-453

Altan, T. and Vazquez, V. (1996) 'Numerical process simulation for tool and process design in bulk metal forming', *Annals of the CIRP,* 45 (2), pp. 599-615.

Altinas,Y., Manufacturing Automation. Metal Cutting Mechanics, Machine Tool Vibrations, and CNC Design, Cambridge University Press, Cambridge, UK, (2000)

Archard, J.F. (1953) 'Wear theory and Mechanisms, in: Peterson, M.B. and Winer, W. (eds.) *Wear Control Handbook.* New York: ASME, pp.35-80.

Armarego, E. J. A., and Brown, R. H., *The Machining of Metals,* Prentice Hall, New Jersey, USA, (1969), pp246-253

Arsecularanatne, J.A., Zhang., L.C., and Montross, C. 'Wear and tool life Of Tungsten Carbide, PCBN and PCD cutting tools', *International Journal of Machine Tools & Manufacture*, 46, (2006) pp.482-491. ISBN: 10: 0-444-52881-4

Astakhov V.P. (2004) 'Tribology of metal cutting', in Liang, H. and Totten G.E. (eds.) *Mechanical Tribology: Materials, Characterization, and Applications*. New York: Marcel Dekker publisher, pp.307-346.

Astakhov, V. P., Turning. In: Davin, J. P. (1st ed) Modern Machining Technology, Woodhead Publishing, Cambridge, UK, (2011), p67

Astakhov, V.P. Effects of the cutting feed, depth of cut, and workpiece (bore) diameter on the tool wear rate, *International Journal of Advanced Manufacturing Technology,* (2006) pp.200-210.

Batista, J. C. A., Joseph, M. C. Godoy, C., and Mathews, A, Micro-abrasion wear testing of PVD TiN coatings on untreated and plasma nitrided AISI H13, Journal of Wear, 249 (2002) pp 971-979

Batista, J.C.A., Joseph, M.C., Godoy, C. and Mathews, A. Micro-abrasion wear testing of PVD TiN coatings on untreated and plasma nitrided AISI H13, *Journal of Wear*, Vol.249, (2002) pp.971-979.

Bayer, R. G., Mechanical Wear Prediction and Prevention, Marcel Dekker publisher, New York, (1994), pp.657 ISBN:

Bhat, D.G. and Woerner, P.F. Coatings for cutting tools, *Journal of Metals and Materials,*Vol.2, (1986) pp.68-69.

Bhushan, B. and Gupta, B.K. (1991) *Handbook of tribology-Materials, coatings, and surface treatments*, New York, NY: McGraw-Hill. ISBN: 1-5752-4050-5

Bhushan, B. Wear and mechanical characterisation on micro- Picoscales using AFM, *International Material Review,* Vol.44 (1999) pp105- 117

Boothroyd, G., and Knight, W.A., (1989) *Fundamentals of machining and machine tools.* 2nd edn. Marcel Dekker, Inc, New York, USA, p.146: ISBN:0-8247-7852-9

Boresi, A. P., Schmidt, R. J., and Sidebottom, O. M., (1993) *Advanced Mechanics of Materials, 5th Ed. John Wiley & Sons,* p123, ISBN: 0-471-55157-0

Borodich, F. M., Harris, S. J., Keer, L. M. and Cooper, C. V. 'Wear and abrasiveness of hard carbon-containing coatings under variation of the load', *Journal of Surface Coating Technology*, Vol.179, (2004), pp.78-82.

Boving, H., Hintermann, H. E., Begelinger, A., De Gee, A. W. J., Load carrying capacity of lubricated steel point contacts coated by Chemical Vapour Deposition, *Journal of Wear Vol.88* (1983) pp13-22

Bromark, M., Hedenqvist, P. and Hogmark, S. 'The Influence of substrate material on the erosion resistance of TiN coated tool steel', *Journal of Wear,* (1995) pp.189-194.

Bull, S. J., Rickerby, D. D., Robertson, T. and Hendry A. 'The role of titanium in the abrasive wear resistance of physically vapour-deposited TiN', *Journal of Surface Coating Technology*, 41(1), (1988) p.743.

Burns, T.J. and Davies, M.A. 'Nonlinear dynamics model for chip segmentation in machining', *Physical Review Letters,* Vol.79 (3), (1997) pp.447-450.

Carroll, J. T., and Strenkowski, J. S.,: Finite Element Models of Orthogonal Cutting with Application to Single Point Diamond Turning, *International Journal of Mechanical Society,* Vol.30, (1988) pp899-920

Cekada, M., Panjan, P., Macek, M. and Amid, P. 'Comparison of structural and chemical properties of Cr-based hard coatings', *Journal of Surface Coatings Technology*, Vol.151-152 (2002) pp.31–35.

Celis, J.P., Ponthiaux, P. and Wenger, F. 'Tribo-corrosion of materials: Interplay between chemical, electrochemical and mechanical reactivity of surfaces', *Journal of Wear, Vol.*261, (2006) pp.939-946.

Childs T.H.C., Maekawa, K., Obikawa, T. and Yamane, Y. (2000) *Metal machining theory and applications*. London: Arnold Publishing.

Clapa, M. and Batory, D. 'Improving adhesion and wear resistance of carbon coatings using TiC gradient layers', *Journal of Achievements in Materials and Manufacturing Engineering, Vol.*20, (2007) pp.415-418.

Colding, B. N. A., Three Dimensional Tool-life equation,: Machining economics, *ASME Journal of Engineering Industry, Vol.81* (1959) pp239-250

Colwell, L.V., Predicting the angle of chip flow for single point cutting tools, ASME Trans. 76(1954) pp199-204.

Davim, J.P. and Astakhov, V.P. (2008) 'Tools (geometry and material) and tool wear', in *Machining fundamentals and recent advances*. Springer. ISBN: 978 1-84800-212-8.

Davis, J.R. (ed.) (2005) *Tool materials*. ASM Specialty Handbook. OH, USA: ASM International, p383

Dechjarern, S. (2002) *Study of the friction and wear behaviour of a coated cutting tool with different surface topologies*. Unpublished PhD thesis, Imperial College London.

Dechjarern, S. '3D finite element investigations of the influence of tool rake face angle on cutting performance', *Asian International Journal of Science and Technology in Production and Manufacturing,* 1(2), (2008), pp. 149-158.

Dechjarern, S., Busso, E. and Hibberd, R. 'Effects of surface roughness on friction and wear behaviour of coated cutting tools: numerical approach', *Proceedings of the International Conference on Tribology in Manufacturing Processes*, 36, (2004), pp.1-5.

Deller, D. L., National Mechanical Tools Builders Association, *IMTS-82 Technical Conference,* (September 8th – 17th 1982) pp290

Dewhurst, W. 'On the non-uniqueness of the machining process', *Proceedings of Royal Society London A*, 360, (1878), pp. 587-609.

Dieter, G. (1976) *Mechanical metallurgy*. New York: McGraw-Hill, p.278.

Dobrzanski L.A., Polok, M., Panjan, P., Bugliosi, S. and Adamiak, M. 'Improvement of wear resistance of hot work steels by PVD coatings deposition', *Journal of Materials Processing Technology*, Vol.155, (2004) pp.1995-2001.

Ee, K. C., Balaji, A. K., and Jawahir, I. S., Progressive Tool Wear Mechanisms and their effects on chip-curl / chip-form in machining with grooved tools: an extended application of the equivalent tool face (ET) model, *Journal of Wear, Vol.255* (2003) pp1404-1413

Ernst, H., and Merchant, M. E., Chip Formation, Friction and High Quality Machined Surfaces, in "Surface Treatment of Metals" *American Society of Metals, New York,* Vol.29, (1941), p299

Eu-Gene, Ng. and Aspinwall, D.K. 'Modelling of hard part machining', *Journal of Materials Processing Technology*, Vol.127, (2002), pp.222-229.

Ezugwu, E. O., High Speed Machining of Aero-engine alloys. *Journal of Brazil Society of Mechanical Science and Engineering. Vol.26,* (2005), pp1-11

Ezugwu, E.O., Olajire, K.A., and Jawaid, A., wear performance of Multilayered carbide tool, *Journal of Machining Science and Technology*, 5(1), (2001) pp115-121

Feinberg, B. 'Longer life from TiN tools', *Manufacturing Engineering Management,*Vol.67, (1971) p.16.

Fenton, R. G., and Oxley, P.l.B., Mechanics of orthogonal machining: Prediction chip geometry and cutting forces from work-material properties and cutting conditions, *Proc. Inst. Mech. Engin.* Vol.184, (1970), p927

Finnie I. and Shaw M. C. 'The friction process in metal cutting', *Transactions of ASME*, Vol.78, (1956) pp.1649-1657.

Fouvry, S. and Kapsa, P. 'An energy description of hard coating wear mechanisms', *Journal of Surface Coatings Technology*,138, (2001), pp.141-148.

Fox-Rabinvich, G.S., Shuster, L. and Dosbaeva, K.L., 'Impact of ion modification of HSS surfaces on the wear resistance of cutting tools with surface engineered coatings', *Journal of Wear*, Vol.294, (2001) pp. 1051-1058.

Franklin, S. E. and Beuger, J. A 'Comparison of the tribological behaviour of several wear-resistant coatings', *Journal of Surface Coatings Technology, Vol. 54/55,* (1992) pp.459-465.

Ghani, J.A., Choudhury, L.A. and Masjuki. H.H. 'Wear mechanisms of TiN coated carbide and uncoated cermets tools at high cutting speed applications', *Journal of Materials Processing Technology*, Vol.153-154, (2004), pp.1067-1073.

Gorczyca, F.Y., (1987) Application of metal cutting Theory, Industrial Press, New York, ISBN: 10:083-1111-76-3

Gordon, M. B., The applicability of binominal law to the process of friction in the cutting of metals, *Journal of Wear, Vol.10 (1967), pp274-290*

Grzesik, W. 'The influence of thin hard coatings on frictional behaviour in the orthogonal cutting processes, *Tribology International Conference*,Vol.33, (2000) pp.131-140.

Harju, E. J., Penttinen, I.M., Korhonen, A.A. and Lappalainen, R. 'Optimisation of wear and corrosion resistance of triode-ion-plated nitride coatings', *Journal of Surface Coatings Technology, Vol.*41, (1990) pp.157-166.

Hedenqvist, P., Olsson, M., Wallén, P., Kassman, A., Hogmark, S. and Jacobson, S. 'How TiN coatings improve the performance of high speed steel cutting tools', *Journal of Surface and Coatings Technology*, 41(2), (1990) pp.243-256.

Hendenqvist, P., Olsson, M. and Söderberg, S. (1988) 'Wear mechanisms of high speed steel and the effect of TiN-coating on wear resistance', presented at the *Nordic Conference on Tribology (NORTRIB'88)*, Trondheim, 26-29June.

Hermann, A.J.M. 'Multicomponent and multiphase hard coatings for tribological applications', *Journal of Surface and Coatings Technology,*Vol.131, (2000)pp.433-440.

Hieronimus, K.(1977) *A few aspects on the development of structural models*. SAE Technical Paper 770598, doi:10.4271/770598.

Hill, R., 'The mechanics of machining: A new approach', *Journal of Mechanics and Physics of Solids*, 3, (1954) pp.47-53.

Holmberg, K. and Mathews, A. (2009) *Coatings tribology properties, mechanisms techniques and applications in surface engineering*. Oxford, England: Elsevier, pp.235-337.

Holmberg, K., Laukkanen, A., Ronkainen, H., Wallin, K., Varjus, S., Koskinen, K., Tribological contact analysis of a rigid ball sliding on a hard coated surface –Part II: Material deformations, influence of coating thickness and Young's modulus. *Journal of Coating Technology, Vol.200*, (2006), pp3810-3823

Holmes, P.M. (1971) 'Factors affecting the selection of cutting fluids', *Journal of Industrial Lubrication Tribology*, 23(2), pp.47-55.

Holubar, P., Jilek, M. and Sima, M. 'Present and possible future applications of superhard nano-composite coatings', *Journal of Surface and Coating Technology,* 133-134, (2000), pp.145-151.

Horlin, N. A., TiC coated cemented Carbides –their introduction and impact on metal cutting, *prod. Engine. (Lond).,* Vol. 50(4-5) (1971) pp153-159

Hurless, B.E and Froes, F.H. (2002) 'Lowering the cost of titanium', *Advanced Materials and Processes Technology Information Analysis Centre (AMPTIAC) Quarterly*, Vol.6 (2), (2002) pp.3–9.

Iliuc, I., Wear micropitting of steel ball sliding against TiN coated steel plate in dry and lubricated conditions, *Journal of Tribology International, Vol.*39, (2006) pp607-615. Isakov, E. (2004) *Engineering formulas for metal cutting industrial*. New York, NY.

Iwata, K., Osakada, K. and Terasaka, Y.(1984)'Process modelling of orthogonal cutting by the rigid–plastic finite element method', *ASME Journal Engineering Materials and Technology*, 106, pp.132-138.

Jacobson, S. and Hogmark, S.(2001) 'The tribological character of boundary lubricated DLC coated components', *2nd World Tribology Congress*, Vienna, Austria, p. 9.

Jacobson, S., Wallén, P. and Hogmark, S. 'Intermittent metal cutting at small cutting depths and cutting forces', *International Journal of Machine Tools and Manufacture*, 28(4), (1987) pp. 551-567.

Jahanmir, S. 'On the wear mechanisms and the wear equations', in Suh, N. P. and Saka, N. (2nd ed.) *Fundamentals of Tribology*. London: The MIT Press, (1980), pp.455-467.

Jahara, A. G., Muhammad, R., Nuwai, M. Z., Haron, C. H. C and Ramli, R., Statistical Analysis for Detection Cutting Tool Wear Based on Regression Model, Lecture Notes in Engineering and Computer Science: Proceedings of the International MultiConference of Engineers and Computer Scientists 2010, IMECS 2010, 17-19 March, 2010, Hong Kong, pp.1784-1788

Jaspers S.P.F.C., Dautzenberg, J.H. and Oosterling, J. A. J. 'Machinability of MMCs using diamond coated tool', *Journal of Science and Engineering of Composite Materials,* 7(4),

(1998), pp.329-332.

Jawahir, I.S., Van Luttervelt, C.A., Recent developments in chip control research and applications, Annals of the CIRP, 42(1993) pp659-693.

Jiang, J. and Arnell, R.D. 'The effects of surface roughness on the wear of diamond-like carbon coatings', *Journal of Wear,*Vol.239, (2000) pp.1-9.

Jiang, J. and Stack, M.M. 'Modelling sliding wear, from dry to wet environments', *Journal of Wear*, Vol. 261, (2006) pp. 954-965.

Juneja, B.L., Nitin, S. and Sekhon, G.S. (2003) *Fundamentals of metal cutting and machine tools*. 2nd Ed. New Delhi, New Age Publisher, p.228.

Kalpakjian, S. and Schmidt, S.R. (2006) *Manufacturing engineering and technology*. Upper Saddle River, NJ: Prentice Hall. P.1039. ISBN: 0-13-197639-7

Karl, E.R., Komvopoulos, K., Three dimensional finite element analysis of surface deformation and stress in an eastic-plastic layered medium subjected to indentation and sliding contact loading, Trans. ASME. Journal of Applied Mechanics 63(1996,b) pp365-375

Kassman, A., Olsson, M., Jacobson, S. and Hogmark, S. (1989) *Internal Representation at UPTEC 89 084R*, Department of Technology, Uppsala University.

Kato, K. and Adachi, K. (2001) 'Wear mechanisms', in Bhushan, B. (ed.) *Modern Tribology Handbook*, New York: CRC Press, Vol. 1, pp.273-300.

Kato, K., Classification of wear mechanisms/models, Proceedings of the Institution of Mechanical Engineers, part J: Engineering Tribology, vol.216 (2002) pp349 – 355

Kickel, J., Shuaib, A. N., Yilbas, B. S., and Nizam, S. M., Evaluation of the wear of the plasma nitride and TiN coated HSS drills using conventional and Micro-PIXE technique, *Journal of Wear*, Vol.234 (2000) pp155- 167

Kim, G .S., Lee, S. Y., Hahn, J. H., Lee, B. Y., Han, J. G., Lee, J. H. and Lee, S. Y. 'Effects of the thickness of Titanium buffer layer on the mechanical properties of TiN coatings', *Journal of Surface Coatings Technology*, 171, (2003), pp.83-90.

Kim, K. W. and Sin, H.-C. 'Development of a thermo-viscoplastic cutting model using finite element method', *International Journal of Machine Tools and Manufacture, Vol.*36(3), (1996) pp.379-397.

Klocke, F. and Krieg, T. 'Coated tools for metal cutting – Features and applications', *Annals of the CIRP,*Vol.48, (1999) pp. 515-525.

Klopstock, H., In Berichte des Versuhsfeldes fur Workzeugmaschinen an der tech. Hocshe, Berlin, Vol.8 (1926) pp45- 50

Komvopoulos, K. and Erpenbeck, S.A. 'Finite element modelling of orthogonal metal cutting', *ASME Journal of Engineering for Industry*, Vol.113, (1991), pp.253-267.

Kopač, J. 'Cutting tool wear during high-speed cutting', *Strojniski Vesnik*, vol.50, (2004) pp.195-205.

Kraft, E.H. (2003) *Summary of emerging titanium cost reduction technologies*. Oak Ridge National Laboratory Report, ORNL/Sub/4000023694/1, December

Kragelskii, I. V., and Marchenko, E. A., Wear of Machine Components, Journal of Lubrication Technology, Trans., ASME, Vol.104, (1982), pp1- 8

Kramer, B.B., Tool Material for high speed machining, ASME J. Eng. Ind. 109(1987) pp87-91

Kuldeep, O., Garg, R.K. and Singh, K.K. 'MRR improvement in sinking electrical discharge machining: A review', *Journal of Minerals and Materials Characterization & Engineering,* 9(8), (2010) pp.709-739.

Kwostubhan, P., Lackner, J.M., Stotter, C., Waldhauser, W., Ebner, R., Lenz., W. and Beutl, M. 'Pulsed laser deposition of diamond-like carbon coatings for industrial tribological applications', *Journal of Surface Coating Technology,*vol.174-175, (2003) pp.402-407.

Landheer, D., and De Gee, Adhesion, Friction Wear, *MRS Bulletin, Oct.*, (1991) pp36-40

Lee, E.H. and Shaffer, B.W 'The theory of plasticity applied to a problem of machining', *ASME Journal of Applied Mechanics*, vol.18, (1951) pp.405-413.

Li, T. S., Li, H., and Pan, F. Microstructure and nano-indentation hardness of Ti/TiN multilayered film, *journal of Surface Coatings Technology*, vol.137, (2001) pp225 -229

Li, T. S., Li, H., and Pan, F., Microstructure and nano-indentation hardness of Ti/TiN multilayered film, Journal of Surface

Lin, Y.J. and Khrais, S. K 'Wear mechanisms and tool performance of TiAlN PVD coated inserts during machining of AISI 4140 steel', *Journal of Wear*, vol.262, (2007) pp.64-69.

Lin, Z.C. and Lin, S.Y. 'A coupled finite element model of thermo-elastic-plastic large deformation for orthogonal cutting', *ASME Journal of Engineering for Industry,* vol.114, (1992) pp.218-226.

Lin, Z.C., Pan, W.C. and Lo, S.P., "A Study of Orthogonal Cutting with Tool Flank Wear and Sticking Behaviour on the Chip-Tool Interface", *Journal of Materials Proc. Tech.*,Vol. 52, (1995) pp. 524-538

Mabuchi, Y., Hamada, T., Kano, M., Yasuda, Y., Ariga, K., Diamond-like carbon coating for reducing valve train friction, in: Proceedings FISTA 2004 World Automotive Congress, F2004F388, STA, Spanish Society for Automotive Engineers (2004) p15

Madhavan, V., Chandrasekar, S. and Farris, T.N. 'Mechanistic model of machining as an indentation process', in Stephenson, D.A. and Stevenson, R. (eds.) *Materials issues in machining III and Physics of machining processes III.* Journal of The Minerals, Metals & Materials Society, (1996) pp.187-208.

Madhaven,V., Chandrasekar, S. And Ferris, T. N., In Materials Issues in Machining III and the Physics of Machining Process, *Journal of Minerals, Metals and Materials Society,* (1988) pp187- 209

Maillet, B., Celis, J.P., Roos, J.R., Stals, L.M. and Van Stappen, M. 'Wear phenomena in the system TiN-coated high speed steel disk against a chromium steel pin', *Journal of Wear,*vol.142,(1991) pp.151-170.

Makarow, A. D., optimisation of cutting processes (in Russian), Machinostroenie, Moscow, (1976) pp100-105

Marinov, V., Experimental study on the abrasive wear in metal cutting, Journal of Wear, 197(1996) pp242-247

Mayrhofer, P.H., Mitterer, C. and Clemens, H. 'Self-organising nanostructures in hard ceramic coatings', *Journal of Advanced Engineering Materials*, vol.7(12).(2006) pp.1071-1082.

McCabe, M.J. 'How PVD coatings can improve high speed machining', *SME Conference, Northbrook, Illinois, September, (2001) pp.20-21,

McGeough, (1988), advanced Method of machining, Chapman Hall, London, pp 22 ISBN: 0-412-31970-5

Meng, H. C., and Ludema, K. C., Wear models and Predictive Equations their Form and Content, *Journal of Wear,*Vol.181/183, (1995) pp443-457

Merchant, M. E. 'Mechanics of the metal cutting process–1. Orthogonal cutting and a type 2 chip', *Journal of Applied Physics,*Vol.16(5), (1945) pp.267-275.

Merchant, M. E., and Zlatin, N., *Mechanical Engineering Vol.67*, (1945), pp737

Merchant, M.E. (1968) 'Friction and adhesion', inKu, P.M. (ed.) *Interdisciplinary approach to friction and wear*. NASA Publication, pp.181-265.

Mohan, D.L., Renganarayanan, S. and Kalanidhi, A.(2001) 'Cryogenic treatment to augment wear resistance of tool and die steels', *Cryogenics*, 41(3), pp.149-155.

Mohd Nor A.M.R., Jaharh, A.G., Eghawail, A.M., Kamal, O., Mohd N.A.R. and Haron, C.H.C. (2010)'Green turning of FCD 700 ductile cast iron using coated carbide tool', *IAENG Transactions on Engineering Technologies*,5, pp.260-266.

Moriwaki, T., Sigimure, N. and Luan, S. 'Combined stress, material flow and heat analyses of orthogonal micromachining of copper', *Annals of the CIRP,* 42, (1993), p.75.

Movahhedy, M. R., Gadala, M. S. and Altintas, Y. 'Simulation of the orthogonal metal cutting process using an arbitrary Lagrangian-Eulerian finite-element method', *Journal of Materials Processing Technology, Vol.*103, (2000) pp. 267-275

Movahhedy, M.R, Altintas, Y. and Gadala, M.S.'Numerical analysis of metal cutting with chamfered and blunt tools', *ASME Journal of Manufacturing Science and Engineering,*124,(2002) pp.178-188.

Navinsek, B., Panjan, P., Uranian, I., Vahte, P. and Gorenjak, F.'Improvement of hot-working process with PVD coatings and duplex treatment', *Journal of Surface Coatings Technology*, Vol.142-144, (2001) pp.1148-1154.

Nuawi, M. Z., Lamin, F., Nor, M. J. M., Jamaluddin, N., Abdullah, S. and Nizwan, C. K. E. 'Intergration of I-Kaz coefficient and Taylor tool life curve for tool wear progression monitoring in machining process', *International Journal of Mechanics,* vol.3(1), (2007) pp.45-50.

Olson, M., Stridh, B. and Söderberg, S. 'Sliding wear of hard materials - The importance of a fresh countermaterial surface', *Journal of Wear*, Vol.124, (1988), pp.195-216.

Oraby, S. E. and Alaskari, A. M. 'Mathematical modelling experimental approach of friction on the tool-chip interface of multicoated carbide turning inserts', *Proceedings of the World Academy of Science Engineering and Technology*, (2011) pp. 577-587.

Oxley, P.L.B. (1989) *Mechanics of machining: An analytical approach to assessing machinability*. New York, NY: Wiley.

PalDey, S., and Deevi, S.C., Single layer and multilayer wear resistant coating on (Ti,Al)N: A Review, *Journal of material science engineering, Vol.342,* (2003), pp58-79

Palmer, W. B., and Oxley, P.L.B., Mechanics of Orthogonal Machining, *Proc. IME*, Vol.173 (1959, p.623

Podgornik, B., Hren, D., Vižintin, I., Jacobson, S., Stavlid, N., Hogmark, S., Combination of DLC coatings and EP additives for improved tribological behaviour of boundary lubricated surfaces, *Journal of wear,* vol.26 (2006) pp32-40

Podgornik, B., Jacobson, S., Hogmark, S., Influence of EP and AW additives on the tribological behaviour of hard low friction coatings, *Journal of surface Coating Technology,* Vol.165(2003), pp168-175

Prengel, H. G., Jindal, P. C., Wendt, K. H., Santhanam, A. T, Hedge, P. L. and Penich, R. M. 'A new class of high performance PVD coatings for carbide cutting tools', *Journal of Surface and Coating Technology, 139,* (2001), pp.25-34.

Puertas, A.I., and Perez, L.C.J., Surface roughness prediction by factorial design of experiments in turning processes, *Journal of materials processing Technology, Vol.143-144* (2003) pp390-396

Rabinowicz, E. (1965) *Friction and wear of materials.* New York: John Willey & Sons, p.244.

Rabinowicz, E. 'The wear coefficient – magnitude, scatter and uses', ASEM Paper, No: 80-C2/Lab-4 Century 2, *ASME-ASLE International Lubrication Conference,* San Francisco, USA,Vol. 8,(1980) p.6.

Rao, S. B., Kumar, K. V. and Shaw M. C. 'Friction characteristics of coated tungsten carbide cutting tools', *Journal of Wear,* 49(2), (1978), p. 353.

Redford A.H., El-Bialy, B.H. and Mills, B. (1986) 'Proposed wear mechanisms for titanium nitride coated high speed steel', *Journal of Surface Engineering,*2(1), p. 29.

Samyn, P., Schoulkens, G., Quintelier, P. and De Baets, P. 'Friction, wear and materials transfer of sintered polyamides sliding against various steel diamond-like carbon coated surfaces', *Journal of Tribology International,* Vol.39, (2006) pp.575-589.

Sandvik Coromant (2008) *Modern metal cutting. A practical Handbook.* N J: Sandvik Coromant.

Schey, J.A., Tribology in metalworking, Journal of American Society for metals, Metal Park, Ohio, 11(1983) pp20-30.

Schulz, U, Peters, M, Fr. Bach, W. and Tegeder, G, Graded coatings for thermal, wear and corrosion barriers, *Journal of Materials Science and Engineering A362* (2003) pp 61-80

Sharif, S. and Rahim, E. A. 'Performance of coated and uncoated-carbide tools when drilling titanium alloy Ti-6A14V', *Journal of Materials Processing Technology,* 185, (2007) pp.90-96.

Shaw, M.C. (2005) *Metal cutting principles*.2nd edn. Oxford University Press, New York, p.330.

Shi, G., Deng, X. and Shet, C.'A finite element study of the effect of friction in orthogonal metal cutting', *Finite Elements in Analysis and Design, Vol.*38, (2002) pp.863-883.

Shih, A.J. and Yang, H.T.Y. 'Experimental and finite element predictions of residual stresses due to orthogonal metal cutting', *International Journal for Numerical Methods in Engineering,* 36,(1993) p.1487.

Shinozuka, J., Obikawa, T. and Shirakashi, T. 'Cutting performance of tools with curved rake face', in Usui, E. (ed.) *Journal ofAdvancement of intelligent production,* (1994) pp. 379-384.

Siniawski, M. T., Harris, S. J., Wang, O., A Universal wear law for abrasion, Journal of Wear, Vol.262, (2007), pp883-888

Smid, P., (2003) *A comprehensive guide to practical CNC programming: CNC programming handbook.*2ndedn. New York: Industrial Press Inc., p.67.

Smith A. B., Abbas, F. M. H., and Williams. R., Proceedings of 1st International Conference on the Behaviour of Materials in Machining (The Institute of Metals), Stratford-upon-Avon, UK November (8–10) (1988) p 38

Söderberg, S., Jacobson, S. and Olsson, M.(1987) *Wear atlas of high speed steel cutting tools*. UPTEC 87130 R. Uppsala University, Institute of Technology (in Swedish).

Söderberg, S., Jacobson, S. and Olsson, M.(1989) in Holmberg, K. and Nieminen, I. (eds.) *Proceedings of the 5th International Congress on Tribology,* Helsinki, Finland, Vol. 1, 12-15 June, p.412.

Soliman, F.A., Abu-zeid, O.A. and Merdan, M.(1987) 'The improvement of the performance of high speed steel turning tools by TiN coatings', *Journal of Wear*, 119, p.199.

Spur, G. and Gerloff, S. 'Modelling the chip formation and their influence on the marginal zone of workpiece by means of 3D-finite element analyses', *Production Engineering*, Vol. 3(1), (1996), pp. 11-14.

145

Spur, G., Byrne, G. and Bienia, B. 'The performance of high speed steel indexible inserts coated by PVD in the milling of ductile materials', *Journal of Surface Coating Technology*, 43/44, (1990), pp.1074-1085.

Stachowiak, G.W. and Batchelor, A.W. (2005) *Engineering tribology*. 3rd edn. Amsterdam, Holland: Elsevier, p.801.

Stephenson, D.A. and Agapiou, J.S. (2006) *Metal cutting theory and practice*. 2nd Ed. New York: Marcel Dekker. P78

Sternberg, K.T.A (1985), Wear Mechanisms of Coated Carbide Tools in Machining of Steel, High Productivity

Stoiber, M, Badisch, E, Lugmair, C and Mitterer, C, Low-friction TiN coatings deposited by PACVD, Journal of Surface and coatings technology, 163-164 (2003) pp 451

Strenkowski, J. S. and Moon, K-J. 'Finite element prediction of chip geometry and tool/workpiece temperatures distributions in orthogonal metal cutting', *ASME Journal of Engineering for Industry,* 112, (1990), pp.313-318.

Strenkowski, J.S. and Carroll, J.T. 'A finite element model of orthogonal metal cutting', *ASME Journal of Engineering for Industry,* Vol.107, (1985), pp.349-354.

Sue, J. A. and Troue H. H. 'Friction and wear properties of titanium nitride coating in sliding contact with AISI steel', *Journal of Surface Coating Technology*, (1) (1990), pp.709-720.

Sundqvist, H. A., Sirvio, E. H. and Kurkien, M. T. 'Wear of metal working tools ion plated with titanium nitride', *Journal of Metrology Technology,* (1983), pp.130-134

Tabor, D. 'Wear - A critical synoptic view', *Journal of Lubrication Technology,* (1977), pp.387-395.

Takadoum, J., Houmid-Bennani, H., Mairey, D. and Zsiga, Z.(1997) 'Adhesion and wear resistance of thin hard coatings', *Journal of the European Ceramic Society,* 17, (1997), p.1929.

Talantov, N. V., Physical Fundamentals of the cutting process, tool wear and failure (in Russian) Machinostroenie, Moscow, (1992) pp 120-126

Tay, A. A. O., The importance of allowing for the variation of thermal properties in the numerical computation of temperature distribution in machining, *Journal of Materials Processing Technology,* 28, (1991) pp. 49-58.

Taylor, F.W. (1907) On the art of cutting metals, *Transactions of ASME, Vol.*28, (1906) p.31

Tecvac Ltd. TiN Coatings Technology. : http://www.tecvac.co.uk/coatings01/php (Accessed: 25 April 2012).

Thornley, R.H. and Upton, D.P. 'Effects of TiN coatings on tools', *Production Engineering*, (1987), p.21.

Timings, R. L., (1998) Manufacturing Technology, Vol.1 3rd Ed, *Addison Wesley Longman, Harlow, England*, pp.189-190: ISBN 0-582-35693-8

Tomadi, S. H., Hassa, M. A., Hamedon, Z., Daud, R. and Khali, A. G. 'Analysis of the influence of EDM parameters on surface quality, material removal rate and electrode wear of tungsten carbide', *Proceedings of the International MultiConference of Engineers and Computer Scientists*, Hong Kong, Vol. II, (2009), pp.1803-1808.

Trent, E.M. and Wright, P.K. (2000), *Metal cutting Mechanics*. 4[th]ed. Butterworth Heinemann, Boston, Massachusetts USA.

Tyan, T. and Yang, W. H. 'Analysis of orthogonal metal cutting process', *International Journal of Numbers Methods Engineering.* 34, (1992) pp.365-389.

Usui and Takeyama, A Photoelastic Analysis of Machining Stresses, ASME Journal of Engineering Industrial, Vol.81, (1960), pp303-308

Usui, E. and Shirakashi, T. 'Mechanics of machining from descriptive to predictive theory', in: *On the art of cutting metals- 75 years later*. American Society of Mechanical Engineers, Vol.7, (1982), pp. 13-35.

Van Luttervelt, C. A, Childs, T. H. C., Jawahir, I. S., Klocke, F. and Venuvinod, P. K. 'Present situation and future trends in modelling of machining operations: Progress report of the CIRP Working Group "Modelling of Machining Operations', *Annals of the CIRP*, 47(2), (1998) pp.587-626.

Venuvinod, P.K., "3-Dimensional cutting force analysis based on the lower boundary of the shear zone .2. 2-edge oblique cutting", *International Journal of Machine Tools & Manufacture*, 36(3), (1996), pp. 325-338

Von Mises, R. 'Mechanik der Festen Korper in plastisch deformablen Zustand', *Göttin Nachr Mathematics Physics*, 1, (1913) pp.582-592.

Walker, P. I., and Dickinson, E. A., Cutting properties of titanium nitride coated high speed steel, *Proceedings Conference towards improved performance of tool materials,* TIPTOM vol.81 (1981), pp1 - 89

Wallén, P. and Hogmark, S., 'Influence of TiN coating on wear of high speed steel at elevated temperature', *Journal of Wear*, 130(1), (1989), pp.123-135.

Watson, M., Byington, C., Edwards, D. and Amin, S. 'Dynamic modelling and wear-based remaining useful life prediction of high power clutch systems', *Journal of Tribology Lubrication,* 61(12), (2005) pp.38-48.

Wellèn, P and Hogmark, S., Influence of TiN coating on wear of high speed steel at elevated temperature, *Journal of Wear*, Vol. 130 (1) (1989) p123- 135

Williams, J.A., Wear and Wear particles-some fundamentals, *Tribology Int.Vol.38* (2005)pp863-870

Wu, D. W. 'A new approach of finding the transfer function for dynamic cutting processes', *ASME Journal of Engineering for Industry*, 111, (1989) pp.37-47.

Wu, J. H., Karthikeyan, S., Falk, M. L., Rigney, D. A., Tribological characteristics of diamond-like carbon (DLC) based nanocomposite coatings, *Journal of Wear, Vol.259*, (2005), pp744-751

Ye, N., and Komvopoulos, K., Three-dimensional finite element analysis of elastic-plastic layered media under thermo-mechanical surface loading. *Trans. ASME, J. Tribology*, Vol.125 (2003) pp.52-59

Yin-Yu, C., Da-Yung, W. and Chi-Yung, H. Structural and mechanical properties of nanolayered TiAlN/CrN coatings synthesised by a cathodic arc deposition process', *Journal of Surface and Coatings Technology,* (2005), pp.1702-1708.

Zenghi, A.E. and Hashmi, M.S.J. 'Comparative wear characteristics of TiN and TiC coated and uncoated tool steel', *Journal of Materials Processing Technology,* 155-156, (2004) pp.1923-1926.

Zhan, G., Mitomo, M., Xie, R. and Kurashima, K., "The deformation mechanisms of superplastic flow in fine-grained beta- silicon nitride ceramics," *Acta Materialia*, Vol. 48, (2000), pp. 2373-2382.

Zhang, B., and Bagchi, A., Finite Element Simulation of Chip Formation and Comparison with Machining Experiment *Journal Eng. for Industrial., Trans. ASME* Vol.116, (1994) pp289-297

Zlatanvic, M., Munz, W.D., Wear resistance of hard plasma-nitrided and sputter-ion plated hobs. *Journal of Surface Coating Technology,* Vo.l41, (1990) pp17-30

Zorev, N. N. *Interrelation between Shear Processes Occurring along Tool face and on Shear Plane in Metal Cutting,* International Research in Production Engineering, Pittsburgh, Pa., (1963), p42
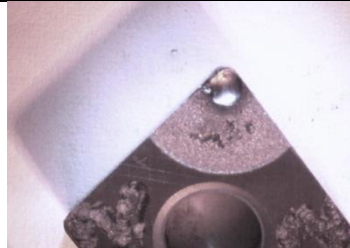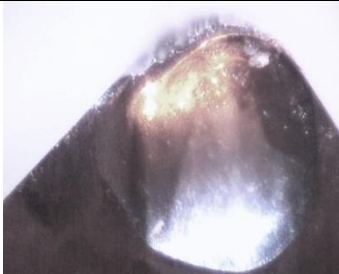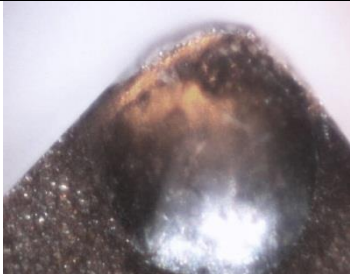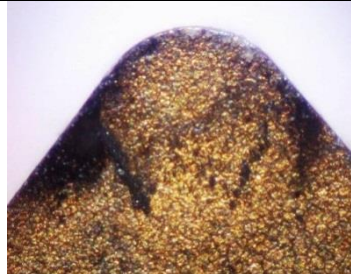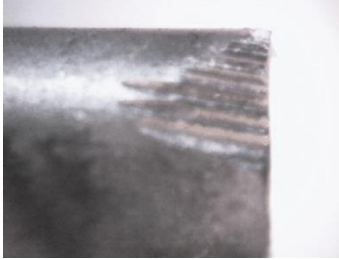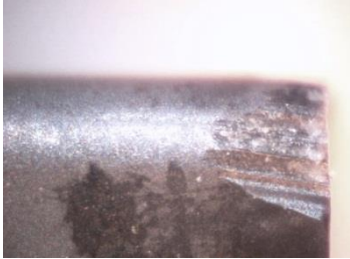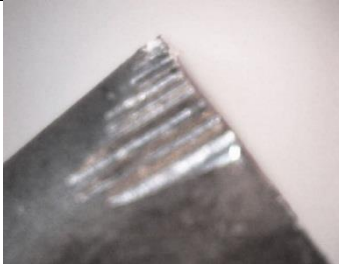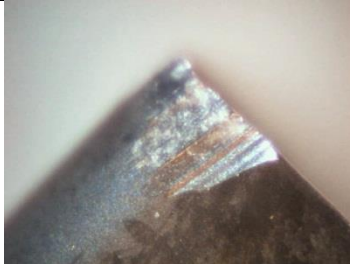
Zorev, N. N., Metal Cutting Mechanics, Pergamon Press, Oxford, (1966)

Cutting Tests Results

Cutting Test No: 01

Fixed Parameters: V = 350 m/min, d = 1 mm, f = 0.28 mm/rev, length of cut = 200 mm.
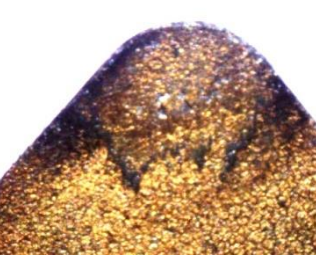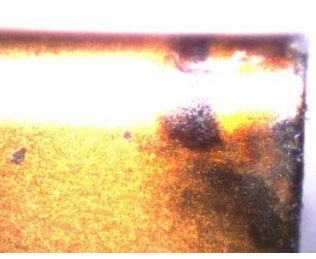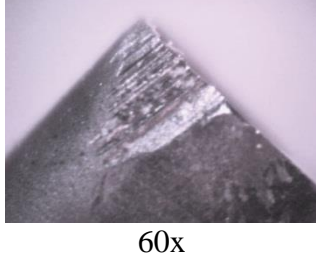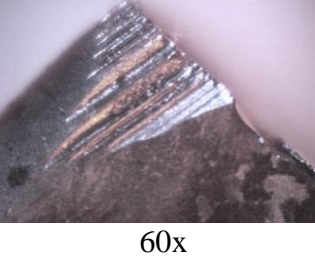
Plain Insert –Control	Uncoated EDMed Insert	Coated EDMed Insert
 10x Rake Face	 10x Rake Face	 10x Rake Face
 60x Rake Face	 60x Rake face	 60x Rake face
 60x Flank	 60x Flank	 60x Flank
 60x After 5 cuts, Flank, Power Load = 65%, Diameter = 61 mm Ra = 2.52 µm (after 2.4 minutes of cutting)	 60x After 4 cuts, Flank, Power Load = 65%, Diameter = 63.8 mm Ra = 3.25 µm (after 1.92 minutes of cutting)	60x After 5 cuts. Flank Workpiece Surface Roughness Ra = 2.41 µm

Appendix 1b
Cutting Tests Results

Cutting Test No: 02

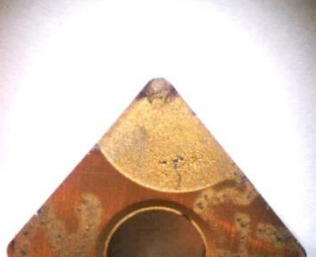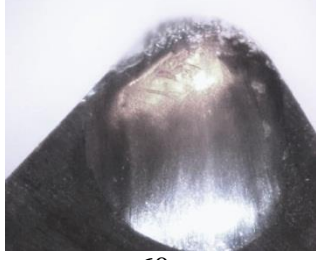Fixed Parameters: V = 350 m/min, d = 1 mm, f = 0.28 mm/rev, length of cut = 200 mm.

Plain Insert –Control	Uncoated EDMed Insert	Coated EDMed Inserts
10x Rake Face	10x Rake Face	10x Rake Face
60x Rake Face	60x Rake Face	60x Rake Face
60x Flank	60x Flank	60x Flank
60x After 5 cuts, Flank, Power Load = 65%, Diameter = 61 mm Ra = 2.64 µm (after 2.4 minutes of cutting)	60x After 5 cuts, Flank, Power Load = 65%, Diameter = 61 mm Ra = 3.42 µm (after 2.4 minutes of cutting)	60x After 10 cuts. Flank Workpiece Surface Roughness Ra = 2.36 µm
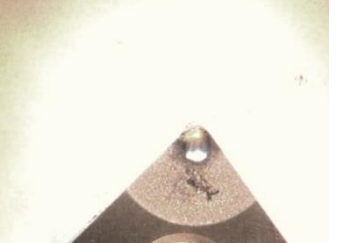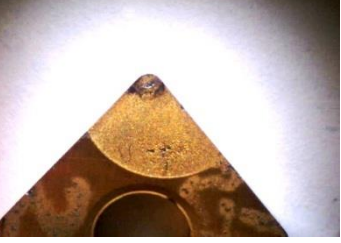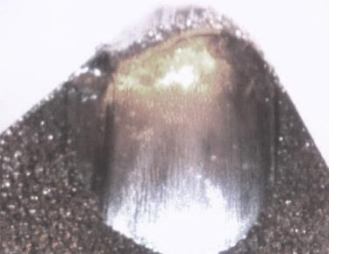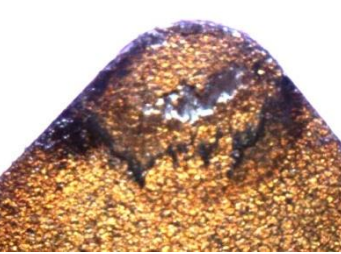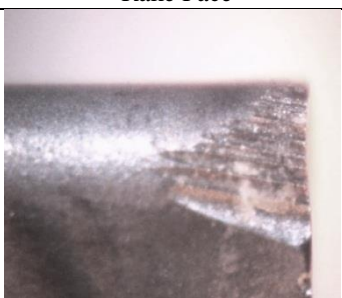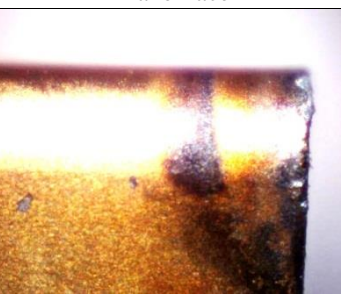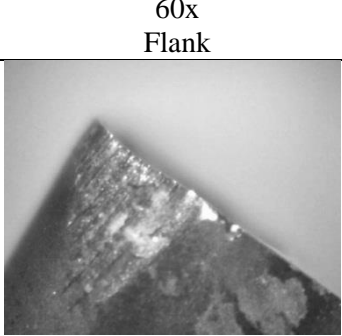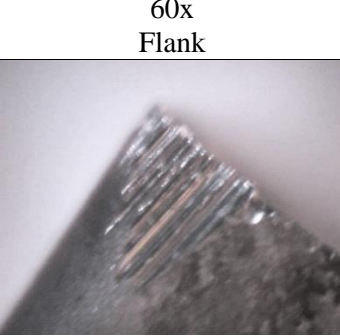
Appendix 1c
Cutting Tests Results

Test No: 03

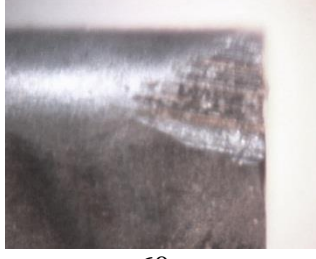Fixed Parameters: V = 350 m/min, d = 1 mm, f = 0.28 mm/rev, length of cut = 200 mm.

Plain Insert –Control	Uncoated EDMed Insert	Coated EDMed Inserts
10x Rake Face	10x Rake Face	10x Rake Face
60x Rake Face	60x Rake Face	60x Rake Face
60x Flank	60x Flank	60x Flank
60x After 5 cuts, Flank, Power Load = 65%, Diameter = 47 mm Ra = 2.58 µm (after 2.4 minutes of cutting)	60x After 5 cuts, Flank, Power Load = 65 %, Diameter = 47 mm Ra = 3.00 µm (after 2.4 minutes of cutting)	After 15 cuts. Flank Workpiece Surface Roughness Ra = 2.59 µm

Appendix II

G-Codes and Modal Program for Turning Operation on 30 HP Hitachi Seiki Lathe Machine

Program for the 250 m/min Cutting Speed
    00001 (**Mild Steel**)
    T0505 (Tool Number 10)
    G50 S2500
    G144 M08
    G18;
    GØ G97 T090900 S110 M03
    G96 S250 M08
    G30 UØ VØ WØ
    GØØ X100.0 Y0.0 Z1.0
    X46.0
    G71 P10 Q5Ø UØ WØ D1000 F0.28
    N10 GØØ X45.0
    N15 G01 Z0.0 F0.15
    N30 Z-200.0
    N50 X75.0 Z-225.0
    GØØ X100.0 Z1.0
    G28 X100.0 Y0.0 Z1.0
    M30

Program for the 300 m/min Cutting Speed
    00002(**Mild Steel**)
    T0505 (Tool Number 10)
    G50 S3000;
    G144 M08;
    G18;
    GØ G97 T090900 S110 M03;
    G96 S300 M08;
    G30 UØ VØ WØ;
    GØØ X100.0 Y0.0 Z1.0;
    X46.0;
    G71 P10 Q5Ø UØ WØ D1000 F0.28;
    N10 GØØ X45.0;
    N15 G01 Z0.0 F0.15;
    N30 Z-200.0;
    N50 X75.0 Z-225.0;
    GØØ X100.0 Z1.0;
    G28 X100.0 Y0.0 Z1.0;
    M30

Program for the 325 m/min Cutting Speed

       00003 (Mild Steel)

       T0505 (Tool Number 10)

       G50 S3250;

       G144 M08;

       G18;

       GØ G97 T090900 S110 M03;

       G96 S325 M08;

       G30 UØ VØ WØ;

       GØØ X100.0 Y0.0 Z1.0;

       X46.0;

       G71 P10 Q5Ø UØ WØ D1000 F0.28;

       N10 GØØ X45.0;

       N15 G01 Z0.0 F0.15;

       N30 Z-200.0;

       N50 X75.0 Z-225.0;

       GØØ X100.0 Z1.0;

       G28 X100.0 Y0.0 Z1.0;

       M30

Program for the 350 m/min Cutting Speed

       00004 (Mild Steel)

       T0505 (Tool Number 10)

       G50 S3500;

       G144 M08;

       G18;

       GØ G97 T070700 S110 M03;

       G96 S350 M08;

       G30 UØ VØ WØ;

       GØØ X100.0 Y0.0 Z1.0;

       X46.0;

       G71 P10 Q5Ø UØ WØ D1000 F0.28;

       N10 GØØ X45.0;

       N15 G01 Z0.0 F0.15;

       N30 Z-200.0;

       N50 X75.0 Z-225.0;

       GØØ X100.0 Z1.0;

       G28 X100.0 Y0.0 Z1.0;

       M30

Appendix III

LOG BOOK DATA FOR CNC MACHINING -COMPARATIVE TESTS

Comparative Results of Surface roughness readings and Power Loads

Insert Type/ specimen	Cutting speed	Number of Cuts	Machining Time (Mins)	Surface Measurement (Ra Value)	Disparity in Ra Values	Motor Power Load (%)	Disparity in power load
Control	250	25	16	2.98	0.54 µm	60	5%
EDMed	250	25	16	3.52		55	
Control	300	25	14	3.32	0.4 µm	55	5%
EDMed	300	25	14	2.92		50	
Control	325	25	12.9	3.00	0.21 µm	60	10%
EDMed	325	25	12.9	2.79		50	
Control	350	25	12	7.30	4.65 µm	70	20%
EDMed	350	25	12	2.65		50	

Appendix IV

BS EN ISO 4287: 1997: **Surface Texture Measurement: Profile method**
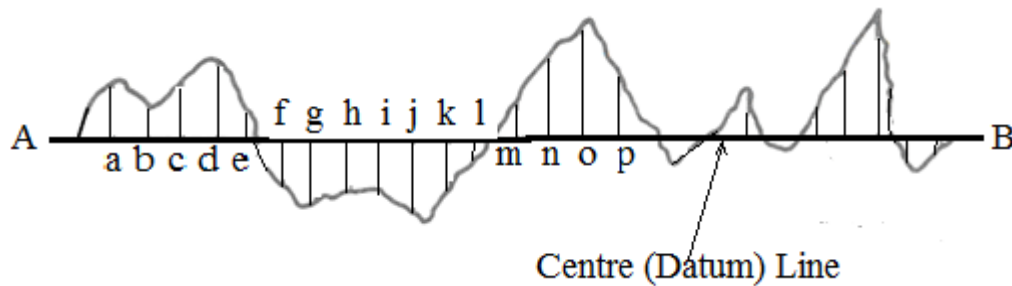
Figure Illustrating Surface Profile Measurements methods

The arithmetical approach in determining the surface roughness (Ra) value is shown in the formula below (BS EN ISO 4287: 1997 *-Surface texture: Profile method –Terms, definitions and surface texture parameters*):

$$R_a = \sqrt{\frac{a^2 + b^2 + c^2 + d^2 + e^2}{n}}$$

From the surface profile measurements, the Roughness Average (R_a) readings were generated within the Taylor Hobson software suite 'Ultra' and results given below:

Appendix V

COATING HARDNESS COMPARED

Table of Properties of Coating Materials

Material and PVD Coatings	Hardness HVN (Kg/mm^2)	Friction Coefficient vs Steel	Maximum Operating Temperature	Coating Thickness (μm)
TiN	2,200	0.4–0.5	600	1–4
TiCN	3,000	0.25–0.4	430	1–7
TiAlN layered	3,300	0.3–0.65	800	2–5
TiAlN monolayered	4,500	0.3–0.65	800	1–5

(Adopted from McCabe (2001))
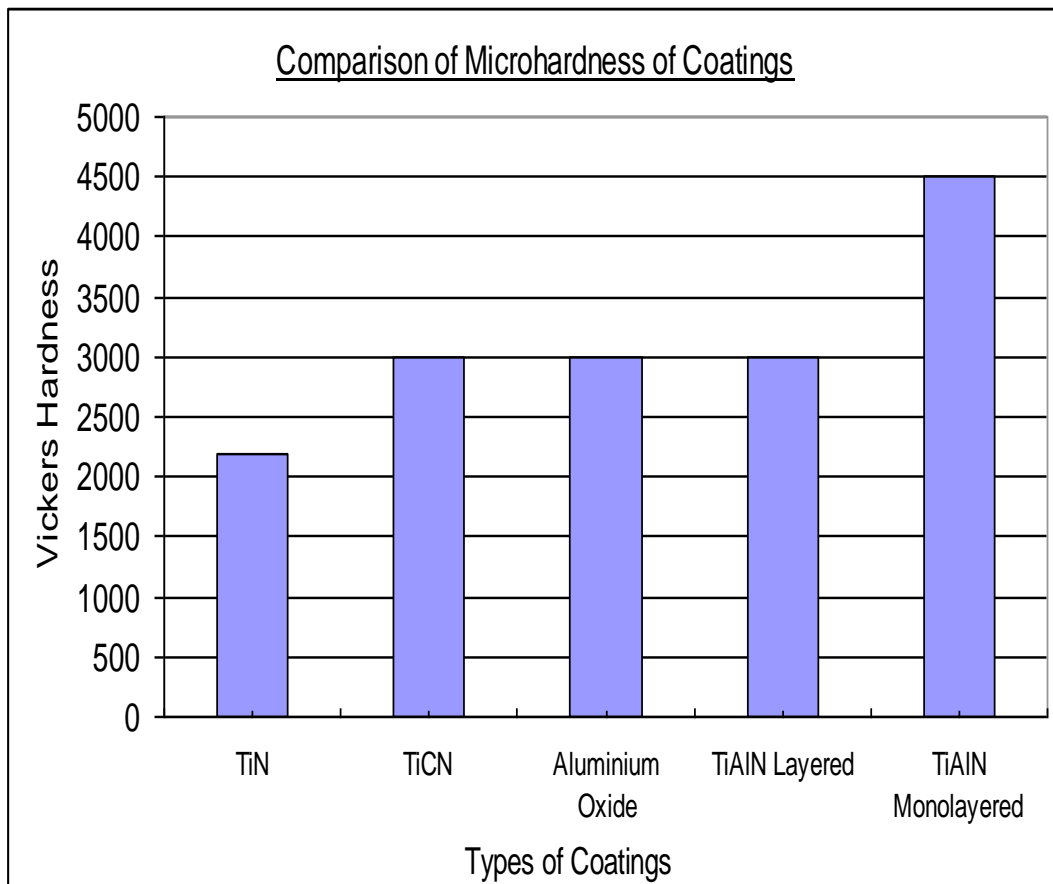
Comparison of Microhardness for different types of coating (Adopted from Stephenson and Agapiou, 2006)

Appendix VI

Titanium Coating Capabilities

Table 1: Physical Properties of TiN

Characteristics	Used	Property
Hardness	Coating cutting tools	2300 Hv
Melting Point	Coating cutting tools	2800 ^{0}C
Density	Coating cutting tools	4.51 gcm^{-3}
Max Operating	Coating cutting tools	500 ^{0}C
Temperature	Coating cutting tools	61.9
Elastic Modulus	Coating cutting tools	600 Gpa
Friction Coefficient	Coating cutting tools	TiN/TiN 0.08–0.25 (Static)
		TiN/TiN 0.15 (Dynamic)
Toxicity	Used in medical prothesis	Nil

(Source: Wallwork HT UK, Heat Treatment and Hard Coating Service 2012
http://www.wallworkht.co.uk/content/commercial_heat_treatment

The effect of the coating method and type in terms of withstanding different types of wear mechanism is illustrated in Table 2.

Table 2: Different Coating Methods Endure Different Wear Mechanisms

Coating	Abrasion Wear	Adhesion Wear	Fatigue Wear	Plastic Deformation	Chipping/ Fracture	Try for a Sharp Edge
PVD	-	+	+	-	+	+
CVD	+	0	0	+	0	-
MT-CVD	+	0	0	+	0	-
TiAlN	+	+	0	+	-	0
TiCN	+	0	0	0	0	0
TiN	0	0	0	0	0	0
Al_2O_3	++	+	-	+	-	-

Note: '+' means Positive impact; '-'means Negative impact; '0' means Neutral impact.
(Courtesy of Sandvik Coromant (2008))

Appendix VII

Material Properties of the Work, Tool and Coating Layer

Tabulation of Material Properties of the Work, Tool and TiN Coating Layer

Conditions / Grade	Symbol	Workpiece Mild Steel	Tool Insert Tungsten Carbide	Titanium Nitride
		EN 3	WC	TiN
Young's Modulus (GPa)	E	208	800	500
Poisson's Ratio	V	0.37	0.2	0.25
Yield Stress (MPa)	Σ	300		600
Ultimate Stress (MPa)		394		
Specific Heat Capacity (J/m^3 K)	Cp		203	2.50×10^6
Thermal Conductivity (W/m K)	Λ		46	90
Vickers Hardness	Hv	145		2600
Mass Density (gcm^{-3})	ρ	7.86	15	4.506
Coefficient of thermal expansion (μm/m^{0}C)	K	$12.4 \times 10^{-6}\,^0$C	4.7 (at 20^{0}C) 4.9 (at 1000^{0}C)	8.5x10-6 k-1
Melting point (^{0}C)			2870 ^{0}C	1668 ^{0}C
Boiling Point (^{0}C)			6000 ^{0}C	3287 ^{0}C
Coefficient of Tool-Face Friction	μ			

Table of Chemical Properties of Mild Steel EN3

Element	Symbol	Quantity
Carbon	C	0.25% max
Silicon	Si	0.05–0.35%
Manganese	Mn	1.0%
Sulphur	S	0.6%
Phosphorus	P	0.06%
Iron	Fe	Remainder

Appendix VIII

Preparation of Steel Substrates

Preparation of steel substrates before application of paints and related products – Surface roughness characteristics of blast-cleaned steel substrates

Method for the calibration of ISO surface profile comparators and for the determination of surface profile – Stylus instrument procedure

1. Scope

This part of ISO 8503 specifies the stylus instrument and describes the procedure for calibrating ISO surface profile comparators conforming to the requirements of ISO 8503.

This part of ISO 8503 is also applicable to the determination of the surface profile, within the range $R_{\ddot{y}5} = 20\mu m$ to $R_{\ddot{y}5} = 200\mu m$, of essentially planar blast-cleaned steel. The determination can be carried out on a representative section of the blast-cleaned surface or, if direct observation of the surface is not feasible, on a replica of the surface (see Annex C).

NOTE: Where appropriate, this procedure can be used to assess the roughness profile of other abrasive blast-cleaned substrates.

An alternative procedure is described in ISO 8503-3.

2. Normative references
The following referenced documents are indispensable for the application of this document. For dated references, only the edition cited applies. For undated references, the latest edition of the referenced document (including any amendments) applies.

ISO 3274. Geometrical Product Specifications (GPS) – *Surface texture: Profile method – Nominal characteristics of contact (stylus) instruments*

ISO 4287: 1997, Geometrical Product Specifications (GPS) – *Surface texture: Profile method – Terms, definitions and surface texture parameters*

ISO 5436-1, Geometrical Product Specifications (GPS) – *Surface texture: Profile method; Measurement standards – Part 1: Material measures*

ISO 5436-2, Geometrical Product Specifications (GPS) – *Surface texture: Profile method; Measurement standards – Part 2: Software measurement standards*

ISO 8503-1, Preparation of steel substrates before application of paints and related products – Surface roughness characteristics of blast –cleaned steel substrates – Part 1: Specifications and definitions for ISO surface profile comparators for the assessment of abrasive blast-cleaned surfaces

Bibliography

1.   ISO 4288:1996, Geometrical Product Specifications (GPS)- Surface texture: Profile method – Rules and procedures for the assessment of surface texture

2.   ISO 8503-2, Preparation of steel substrates before application of paints and related products – Surface roughness characteristics of blast-cleaned steel substrates – Part 2: Method for the grading of surface profile of abrasive blast-cleaned steel – Comparator procedure

3.   ISO 8503-3, Preparation of steel substrates before application of paints and related products – Surface roughness characteristics of blast-cleaned steel substrates – Part 3: Method for the calibration of ISO surface profile comparators and for the determination of surface profile – Focusing microscope procedure

4.   ISO 8504-2, Preparations of steel substrates before application of paints and related products – Surface preparation methods - Part 2: Abrasive blast-cleaning

Form for recording surface profile measurements made in accordance with ISO 8503-4

Test Laboratory and Address					
Stylus Instrument Manufacturer……………….. Type:……………….. Model:………………………….			Tip Radius = …….µm Evaluation Length, ln = ….mm Sampling Length, l, = …..mm		
Reading Number	Segment 1	Segment 2	Segment 3	Segment 4	Steel Substrate Replica
Max value of R_y[5]					
Grand Mean					
Standard deviation					
A delete as appropriate B if profile measurement is of i) a steel substrate or ii) a replica, give details					

Appendix IX

Evidence of components made during Field Tests

Sample of components prepared during the field test at Kennics Engineering
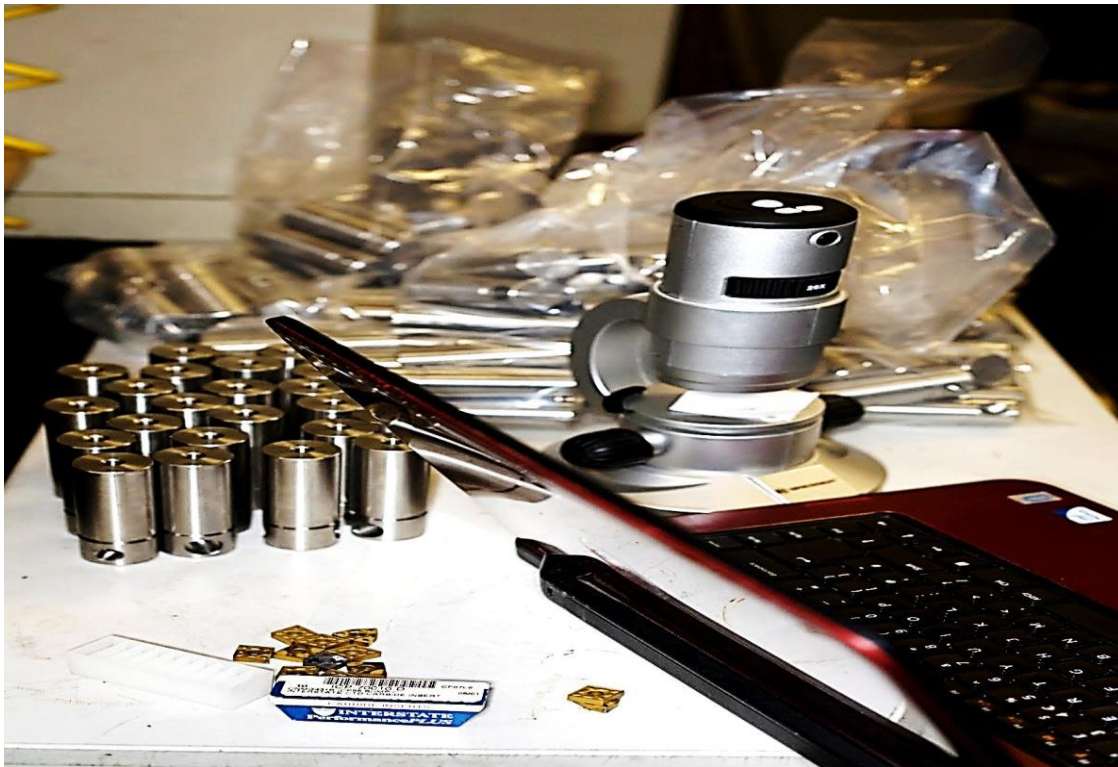
Samples of Components prepared in the Second Field Test at Newton Engineering.

Appendix X

SIMULATION MODELLING PARAMETERS

AdvantEdge^{TM}: Version = 5.9011
Project / Job Name = Super
Job Description = Oblique Cutting in 2D
Units = SI
Process Type = Turning
Workpiece Type = Mild Steel EN-3
Tool Type = TiN Coated EDMed Customised
Tool Material Type = Tungsten Carbide

a) **STANDARD WORKPIECE**
   Workpiece length = 50 mm
   Workpiece Diameter = 20 mm
   Material = AISI-1045_200Bhn
   Workpiece Material Hardness = 200

b) **CUSTOM TOOL**
   Tool File = Super.twt
   Tool Process Type = OBLIQUE
   Tool Material = Carbide-Grade-K
   Minimum Tool Element Size = 0.02 mm
   Maximum Tool Element Size = 0.1 mm
   Mesh Grading = 0.4
   Coating Layer No. = 1
   Coating Material 1 = TiN
   Coating Thickness 1 = 0.004 mm
   Aggregate Layer = ON

c) **PROCESS**
   Depth of cut = 1 mm
   Length of cut = 4.2 mm
   Feed = 0.28 mm
   Cutting speed = 350 m/min
   Initial temperature = 20 ^{0}C
   Friction coefficient = 0.4
   Cutting mode = General
   External Coolant = ON
   Heat Transfer Coefficient = 10000 W/(m2.K)
   Coolant Temperature = 20 ^{0}C
   Coolant Nozzle Location X = 4.0 mm
   Coolant Nozzle Location Y = 3.0 mm
   Jet Radius (R) = 20.0 mm
   Jet Angle (A) = -50 ^{0}
   Jet Velocity = 50 m/s
   Internal Primary Coolant = OFF
   Internal Secondary Coolant = OFF

d)   SIMULATION

Simulation Mode = Standard
Steady state analysis = 1
Avg. Length of Cut Ratio = 10
Chip breakage = 0
Max. number of nodes = 24000
Max Element Size = 0.1 mm
Min Element Size = 0.02 mm
Fraction of Radius = 0.6
Fraction of Feed = 0.1
Mesh Refine = 2
Mesh Coarse = 6
Output Frame = 30
Number of Threads = 1

Appendix XI

AdvantEdge$^{\text{TM}}$ V.5.9011 software Formula for Heat Distributions

In AdvantEdge$^{\text{TM}}$, V. 5.9011, the material behaviours are governed by the following equations

$$\left(1 + \frac{\dot{\varepsilon}^P}{\dot{\varepsilon}_0^P}\right) = \left[\frac{\bar{\sigma}}{g(\varepsilon^P)}\right]^{\text{m1}} , \text{if } \dot{\varepsilon}^P \leq \dot{\varepsilon}_t \qquad\qquad \text{Equation 1}$$

$$\left(1 + \frac{\dot{\varepsilon}^P}{\dot{\varepsilon}_0^P}\right)\left[1 + \frac{\dot{\varepsilon}_t}{\dot{\varepsilon}_0^P}\right]\frac{m2}{m1} - 1 = \left[\frac{\sigma}{g(\varepsilon^P)}\right]^{\text{m2}} , \text{if } \dot{\varepsilon}^P > \dot{\varepsilon}_t \qquad\qquad \text{Equation 2}$$

$$g(\varepsilon^P) = \sigma_0 \theta(T)\left[1 + \frac{\varepsilon^P}{\varepsilon_0^P}\right]\frac{1}{n} \qquad\qquad \text{Equation 3}$$

Appendix XII

DATASHEET / FACT SHEET

This is a PATENT sales Promotional datasheet published by Imperial Innovations Ltd. Part of Imperial College, University of London. The company (Imperial Innovations Ltd) is a partner in the PATENT Registration/ Application (US2005/181174) of this novel/original study. Consumables for this project were wholly financed by Imperial Innovations Limited. They hold the highest stake in terms of money invested for this research and Patent development.

- The Document is in public domain and that explains why it is presented in this Thesis.

- In the document, the Pictures showing wear on tool rake face were taken from appendix 1b and 1c of this thesis.

SUMMARY - BENEFITS

This technology is a patent-protected, low cost surface treatment of cutting tool inserts. The technique leads to improved productivity, reduced power consumption and enhanced work-piece surface finish.

Extensive tests have been conducted on a titanium nitride coated carbide cutting tool tip, treated with the surface enhancement. When operated 40% faster than the recommended standard speed, the tips demonstrated not only increased productivity, but also better surface finish and reduced power loading by 18%. Tool wear characteristics did not affect dimensional accuracy of the work-piece. Tool service life was equivalent, if not longer.
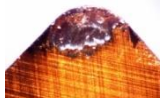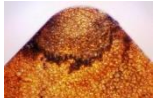
This step-change performance improvement can be incorporated into any coated tool at a marginal cost and particularly where the insert is produced using a sintering process, the production cost is negligible.

HOW IT WORKS

The surface enhancement, called 'residual island' treatment, produces an undulating surface topography on the tool. As the tool wears, 'islands' of residual titanium nitride remain in the valleys, which continue to provide wear resistance. It is expected that residual island effect would occur for most, if not all, types of coating.

STAGE OF DEVELOPMENT

The innovative undulating surface topography has been developed and optimised through several years' research. More recently, tests have been made to compare Kennametal tips with and without the undulating surface topography, at both recommended and over-speed conditions. 75mm diameter mild steel bar billets were machined at constant surface speed. The surface finish on the billets, rake and flank wear on the tip and power load used by the machine were monitored. Table 1 summarises a set of results for a cutting speed of 325 m/min.

Table 1: Speed 325 m/min, feed 0.28mm/rev, depth of cut 1.0mm, cutting time 16min.		
	Standard	Modified
Surface Finish (Ra µm)	3.22	2.44
Power load % of max power	65	53
Rake face after 5 passes (2.5 min)		

A substantial wear land was visible on the rake face of the 'standard' tips after only 5 passes; the wear on the modified tips became apparent after about 15 passes. At 350 m/min, which is 40% above the recommended speed, the 'standard' tips failed repeatedly around 27 passes, while the modified tips continued to perform without failure even after 35 passes. Figure 2 below shows the two tool tips after the 350 m/min test:

Fig 2a- Rake face standard tip after 27 passes

Fig 2b- Rake face modified tip after 30 passes

Fig 2c-Side view
(flank) standard tip
after 27 passes

Fig 2b-Side view
(flank) modified tip
after 30 passes

NEXT STEPS

Imperial Innovations is seeking development partners to explore the full range of capability of this technology. Our intention is to bring the technology to market via licensing.

ABOUT IMPERIAL INNOVATIONS

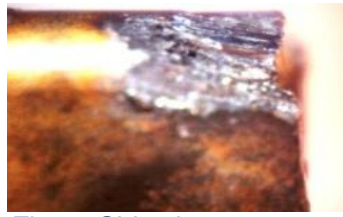Imperial Innovations is one of the UK's leading technology transfer and commercialisation companies. Our goal is to bring valuable ideas to market either by building businesses or licensing to industry.

Imperial Innovations is active across a wide range of areas, including healthcare, energy, environment and other emerging technology. The company's integrated approach encompasses the identification of ideas, protection of intellectual property, licensing of technology, formation & incubation of technology businesses, and subsequent investment activities.

Based at Imperial College London, the company has established equity holdings in 89 technology businesses and is managing 156 commercial agreements as of 31 July 2008. Imperial College is our main partner and major source of ideas. We also provide commercialisation services to a number of external research-intensive organizations, in both the public and private sectors. The company was founded in 1986 and its ordinary shares admitted to trading on the AIM Market of the London Stock Exchange in July 2006 (symbol: IVO).

ABOUT IMPERIAL COLLEGE

Consistently rated amongst the world's best universities, Imperial College London is a science-based institution with a reputation for excellence in teaching and research. The College attracts 12,000 students and 6,000 staff of the highest international quality. Innovative research at the College explores the interface between science, medicine, engineering and business, delivering practical solutions that improve quality of life and the environment.

Since its foundation in 1907, Imperial's contribution to society has been immense. Innovations have included the discovery of penicillin, the development of holography and the foundations of fibre optics. This commitment to the application of research for the benefit of all continues today. Current research focuses include interdisciplinary collaborations to improve health, tackle climate change and develop clean and sustainable sources of energy.

Imperial Innovations

Level 12, Electrical & Electronic Engineering Building
Imperial College London SW7 2AZ, United Kingdom
Telephone: +44 (0)20 7581 4949, Fax: +44 (0)20 7589 3553
www.imperialinnovations.co.uk. www.imperial.ac.uk

Appendix XIII

Lists of Published Works/ Papers Related to this study

1) Titus .B. Watmon and Anthony .C. Ijeh, Coating Cutting Tools with Hard Substance Lowers Friction Co-efficient and Improves Tool Life - A Review, *Proceedings of the International MultiConference of Engineers and Computer Scientists 2010, IMECS* 2010, 17-19 March, 2010, Hong Kong; ISSN: 2078-0966

2) Watmon, T. B., Xiao, D., and Weerasinghe, V, Enhanced tool wear characteristics of carbide tool inserts having a novel surface structure, *Proceedings of Advances in Computing and Technology, (AC&T) The School of Computing and Technology 5th Annual Conference, University of East London,* (2010), pp.33-37 ISBN: 978-0-9564747-0-4

3) Watmon T. B., and Ssengonzi J. B., Application of Finite Element in Metal Cutting Analysis, *World Academy of Science, Engineering and Technology* Vol.66 (2010) pp.261-263; ISSN: 2070-3724

4) Watmon T. B., and Ssengonzi J. B , Review of Finite Element Analysis of Single Point Cutting Process, *World Academy of Science, Engineering and Technology* Vol.66 (2010) pp.264-266; ISSN: 2070-3724

5) Titus B. Watmon, David D. Xiao, study of deformation of coated tools in orthogonal metal cutting process using FEA, *Proceedings of Advances in Computing and Technology, (AC&T) The School of Computing and Technology 4*[th] *Annual Conference, University of East London (2011). Pp.86-90, ISBN: 978-0-9564747-1-1*

6) Watmon, T. B., Coated Tools with Crater-Like Surface Structures Have Enhanced Performance, *American Institute of Physics Conference Proceedings. VOL.5 (*1285) (2011), pp. 279-285; ISBN: 978-0-7354-0839-5, ISSN: 0094-243X

Appendix XIII

Coulomb Friction Forces generated in AdvantEdge^{TM} v.5.9011 and viewed in Tecplot windows and imported into excel spreadsheets for computation.

TITLE : VARIABLES =	TiN Coated Plain Surface Tool		TITLE : VARIABLES =	TiN Coated Undulating Surface Tool	
	Fx (N)			Fx (N)	
	Fy (N)			Fy (N)	
	Von Mises = 1000 MPa			Von Mises = 1000 MPa	
	µ Average = 0.50			µ Average = 0.36	

Fx(N)	Fy(N)	µ = Fy/Fx	Fx(N)	Fy(N)	µ = Fy/Fx
6.35E+00	3.49E+00	0.55	6.20E+00	1.81E+00	0.29
6.38E+00	3.57E+00	0.56	6.24E+00	1.81E+00	0.29
6.41E+00	3.58E+00	0.56	6.28E+00	1.82E+00	0.29
6.47E+00	3.37E+00	0.52	6.33E+00	1.83E+00	0.29
6.22E+00	3.16E+00	0.51	6.41E+00	1.84E+00	0.29
6.43E+00	3.36E+00	0.52	6.49E+00	1.86E+00	0.29
6.39E+00	3.42E+00	0.54	6.47E+00	1.85E+00	0.29
6.47E+00	3.25E+00	0.50	6.46E+00	1.85E+00	0.29
6.38E+00	3.39E+00	0.53	6.44E+00	1.85E+00	0.29
6.21E+00	3.32E+00	0.55	6.43E+00	1.85E+00	0.29
6.33E+00	3.34E+00	0.56	6.40E+00	1.84E+00	0.29
6.40E+00	3.52E+00	0.56	6.38E+00	1.84E+00	0.29
6.40E+00	3.55E+00	0.52	6.37E+00	1.84E+00	0.29
6.47E+00	3.43E+00	0.51	6.35E+00	1.83E+00	0.29
6.47E+00	3.40E+00	0.52	6.34E+00	1.83E+00	0.29
6.44E+00	3.42E+00	0.54	6.30E+00	1.82E+00	0.29
6.44E+00	3.58E+00	0.50	6.31E+00	1.83E+00	0.29
6.47E+00	3.58E+00	0.53	6.27E+00	1.82E+00	0.29
6.24E+00	3.56E+00	0.54	6.26E+00	1.82E+00	0.29
6.27E+00	3.57E+00	0.53	6.22E+00	1.81E+00	0.29
6.25E+00	3.53E+00	0.55	6.23E+00	1.81E+00	0.29
6.18E+00	3.52E+00	0.55	6.10E+00	1.79E+00	0.29
6.21E+00	3.56E+00	0.53	6.19E+00	1.80E+00	0.29
6.47E+00	3.55E+00	0.53	6.18E+00	1.80E+00	0.29
6.47E+00	3.52E+00	0.53	6.14E+00	1.79E+00	0.29
6.43E+00	3.53E+00	0.56	6.11E+00	1.79E+00	0.29
6.39E+00	3.44E+00	0.55	6.13E+00	1.79E+00	0.29
6.38E+00	3.47E+00	0.57	6.09E+00	1.79E+00	0.29
6.35E+00	3.53E+00	0.57	6.07E+00	1.78E+00	0.29
6.35E+00	3.57E+00	0.56	5.83E+00	1.74E+00	0.29
6.46E+00	3.34E+00	0.57	5.81E+00	1.74E+00	0.29
6.32E+00	3.56E+00	0.57	5.82E+00	1.74E+00	0.29
6.30E+00	3.57E+00	0.55	5.84E+00	1.74E+00	0.29

6.47E+00	3.28E+00	0.54		5.85E+00	1.74E+00	0.29
6.46E+00	3.31E+00	0.55		5.89E+00	1.75E+00	0.29
6.31E+00	3.53E+00	0.54		5.90E+00	1.75E+00	0.29
6.33E+00	3.49E+00	0.54		5.99E+00	1.77E+00	0.29
6.31E+00	3.49E+00	0.56		5.93E+00	1.76E+00	0.29
5.92E+00	3.49E+00	0.56		5.94E+00	1.76E+00	0.30
6.03E+00	3.57E+00	0.52		6.16E+00	1.80E+00	0.30
6.12E+00	3.47E+00	0.56		6.15E+00	1.80E+00	0.30
6.10E+00	3.47E+00	0.57		6.06E+00	1.78E+00	0.30
6.00E+00	3.56E+00	0.51		6.05E+00	1.78E+00	0.30
6.17E+00	3.56E+00	0.51		6.04E+00	1.78E+00	0.30
6.28E+00	3.48E+00	0.56		6.03E+00	1.77E+00	0.30
6.22E+00	3.42E+00	0.55		5.98E+00	1.77E+00	0.30
6.16E+00	3.46E+00	0.55		6.01E+00	1.77E+00	0.30
6.38E+00	3.28E+00	0.59		6.00E+00	1.77E+00	0.30
6.43E+00	3.29E+00	0.59		5.97E+00	1.76E+00	0.29
6.38E+00	3.25E+00	0.57		5.95E+00	1.76E+00	0.29
6.44E+00	3.24E+00	0.57		5.91E+00	1.75E+00	0.29
6.14E+00	3.56E+00	0.59		5.92E+00	1.76E+00	0.29
6.12E+00	3.53E+00	0.58		5.86E+00	1.75E+00	0.29
6.12E+00	3.57E+00	0.55		5.87E+00	1.75E+00	0.29
5.94E+00	3.53E+00	0.55		5.80E+00	1.73E+00	0.30
5.97E+00	3.56E+00	0.56		5.79E+00	1.73E+00	0.29
5.61E+00	3.57E+00	0.52		5.67E+00	1.71E+00	0.30
5.63E+00	3.54E+00	0.51		5.52E+00	1.69E+00	0.30
5.64E+00	3.57E+00	0.51		5.51E+00	1.68E+00	0.30
6.11E+00	3.24E+00	0.50		5.57E+00	1.69E+00	0.30
5.97E+00	3.16E+00	0.58		5.61E+00	1.70E+00	0.30
6.02E+00	3.53E+00	0.58		5.40E+00	1.67E+00	0.30
6.07E+00	3.47E+00	0.58		5.43E+00	1.67E+00	0.30
6.04E+00	3.46E+00	0.59		5.74E+00	1.73E+00	0.30
5.79E+00	3.07E+00	0.60		5.76E+00	1.73E+00	0.30
5.62E+00	3.49E+00	0.64		5.53E+00	1.69E+00	0.30
5.96E+00	3.32E+00	0.63		5.54E+00	1.69E+00	0.31
5.98E+00	3.43E+00	0.63		5.47E+00	1.68E+00	0.31
5.84E+00	3.35E+00	0.53		5.48E+00	1.68E+00	0.30
5.84E+00	3.58E+00	0.53		5.49E+00	1.68E+00	0.30
5.87E+00	3.57E+00	0.59		5.44E+00	1.67E+00	0.31
5.80E+00	3.50E+00	0.57		5.44E+00	1.67E+00	0.31
5.75E+00	3.45E+00	0.57		5.40E+00	1.66E+00	0.30
5.69E+00	3.49E+00	0.53		5.39E+00	1.66E+00	0.30
5.64E+00	3.49E+00	0.62		5.78E+00	1.73E+00	0.31
5.74E+00	3.57E+00	0.56		5.77E+00	1.73E+00	0.30
6.47E+00	3.22E+00	0.57		5.70E+00	1.72E+00	0.31
5.44E+00	3.32E+00	0.57		5.71E+00	1.72E+00	0.31

5.57E+00	3.53E+00	0.61	5.41E+00	1.67E+00	0.31
5.59E+00	3.57E+00	0.61	5.42E+00	1.67E+00	0.31
6.09E+00	3.57E+00	0.60	5.55E+00	1.69E+00	0.31
6.08E+00	3.53E+00	0.60	5.56E+00	1.69E+00	0.31
6.06E+00	3.57E+00	0.61	5.50E+00	1.68E+00	0.31
5.76E+00	3.57E+00	0.62	5.51E+00	1.68E+00	0.30
5.81E+00	3.58E+00	0.62	5.60E+00	1.70E+00	0.30
5.79E+00	3.55E+00	0.50	5.66E+00	1.71E+00	0.30
5.67E+00	3.57E+00	0.61	5.62E+00	1.70E+00	0.30
5.71E+00	3.57E+00	0.63	5.63E+00	1.70E+00	0.31
5.70E+00	3.54E+00	0.64	5.63E+00	1.71E+00	0.31
5.45E+00	3.57E+00	0.59	5.45E+00	1.67E+00	0.30
5.50E+00	3.53E+00	0.58	5.46E+00	1.68E+00	0.30
5.49E+00	3.57E+00	0.59	5.68E+00	1.71E+00	0.31
5.47E+00	3.57E+00	0.62	5.69E+00	1.72E+00	0.31
5.37E+00	3.57E+00	0.62	5.38E+00	1.66E+00	0.30